CATALYTIC EFFECTS OF THE γ-FeOOH (LEPIDOCROCITE)

SURFACE ON THE OXYGENATION REMOVAL KINETICS OF Fe(II) and Mn(II)

Thesis by

Windsor Sung

In Partial Fulfillment of the Requirements

for the Degree of

Doctor of Philosophy

California Institute of Technology

Pasadena, California

1981

(Submitted July 30, 1980)

ACKNOWLEDGMENTS

I wish to thank my advisor, James J. Morgan, for his patience. His timely criticisms were very helpful.

Thanks are due to the following professors who have served on my committees: F. C. Anson, N. H. Brooks, R. C. Flagan, W. L. Johnson, W. J. North and G. R. Rossman. R. B. Burns at MIT has been a most stimulating professor during my undergraduate days and continues to be of much support.

Technical help has been invaluable from the following: P. E. Duwez, S. Kotake and S. Samson for X-ray diffraction. R. Potter and G. R. Rossman for instructions on the infrared spectroscopy work. J. B. Earnest kindly did the BET surface area measurements for me in his spare time at JPL. Heartfelt thanks are due to Elaine Granger for typing my manuscript efficiently.

Discussions with J. R. Hunt and J. R. Young have helped clear my thinking. I thank their patience for those uninvited walk-in discussions. Mr. and Mrs. K. Y. Ho and Mr. and Mrs. Z. K. Sung provided much needed moral support.

Caltech has been an enjoyable institution to pursue academic work. Classical guitar lessons with D. Denning provided cultural breaks. Financial support from the Dupont and Union Oil companies is gratefully acknowledged.

Dedicated to my wife,Mei Ling.

ABSTRACT

Previous investigations of Fe(II) oxygenation had resulted in a
wide range in the reported rate constant(s). While Fe(II) oxygenation
rates are fast in simple laboratory systems (seconds to minutes when
pH > 7), actual rates observed in natural waters can be orders of
magnitude lower. Conversely, while Mn(II) oxygenation rates are slow
in laboratory systems (days when pH < 9), much faster rates are observed
in natural waters or implicated in model studies.

The influences of ionic strength, temperature and anions on the
Fe(II) homogeneous oxygenation rates were examined in this study. Other
rate constants from the literature were successfully incorporated into
this framework. Complexation by major anions (e.g., SO_4^{2-} and Cl^-) and
ionic strength effects were sufficient to account for the retardation of
Fe(II) oxygenation in seawater. Autocatalysis of Fe(II) oxygenation was
observed for pH > 7. A general integrated autocatalytic rate expression
suitable for Fe(II) or Mn(II) oxygenation was used to interpret laboratory-
obtained kinetic data. Oxidation of Fe(II) in various laboratory systems
with characteristics like those of natural water was shown to form the
allotrope γ-FeOOH. The γ-FeOOH surface was shown to be an excellent
catalyst for Fe(II) and Mn(II) oxygenation.

The γ-FeOOH surface obtained by oxidizing milli-molar levels of
Fe(II) in 0.7 M NaCl was studied in the following ways: surface charge
characteristics by acid/base titration; adsorption of Mn(II) and surface
oxidation of Mn(II). A rate law was formulated to account for the
effects of pH and the amount of surface on the surface oxidation rate of

Mn(II). The presence of milli-molar levels of γ-FeOOH was shown to reduce significantly the half-life of Mn(II) in 0.7 M NaCl from hundreds of hours to hours. The γ-FeOOH surface was shown to be as effective as colloidal MnO_2 in catalysing Mn(II) oxygenation.

TABLE OF CONTENTS

TABLE OF CONTENTS (Continued)

LIST OF FIGURES

LIST OF FIGURES (Continued)

LIST OF TABLES

NOTATIONS AND SYMBOLS

[i] concentration of species i, usually in moles/L (M)

{i} thermodynamic activity of species i, in M

A specific surface area (m^2/g)

b gas transfer coefficient (min^{-1})

C Capacitance (coulombs/volt m^2 = Farads/ m^2)

ε dielectric constant, 89×10^{-12} coulomb/volt cm

E potential of the glass-reference electrode (mv)

F Faraday's constant, 96500 coulombs/equivalent

Fe(II) total iron in the +2 oxidation state

Fe(III) total iron in the +3 oxidation state

Fe^{2+} the chemical species $Fe(H_2O)_6^{2+}$

k rate constants

κ reciprocal double layer thickness (cm^{-1})

K equilibrium constants

K_W ionic product of water $^cK_W = [H^+][OH^-]$

Mn(II) total manganese in the +2 oxidation state

Mn(IV) total manganese in the +4 oxidation state

Mn^{2+} the chemical species $Mn(H_2O)_6^{2+}$

M(moles/L)

pH: $-\log\{H^+\}$ = p_cH when ionic strength > 0.11 M

p_cH: $-\log[H^+]$

pH_{zpc} the pH value for a solid/solution interface where the total surface charge on the surface is zero

Γ surface excess of protons (moles/g)

σ surface charge density (coulombs/m^2)

S surface site

ψ surface potential (mv)

CHAPTER 1

INTRODUCTION

1.1 Interest in Iron and Manganese

Iron(Fe) and manganese(Mn) are important elements in environmental geochemistry. If one may gauge the importance of a subject by the number of publications about it, iron and manganese certainly rank high. A 1973 National Academy of Sciences report on manganese listed 555 references and a later 1977 National Research Council (NRC) report on geochemistry and the environment listed 87 references under the section on manganese. A 1979 NRC report on iron listed 873 references.

There are five reasons for the interest in iron and manganese.

1. Abundance: Iron and manganese rank fourth and twelfth,respectively, in crustal abundance of elements. Among metals, iron is second after aluminum in abundance. Among heavy metals, iron is ranked number one and manganese is second in crustal abundance. According to Mason (1958), average crustal composition is 5 percent iron and 0.1 percent manganese by weight.

2. Micronutrient requirements: Iron and manganese are essential micro-nutrients to organisms, both plant and animal. According to Bowen (1966), the function of iron involves its ability to activate a number of oxidases (oxidizing enzymes); it is also a constituent of many oxidizing metallo-enzymes and respiratory pigments. The biological function of manganese is similar; it activates a host of enzymes such as peptidases and phosphatases. See also Phipps (1976).

3. <u>Surface properties of hydrous iron and manganese oxides</u>: Goldberg (1954) and Krauskopf (1956) were among the first to suggest control of heavy metal concentrations in seawater by adsorption on hydrous iron and manganese oxides. Jenne (1968) extended the role of the oxides to control of trace metals to soils and sediments. Numerous studies have since been made of the adsorption properties of these oxides, and field studies have indicated that these oxides are indeed important sinks and modes of transport for other heavy metals in the environment. Table 1.1 summarizes some of the recent laboratory work on metal adsorption on hydrous iron and manganese oxides.

4. <u>Ferromanganese nodules</u>: Ferromanganese nodules are abundant in marine, freshwater and soil environments. The origins of these deposits are still being debated. Goldberg (1961) first suggested catalytic oxidation of manganese by dissolved oxygen on an iron oxide surface as a possible mechanism; other suggestions include hydrothermal activity, nucleation and epitaxial growth, and microbial activity. Related to ferromanganese nodules are desert varnish and stream bed iron and manganese deposits.

5. <u>Water quality</u>: Iron and manganese are also of environmental concern in water use. Their presence in concentrations greater than several ppm impart undesirable taste and color to the water. The deposition of precipitated iron and manganese causes staining of plumbing fixtures and laundry. Growth of microorganisms that utilize the redox cycle of iron and manganese as a source of energy in water distribution systems can lead to reduction in pipeline carrying capacity and clogging of meters and valves.

Table 1.1 Summary of some metal adsorption

work on hydrous iron and manganese oxides

OXIDE	INVESTIGATOR	SYSTEM[a]
HYDROUS FERRIC OXIDE		
1.Amorphous FeOOH	Gadde & Laitinen(1974)	Pb;Zn;Cd;Tl;
	Davis & Leckie (1978)	Pb;Cd;Cu;Ag in 0.1M $NaNO_3$
	Swallow(1978)	Pb;Cu in synthetic seawater
2.α-FeOOH	Grimme(1968)	Cu;Zn;Co;Mn in0.1M KNO_3
	Forbes,Posner & Quirk (1974)	Hg;complexed Co in 0.075M $NaNO_3$ or NaCl; $20^{o}C$
	ibid (1976)	Cu;Pb;Zn;Co;Cd in 0.075M $NaNO_3$ or KNO_3; $20^{o}C$
HYDROUS MANGANESE OXIDE[b]		
	Murray, Healy&Fuerstenau (1968)	Ni;Cu;Co
	Posselt,Anderson & Weber (1968)	Ag;Ba;Ca;Mg;Mn;Nd;Sr in $10^{-2}M$ $NaClO_4$;ambient T
	Loganathan & Burau (1972)	Co;Zn;Ca;Na in $10^{-3}M$ $NaClO_4$; $24^{o}C$
	Anderson, Jenne & Chao (1973)	Ag in 0.082M $NaClO_4$
	Gadde & Laitinen(1974)	Pb;Zn;Cd;Tl
	Murray (1975)	Co;Mn;Zn;Ni;Ba;Sr;Ca;Mg in 0.1M NaCl
	Van der Weijden(1976)	Zn;Cd in 0.01 M $NaNO_3$ and synthetic seawater

a. Temperature is assumed to be $25^{o}C$ unless otherwise noted

b. The major phase used by these investigators is δ-MnO_2 although in some cases the related phase birnessite was used.

The United States Public Health Service standards for iron and manganese
in potable water are 0.3 mg/L (5.3 μM) and 0.05 mg/L (0.91 μM), respec-
tively. Common methods of control involve precipitation (by aeration or
addition of oxidizing agents such as $KMnO_4$) and filtration.

1.2 Brief Overview of Iron and Manganese Chemistry

The aqueous chemistries of iron and manganese have been summarized
by Stumm and Morgan (1970) and Hem (1972). Iron and manganese are
elements of the first transition series in the periodic table. Transition
metals can be loosely defined as those elements which have a partially
filled set of d-orbitals. Their ability to exist in various oxidation
states is an important characteristic. The chemistry of aqueous iron
involves the II(ferrous) and III(ferric) oxidation states while in the
case of manganese, the II(manganous), divalent, or III(trivalent) and
IV states are important.

Generally speaking, acid anaerobic conditions favor the formation of
the more soluble and therefore mobile forms: iron (II) and manganese(II).
Alkaline aerobic conditions favor the formation of the oxidized forms
which tend to have low solubilities, and thus low mobilities. In simple
inorganic laboratory systems, the kinetics of Fe(II) and Mn(II) oxygenation
are strong functions of pH, rapid (on the order of minutes) when pH is
above 6.5 and 9.6, respectively. The chemistry of the transition metals
is dominated by their ability to act as Lewis acids, forming stable complexes
with a variety of Lewis bases. We would expect that formation of complexes
with organic and inorganic ligands can favor one oxidation state over the
other.

1.3 The Objective of This Study

1.3.1 General Considerations

This thesis is concerned with the oxygenation kinetics of Fe(II) and Mn(II) to higher oxidized forms in well defined systems. Three questions were asked:

1. How can the reported rate constants for Fe(II) and Mn(II) oxygenation be placed in a consistent framework?

2. What is the particular phase that is formed when Fe(II) is oxygenated?

3. Can the phase that is formed in Fe(II) oxygenation catalyse the oxygenation of Mn(II)?

1.3.2 Experimental Design

For Fe(II) oxygenation kinetics the following physical chemical parameters were explored:

1. Ionic strength: $NaClO_4$ was used to study ionic strength effects with minimum complexation.

2. Temperature: the range 5-30°C was explored.

3. pH was varied from 6.5 to 7.2.

4. Solution composition: NaCl, $NaClO_4$ and Na_2SO_4 were studied.

For Mn(II) oxygenation in the presence of a surface a seawater-like medium was used: 0.7 M NaCl and mM levels of $NaHCO_3$ for pH regulation. Temperature was fixed at 25°C. The two main variables studied were pH, which was varied from 8 to 9, and the amount of iron oxide surface, which was varied from 10^{-4} to 10^{-3}M Fe(III).

CHAPTER 2

EXPERIMENTAL TECHNIQUES

2.1 General Information

All chemicals used in this study were of A.C.S. analyzed reagent
grade unless otherwise noted. The water used for the experiments was
re-distilled tap deionized water. All solutions were filtered through
0.45 µm Millipore® filter as a purification step. Glassware was soaked
in a detergent solution overnight (PEX laboratory detergent), rinsed with
top deionized water, 4 M HNO_3 and finally with distilled deionized water.
The reaction vessel was cleansed by soaking in hot 4 M HCl, rinsed with
tap deionized water and finally with distilled-deionized water.

2.2 Reaction Vessel

Experiments were carried out in a one-liter borosilicate beaker with
a water jacket. The beaker was sandwiched between 1/2-inch lucite covers
and bolted together by wing bolt nuts. The top cover was recessed 0.125
inch to fit the flange of the vessel, and holes to accommodate No. 5 rubber
stoppers were provided for the insertion of electrodes, thermometer and
glass delivery tubes. A sketch of the vessel is shown in Figure 2.1.

Temperature was maintained at 25°C ± 0.5°C by the circulation of water
from a Haake FK constant temperature circulator. For cooling below 25°C,
a Heto cooling unit was employed.

pH was maintained by a HCO_3^-/CO_2 buffer. See Appendix A for a descrip-
tion of the buffer. The air-CO_2 compressed gas mixtures were prepared
and analyzed by Matheson Gas Co. (Cucamonga, California) and were used
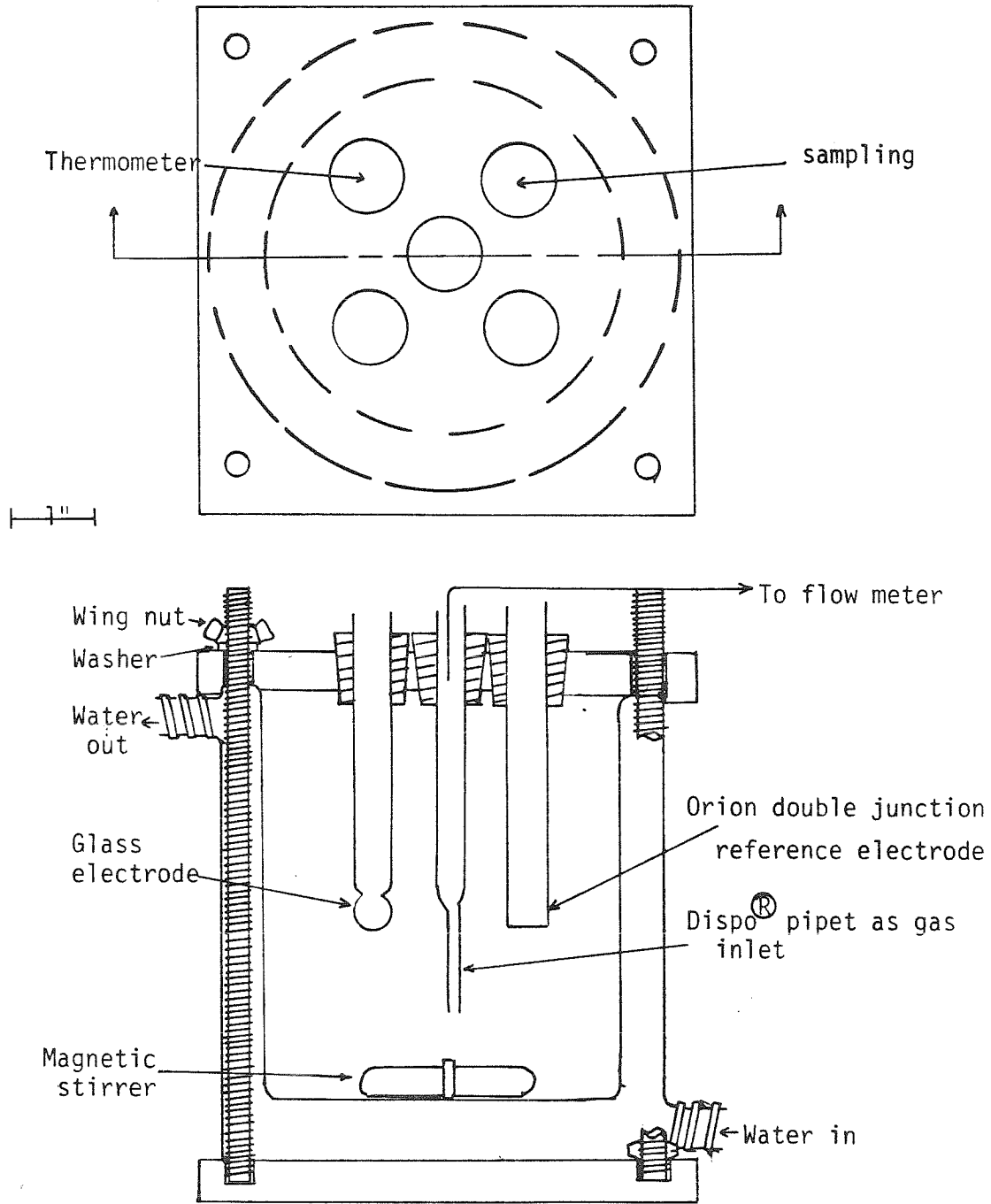
Figure 2.1 Schematic sketch of the reaction vessel

without further purification. The pH was monitored continuously with a Beckman glass electrode and an Orion double-junction reference electrode via an Orion 801A pH meter. See Appendix B for a description of the calibration procedure.

2.3 Analytical Methods

Both atomic absorption and visible spectroscopy were explored as analytical methods for iron and manganese. For μM levels their precisions and accuracies were similar ($\pm 1\%$). Visible spectroscopy was adopted for the reason of simpler instrumentation.

2.3.1 Iron Analysis

Ferrous iron concentration was determined spectrophotometrically with 1,10-phenanthroline using fluoride as a masking agent for ferric iron. The procedure employed is essentially that of Tamura et al. (1974). Ten-mL samples were quenched in 1 mL of 3.6 M H_2SO_4, 2 mL of 2 M ammonium fluoride, 1 mL of 1% 1,10-phenanthroline and 5 mL of 2M hexamethylene-tetramine were then added in that order; swirling the solution after the addition of each reagent. The solution was diluted with distilled deionized water to 25 mL and the absorbance measured at 510 nm. Five-cm cells were used with a Beckman Acta CIII spectrophotometer. Beer's law was obeyed with Fe(II) as high as 125 μM (7 mg/L) and a ferric iron background of 45 mM (2500 mg/L). The molar absorptivity at 510 nm was determined to be 1.05×10^4 $M^{-1} cm^{-1}$ with an accuracy of better than 1% and it was not significantly affected by ionic strength (up to 0.28 M NaCl).

Standard ferrous iron solutions were prepared by dissolving weighed

amounts of ferrous perchlorate in dilute $HClO_4$ acid or by dissolving

weighed amounts of electrolyte grade iron powder in known stoichiometric

amounts of redistilled $HClO_4$ or HCl to desired pH values.

Manganous manganese forms a colorless complex with the phenanthroline

reagent. Solution blanks were always checked for contaminations.

2.3.2 Manganese Analysis

Soluble manganese as Mn(II) was determined by spectrophotometric

analysis of 0.22 μm Millipore® filtered filtrate with formaldoxime reagent.

The procedure is essentially that of Morgan and Stumm (1965). Formaldoxime

reagent was prepared by dissolving 20 g of hydroxylamine hydrochloride in

200 mL water, adding 10 mL of 37% formaldehyde to the solution and

diluting to 500 mL. Ten-mL of filtrate was pipetted into a 25 mL volu-

metric flask, 2 mL of the formaldoxime reagent and 5 mL of 5 M NaOH were

then added and the contents diluted to the mark with distilled deionized

water. For adsorption studies, where oxygen was excluded, the contents

were aerated with pure oxygen for 30 sec before dilution to the mark.

Full color development is usually complete in 2 minutes. The Millipore

filters were pre-wet once, and distilled deionized water filtered to ensure

full recovery of Mn(II). The absorbance was measured at a wavelength of

450 nm and the molar absorptivity was determined to be 1.08×10^4 $M^{-1}cm^{-1}$;

it was not affected by ionic strengths as high as 0.28 M NaCl.

Manganese standards were prepared by dissolving weighed amounts of

manganous perchlorate in dilute $HClO_4$ or by dissolving weighed amounts of

pure manganese metal (National Science Supplies) in known stoichiometric

amounts of redistilled $HClO_4$ or HCl to desired pH values.

Iron and other metals form colored complexes with formaldoxime reagent. Solution blanks were monitored for Fe(II) by 1,10-phenanthroline and checked for contaminations.

Leuco crystal violet dye was used to check for oxidized Mn with the procedure of Kessick et al. (1972). Beer's law was obeyed for a final ionic strength of 0.28 M NaCl with MnO_2 concentration of 20 µM and a molar absorptivity of 4.8×10^4 $M^{-1} cm^{-1}$ at 591 nm. The corresponding molar absorptivity at low ionic strengths was reported by Kessick et al. (1972) to be $8.5 \times 10^4 M^{-1} cm^{-1}$. This procedure was not deemed to be a quantitative measure for oxidized manganese in the presence of a iron oxyhydroxide surface because conventional ways of separation (filtration, centrifugation) invariably decreased the absorbance value. As such, it was used only to show qualitatively the presence of oxidized manganese for the surface catalysis experiments.

2.4 X-ray Diffraction

Because of the small amounts of product obtained during any one experiment (less than 1 mg), X-ray powder patterns were obtained using Debye-Scherrer cameras. Oxygenation products were placed in 0.3 mm glass capillary tubes and mounted. Iron-filtered chromium radiation was used for the iron studies while vanadium-filtered chromium radiation was used for the manganese studies. Figure 2.2 summarizes the interpretation of X-ray power patterns. Standard diffraction patterns were obtained for the iron oxyhydroxides. See Appendix C for the synthetic scheme for iron oxyhydroxides.
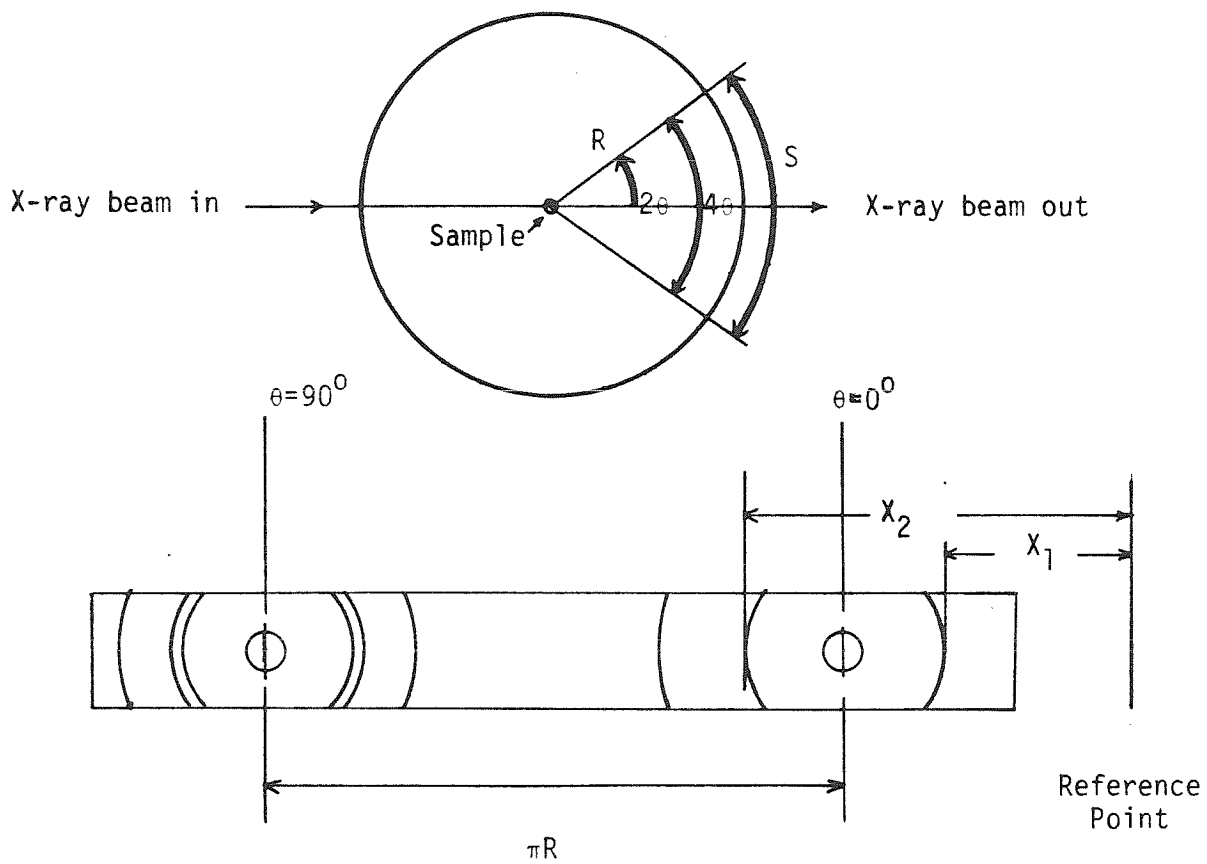
Bragg's equation: $d = \dfrac{\lambda}{2\sin\theta}$

$\lambda = 2.2909\ \overset{o}{A}\ Cr$

$1.7902\ \overset{o}{A}\ Co$

$\theta = (\ 180/4\ \pi R)S$ degrees

$S = X_2 - X_1$

Figure 2.2 Schematic presentation of X-ray film
interpretation

2.5 Infrared (IR) Spectroscopy

X-ray diffraction patterns are characteristic of the atomic arrangements of a particular solid. However, the finely-particulate size and disordered nature of iron and manganese oxides makes the interpretation of X-ray patterns difficult. IR is sensitive to the metal-oxygen bond environment and the structural environment of hydrous components. It is not a primary structural technique but once calibrated against a good set of standards it can be used to identify phases. Powers (1975) discussed the application of IR and paramagnetic measurements for the study of the ferric oxyhydroxides. Potter and Rossman (1979) discussed the application of IR to the study of tetravalent manganese oxides.

Samples of 0.5 to 1 mg were weighed out on a Cahn electrobalance and dispersed in 200 mg KBr. Pellets of 13 mm diameter were pressed at 18,000 psi for one minute under vacuum on a Carver lab press. The thickness of the pellet is of the order of 0.57 mm. IR spectra were obtained with a Perkin-Elmer model 180 spectrophotometer for the 1400 cm^{-1} to 200 cm^{-1} region.

2.6 Synthetic Scheme of γ-FeOOH For Surface Experiments

In the following chapter we will describe the identification of the oxygenation product of Fe(II) to be γ-FeOOH, lepidocrocite. This surface was studied for its catalytic effect on manganese oxygenation kinetics. Two procedures were employed to synthesize the surface. Procedure A was to generate a 10^{-3} M γ-FeOOH suspension suitable for immediate adsorption or oxygenation experiments. Procedure B was to synthesize a stock 5×10^{-3} M γ-FeOOH suspension. The same batch was diluted in aliquots to study

surface loading effects.

Stock 10^{-2} M Fe(II) solution was prepared by dissolving 0.5585 g of electrolyte grade iron powder in 500 mL of 6×10^{-2} M HCl and dilute to one-liter. The final solution composition was thus: 10^{-2} M Fe(II), 10^{-2} M H^+, 3×10^{-2} M Cl^- since the dissolution reaction is:

$$Fe(s) + 2H^+ = Fe(II) + H_2(g) \uparrow \qquad (2.1)$$
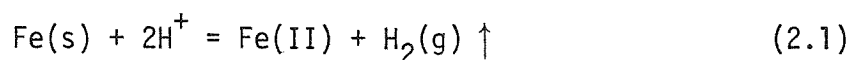
2.6.1 <u>Procedure A Generation of 10^{-3} M γ-FeOOH</u>

1. Add 100 mL 3.5 M NaCl, 4 mL 1.0 M NaHCO$_3$ to 341 mL distilled deionized water. This gave a total volume of 445 mL and a composition of 0.787 M NaCl and 8.99 mM NaHCO$_3$.

2. Pre-mixed gas of the composition 1.1% CO_2, 20.4% O_2 and 78.5% N_2 was bubbled into the solution for 30 minutes until the pH reading stabilized. The pH reading should be on the order of 7.4.

3. Add 50 mL of the stock Fe(II) solution and oxygenate for 60 minutes. The pH should decrease to about 7.2, since we are introducing and generating protons:

$$Fe^{2+} + 3/2 \ H_2O + 1/2 \ O_2 = FeOOH(s) + 2H^+ \qquad (2.2)$$
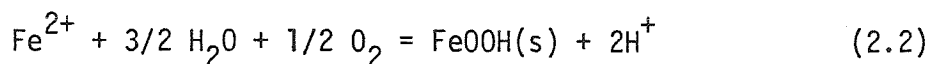
4. The final volume was made up to 500 mL by adding 5 mL of distilled deionized water, stock Mn(II), acid or base depending on the experiment. This gives a final composition of 0.7 M Cl^-, 5 mM HCO_3^- and 1 mM Fe(III).

The amount of solids captured when 50 mL of this preparation was filtered through 0.22 μm Millipore® filter was 4.3 mg after drying at 60°C for 24 hours. This implied a solids concentration of 8.6×10^{-2} g/L. Since the molecular weight for FeOOH is 88.86 g/mole and by design the final Fe(III) was 10^{-3} M we were off by about 3%. The variation of the desired total Fe(III) loading from the observed one from experiment to experiment was estimated to be no greater than ±4%.

2.6.2 <u>Procedure B   Generation of 5 mM γ-FeOOH</u>

1. Add 160 mL 3.5 M NaCl, 20 mL of 1.0 M $NaHCO_3$ and 220 mL distilled deionized water to the reaction vessel. This gave a total volume of 400 mL and a composition of 1.4 M NaCl and 5×10^{-2} M $NaHCO_3$.

2. Pre-mixed gas of composition 1.1% CO_2, 20.4% O_2 and 78.5% N_2 was bubbled in the solution for 30 minutes with a gas flow rate of one-liter/minute.

3. Add 400 mL of stock Fe(II) at increments of 100 mL per 15 minutes.

4. The gas flow was terminated after 60 minutes. The final composition was 0.7 M Cl^-, 5×10^{-3} M Fe(III) and 10^{-2} M HCO_3^-.

5. The preparation was stored in volumetric flasks and aged at room temperature for two weeks before further experiments.

CHAPTER 3

KINETICS AND PRODUCT OF Fe(II) OXYGENATION IN AQUEOUS SYSTEMS

3.1 Homogeneous Oxygenation

The kinetics of Fe(II) oxygenation in laboratory systems have been studied by Stumm and Lee (1961), Morgan and Birkner (1966), Schenk and Weber (1968), Theis (1972), Tamura et al. (1976a), and Liang and Kester (1977); the general rate law was found to be:

$$-\frac{d[Fe(II)]}{dt} = k[OH^-]^2 P_{O_2}[Fe(II)] \qquad (3.1)$$

where k is the homogeneous constant with units $M^{-2}atm^{-1}min^{-1}$, $[OH^-]$ denotes the concentration of hydroxyl ions and $[Fe(II)]$ denotes the concentration of total ferrous iron. At constant pH and P_{O_2} equation (3.1) reduces to a first-order equation:

$$-\frac{d[Fe(II)]}{dt} = k_1[Fe(II)] \qquad (3.2)$$

where $k_1 = k[OH^-]^2 P_{O_2}$ and has units of inverse time, equation (3.2) integrates to:

$$[Fe(II)] = [Fe(II)]_0 exp(-k_1 t) \qquad (3.3)$$

and we can define $\tau_{1/2}$ as the time when $[Fe(II)] = [Fe(II)]_0/2$

$$\tau_{1/2} = \frac{\ln 2}{k_1} \qquad\qquad (3.4)$$

Psuedo-first order kinetics with respect to ferrous iron were also observed in water treatment plants or in seawater by Ghosh et al. (1966), Larson (1967), Kester et al. (1975) and Murray and Gill (1978). Table 3.1 summarizes the values of k inferred from the reported results.

Since the rate is strongly dependent on pH, one of the major uncertainties in the numerical value for the rate constant arises from variation of pH during an experiment. Reported variations range from ±0.02 to 0.05 pH units. Figure 3.1 shows typical variation in pH during an oxygenation experiment. The initial drop in pH coincides with the addition of the stock Fe(II) solution, which is also a source of strong-acid protons. The subsequent increase in pH can be attributed to the slow, diffusion-controlled loss of aqueous CO_2 from the solution. Substantial error can be introduced if the oxygenation kinetics are studied on the same time scale of about 20 minutes. To cope with this difficulty the variation of Fe(II) was plotted arithmetically versus time and slopes were constructed to obtain instantaneous rates. These were then normalized with respect to the instantaneous $[OH^-]$, P_{O_2} and [Fe(II)] measured at that time. Rate constants obtained this way have about 20% variability (2σ) and compare well with the rate constants obtained by linear regression from first order plots.

3.1.1 Ionic Strength Effects

A series of experiments with ionic strength varying from 9×10^{-3}M to 0.11 M was initiated at 25°C. The results are summarized in Table 3.2.

Table 3.1 Summary of previous results
on Fe(II) oxygenation kinetics

INVESTIGATOR	SOLUTION CHARACTERISTICS[a]			REPORTED RATE INFORMATION	REDUCED k $(M^{-2} atm^{-1} min^{-1})$
	$T(^oC)$	$P_{O_2}(atm)$	Alk. (meq/L)		
Stumm & Lee(1961)	20.5	varies	29-39 as $NaHCO_3$		$8.0 \pm 2.5 \times 10^{13}$
Morgan & Birkner(1966)	25	0.6	32 as $NaHCO_3$	$\tau_{1/2} \simeq 47$ min at pH=6.5 $\tau_{1/2} \simeq 16$ min at pH=6.7	1.7×10^{13} 2.0×10^{13}
Schenk & Weber(1968)	25	0.21	30-50 as $NaHCO_3$		$2.1 \pm 0.5 \times 10^{13}$
Theis (1972)	25	0.5	15.8 as NaOH initially	$\tau_{1/2} = 25.4$ min at pH=6.3	1.4×10^{14}
Kester et al (1975)	?	0.21	Naragansett seawater Sargasso seawater	$\tau_{1/2} = 5.5$ min at pH=8.0 $\tau_{1/2} = 3.3$ min at pH=8.0	6.0×10^{11} [b,c] 1.0×10^{12}
Tamura et al (1976a)	25	varies	10 as $NaHCO_3$ Total ionic strength=0.11 M	0.1 M $NaClO_4$ 0.1 M $NaNO_3$ 0.1 M NaCl 0.1 M NaBr;0.1 M NaI;0.033M Na_2SO_4	1.8×10^{13} [d] 1.6×10^{13} 1.2×10^{13} 1.0×10^{13}
Murray & Gill(1978)	?	?	Puget Sound seawater	$\tau_{1/2} = 3.9$ min at pH=8.0	8.9×10^{11} [e]

a. For solutions with $NaHCO_3$ alone for alkalinity control, the ionic strength is assumed to be dominated by the bicarbonate ion. e.g. Stumm & Lee's 29-39 meq/L alk. would imply an average ionic strength of 34 mM.

b. The kinetics were followed by ferric iron absorbance in the u.v. and showed catalytic features for t>20min;

c. The reported k is obtained assuming $pK_w=14$ for seawater, not a good assumption.

d. The reported k's were reported in units $M^{-3} s^{-1}$. The Henry's law constant 0.00127M atm^{-1} was used for conversion

e. Same comment as c.

Figure 3.2 shows the variation of log k with $\sqrt{I}$. The plotting form is suggested by transition state theory, which utilizes the Debye-Huckel limiting law for the activity coefficients of the reactants and activated complex. When due regard was given to ionic strength differences, the rate constants of Morgan and Birkner (1966), Schenk and Weber (1968) and Tamura et al. (1976a) are found to be in reasonable agreement with those obtained in this study. Better agreement with the data of Tamura et al. (1976a) can be obtained if further normalization with respect to the activity coefficient of the OH^- is carried out. The result of Theis (1972) is at variance with results of this study, and no satisfactory explanation is evident. The previously observed role of alkalinity in iron oxygenation kinetics lies in its buffering capacity for acidity and also in its contribution to the ionic strength.

Tamura et al. (1976a) proposed the following reaction as the rate limiting step:

$$FeOH^+ + O_2OH^- \rightarrow Fe(OH)_2^+ + O_2^- \qquad (3.5)$$
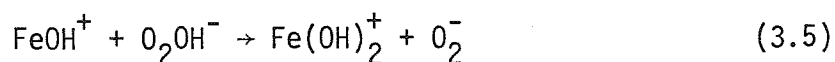
If this were true, the plot in Figure 3.2 should yield a slope of -1 (the product of the charges of the rate-limiting species). Instead, the plot shows a slope of -2. Application of Weiss's mechanism to the system was discussed by Goto et al. (1970), but Michelson et al. (1977) pointed out the lack of experimental evidence for that mechanism. In light of the difficulty of mechanistic interpretations from rate data alone, the present discussion will not dwell on mechanisms.
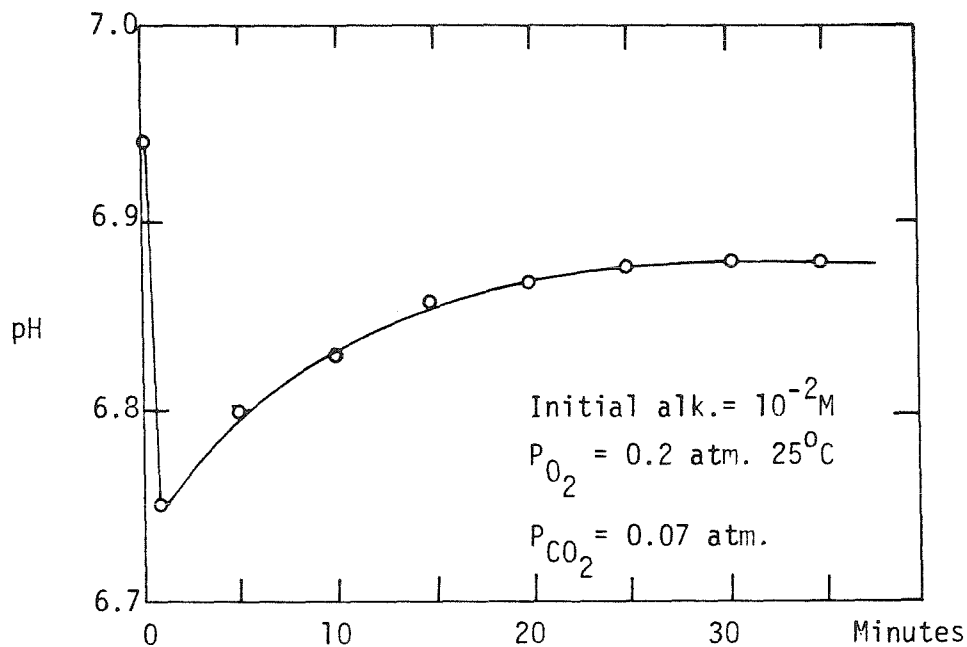
Figure 3.1 Variation of pH during an oxygenation
experiment.The initial drop in pH coincides with
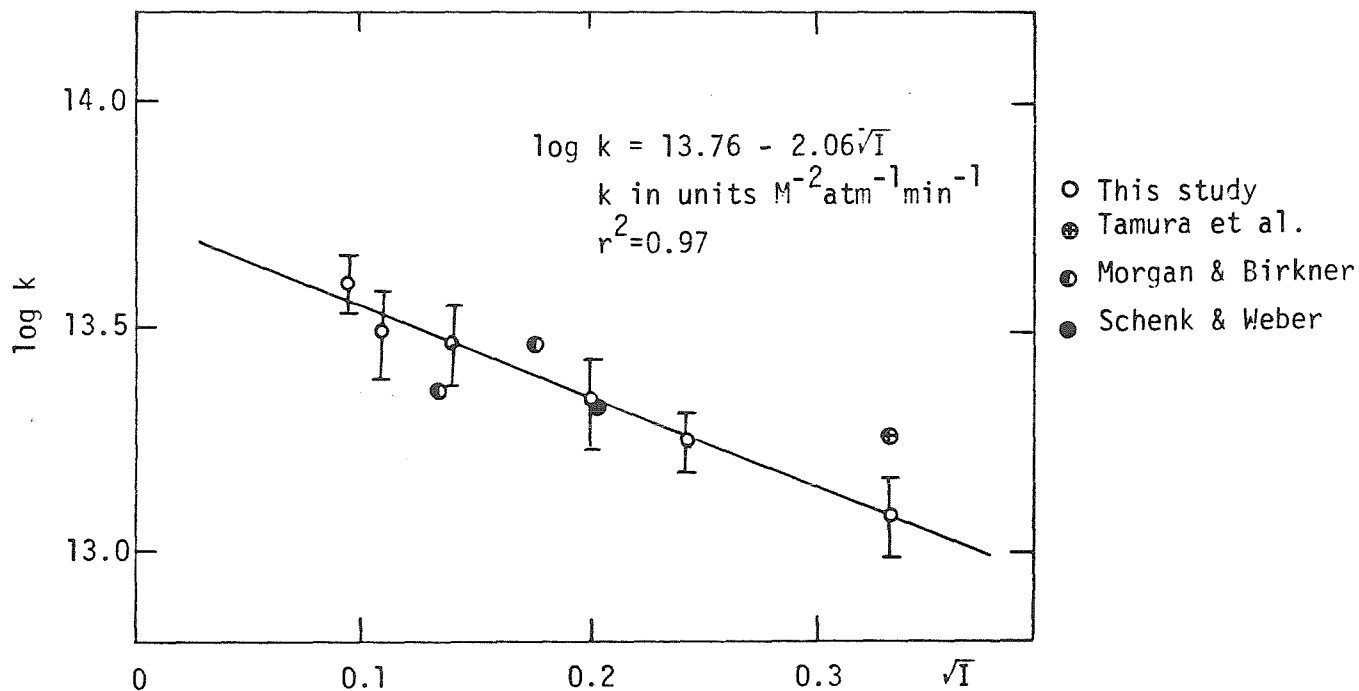the addition of stock Fe(II) solution which introduces
one milli-molar protons.

Figure 3.2 The effect of ionic strength on the rate constant
of Fe(II) oxygenation. See Table 3.2 for details.

3.1.2 Temperature Effects

Stumm and Lee (1961) reported that for a given pH, the rate increases about 10-fold for a 15°C temperature increase. A series of experiments was initiated with temperature ranging from 5° to 30°C. Figure 3.3 shows first-order plots for these experiments. The temperature effect appears to be large, $\tau_{1/2} = 316$ min at 5°C decreased to $\tau_{1/2} = 4$ min at 30°C. But when normalization with respect to changes in K_W and O_2 solubility with temperature was carried out, as in Table 3.3, the rate constant was seen to vary only slightly with temperature. When proper attention was given to ionic strength, it was found that the results of this study compare well with those of Stumm and Lee (1961). The error bars on the derived rate constant were sufficiently large to make meaningful calculations of activation energy impossible, however.

3.1.3 Anion Effects

Tamura et al. (1976a) studied the effects of anions on the oxygenation kinetics of Fe(II) and found the rate constant to decrease in the order $ClO_4^- > NO_3^- > Cl^- > Br^- = I^- = SO_4^{2-}$, at the same ionic strength. Kester et al. (1975) and Murray and Gill (1978) reported $\tau_{1/2}$ of Fe(II) in seawater to be in the range of 3-6 min. The present study confirms the order of ClO_4^-, Cl^- and SO_4^{2-}. Figure 3.4 shows first-order plots of Fe(II) oxygenation in chloride media. The rate decreases with increasing chloride concentration, but not linearly. The rate in ClO_4^- media is a factor of 3 higher than that in Cl^-, and a factor of 4 higher than that in SO_4^{2-}. Tamura et al. (1976a) suggested that this can be
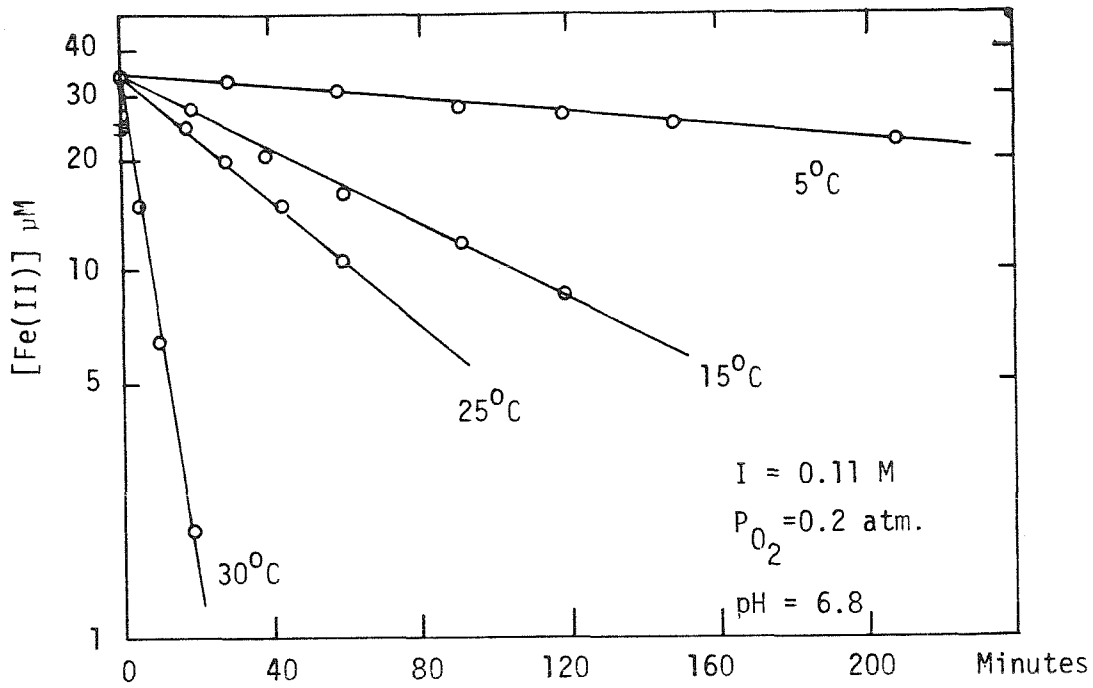
Figure 3.3 The effect of temperature on the oxygenation
kinetics of Fe(II). See Table 3.3 for details.
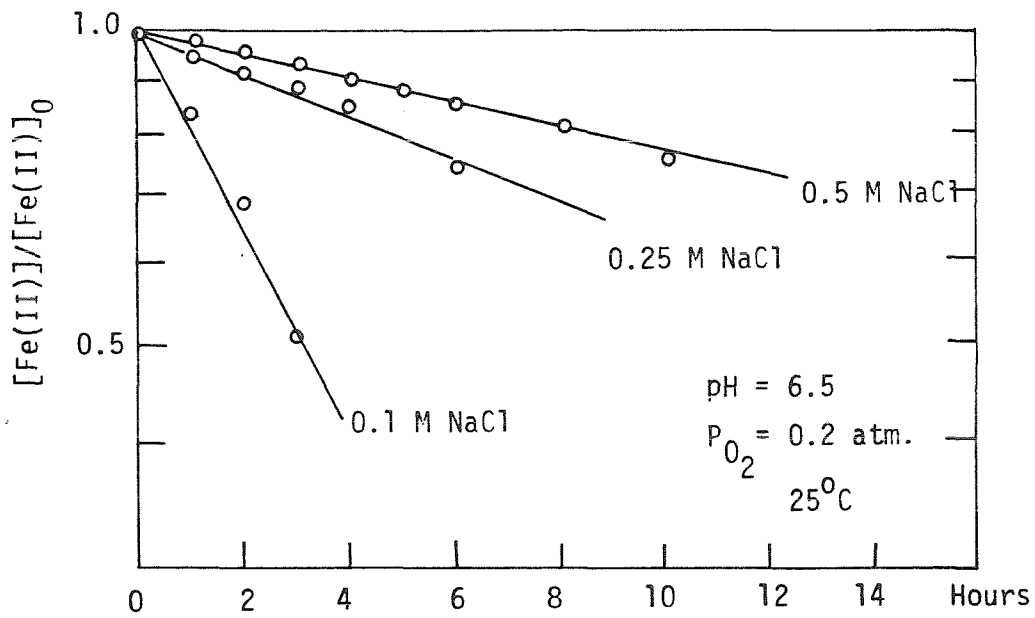
Figure 3.4 Effect of Cl⁻ anions on the oxygenation
kinetics of Fe(II).

TABLE 3.2 <u>VARIATION OF k WITH IONIC STRENGTH (adjusted by NaClO$_4$)</u>

(T = 25°C, Alk. = 9x10^{-3}M NaHCO$_3$, [Fe(II)]$_0$ = 34.7 μM,P$_{O_2}$ = 0.20 atm)

pH $\overset{\sim}{\sim}$ 6.84

Ionic Strength (M)	$\tau_{1/2}$min. (least square)	k M^{-2}atm^{-1}min^{-1}
0.009	18.0	4.0 ± 0.6 x 10^{13}
0.012	18.2	3.1 ± 0.7 x 10^{13}
0.020	18.5	2.9 ± 0.6 x 10^{13}
0.040	21.5	2.2 ± 0.5 x 10^{13}
0.060	26.8	1.8 ± 0.3 x 10^{13}
0.110	37.9	1.2 ± 0.2 x 10^{13}

TABLE 3.3 <u>VARIATION OF k WITH TEMPERATURE</u>

(Alk. = 9 x 10^{-3}M NaHCO$_3$, ionic strength = 0.11 M adjusted by

NaClO$_4$. P$_{O_2}$ = 0.20 atm [Fe(II)]$_0$ = 34.7 μM)

T(°C)	$\tau_{1/2}$(min)	pH	K$_W$ x 10^{14}	O$_2$saturation x 10^{4}M	k(M^{-3}min^{-1})
5	315.6	6.76	0.1846	3.81	2.7±0.5x10^{16}
15	63.1	6.80	0.4505	3.06	2.2±0.3x10^{16}
20.5*			0.70		
25	37.9	6.84	1.008	2.50	9.4±1.7x10^{15}
30	4.1	6.88	1.469	2.28	3.3±0.7x10^{16}

*Stumm & Lee (1961)

k = 8.0 ± 2.5 x 10^{13}M^{-2}atm^{-1}min^{-1}

k = 5.8 ± 1.8 x 10^{16}M^{-3}min^{-1} at 34 mM ionic strength

k = 2.9 ± 0.9 x 10^{16}M^{-3}min^{-1} at 0.11 M ionic strength

using the -2 slope dependence of log k on

$\sqrt{I}$

explained by the formation of a ferrous complex which has a different reactivity than that of the uncomplexed ferrous iron. A detailed quantitative check of this theory was not possible because of the lack of knowledge of the actual mechanisms. However, this work does agree with that of Liang and Kester(1977) which showed that the presence of Cl^- and SO_4^{2-} anions can effectively reduce the oxygenation rate to that of its counterpart in seawater. The reduction of the rate is due to combined effects of ionic strength (a factor of some 20 fold) and complexation.

3.2 Heterogeneous Oxygenation

Takai (1973) studied the catalytic oxidation-removal of Fe(II) by α-FeOOH and γ-FeOOH experimentally and found the latter solid to be effective. Tamura et al. (1976b) studied the effect of ferric hydroxide on the oxygenation of Fe(II) in neutral solutions and found that at constant pH and O_2 that the rate is:

$$\frac{-d[Fe(II)]}{dt} = (k_1 + k_2[Fe(III)])[Fe(II)] \qquad (3.6)$$

where k_1 is the homogeneous rate constant, with inverse time units, and k_2 is the heterogeneous rate constant, with inverse concentration and time units ($M^{-1}min^{-1}$). They also showed that:

$$k_2 = k_s[O_2]K/[H^+] \qquad (3.7)$$

where k_s is the surface rate ($4380 \ M^{-1}min^{-1}$), $[O_2]$ is the concentration of oxygen in solution, and K is the adsorption constant of Fe(II) on ferric hydroxide, whose numerical value was determined to be $10^{-9.6}$ mol mg^{-1} for amorphous ferric hydroxide (formed by hydrolyzing Fe(III) perchlorate at pH 7.0), which converts to the dimensionless value of $10^{-4.85}$. The implicit assumption is that the adsorption step is fast compared to both the homogeneous and surface oxygenation steps. K was written as $[Fe^{2+}]_{ads}[H^+]/[Fe(III)][Fe^{2+}]$, where $[Fe^{2+}]_{ads}$ denotes adsorbed ferrous iron concentration.

For a system with ferric iron initially absent, we can write the mass balance for any time:

$$[Fe(III)] + [Fe(II)] \approx [Fe(II)]_0 \qquad (3.8)$$

The mass balance is approximate since we are ignoring the adsorbed Fe(II). Substituting (3.8) into (3.6), we obtain the autocatalytic rate law:

$$\frac{-d[Fe(II)]}{dt} = \{k_1 + k_2([Fe(II)]_0 - [Fe(II)])\} \, [Fe(II)]$$

$$= (k_1 + k_2 [Fe(II)_0]) \, [Fe(II)] - k_2[Fe(II)]^2 \qquad (3.9)$$

This can be readily integrated for the condition $[Fe(II)] = [Fe(II)]_0$ at $t = 0$ to give:

$$[Fe(II)] = \frac{[Fe(II)]_0 \, (k_1 + k_2 \, [Fe(II)_0])}{k_2[Fe(II)]_0 + k_1 \, exp[(k_1 + k_2[Fe(II)]_0)t]} \qquad (3.10)$$

we can also define $\tau_{1/2}$ as the time when $[Fe(II)] = [Fe(II)]_0/2$:

$$\tau_{1/2} = \frac{\ln(2k_1 + k_2 X_0)/k_1}{k_1 + k_2[Fe(II)]_0} \qquad (3.11)$$

We note that in the case when $k_1 >> k_2[Fe(II)]_0$, Eqs. (3.10) and (3.11) readily reduce to their first-order counterparts, Eqs. (3.3) and (3.4), respectively. For $k_2[Fe(II)]_0 >> k_1$ and long times, such that k_1 exp $[(k_1 + k_2[Fe(II)]_0)t] >> k_2[Fe(II)]_0$, Eqs. (3.10) can be written as an exponentially-decaying function:

$$[Fe(II)] = [Fe(II)]_0 \frac{(k_1 + k_2[Fe(II)]_0)}{k_1} \exp[-(k_1 + k_2[Fe(II)]_0)t] \qquad (3.12)$$

Figure 3.5 shows data for oxygenation of Fe(II) in ClO_4^-, Cl^- and SO_4^{2-} media at pH 7.2. There are two ways to obtain the rate constant k_2. We can first get the homogeneous rate constant, k_1, at lower pH values and use the $[OH^-]^2$ dependence to obtain the suitable k_1 at the higher pH. Then k_2 can be adjusted until a good fit is obtained between calculated values with (3.10) and the experimental data. This approach is illustrated by Figure 3.6. Alternatively, one can utilize plots of $\log\{([Fe(II)]_0 - [Fe(II)]) + (k_1/k_2)]/[Fe(II)]\}$ vs. time, assuming in a first trial that k_1/k_2 is small and plotting $\log\{([Fe(II)]_0 - [Fe(II)])/[Fe(II)]\}$ vs. time. The straight line will have a slope of $(k_1 + k_2[Fe(II)]_0/2.303$ and an intercept of $\log(k_1/k_2[Fe(II)]_0)$. The values of k_1 and k_2 thus obtained can be substituted in a second trial and the log function plotted again
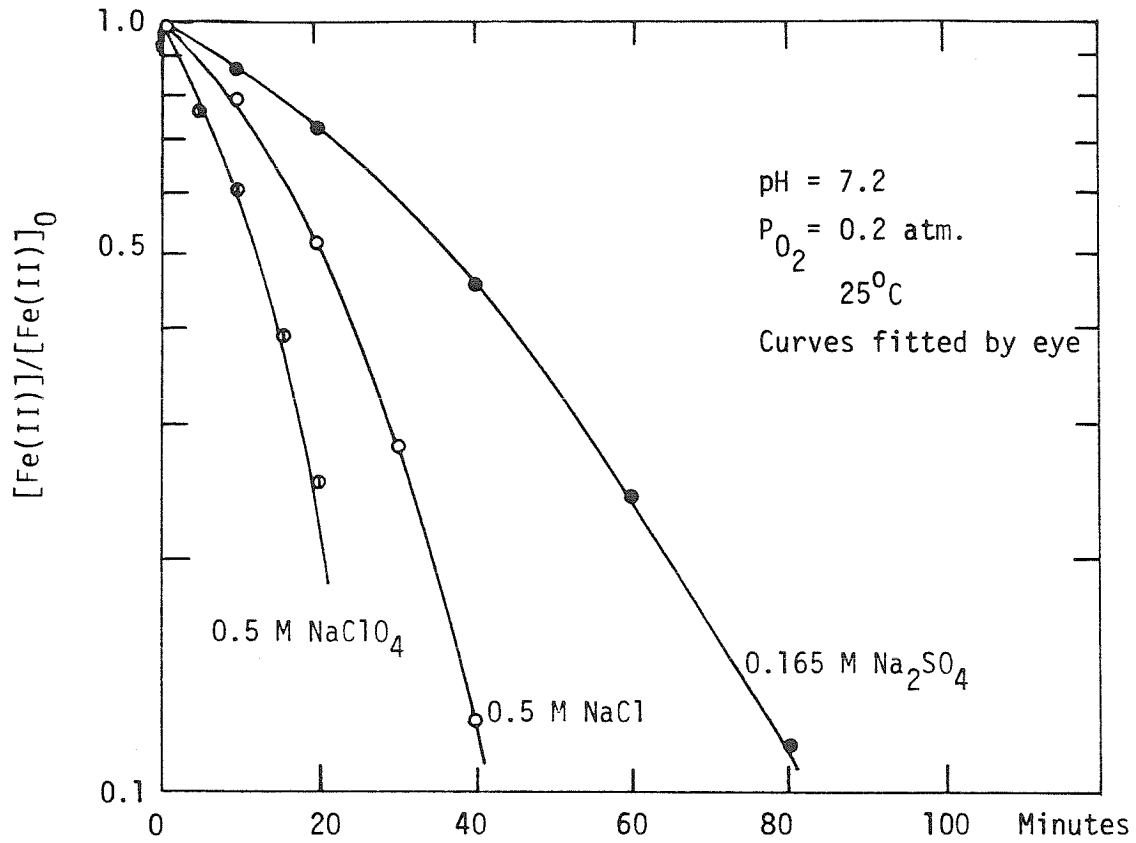
Figure 3.5 Effect of anions on Fe(II) oxygenation kinetics.
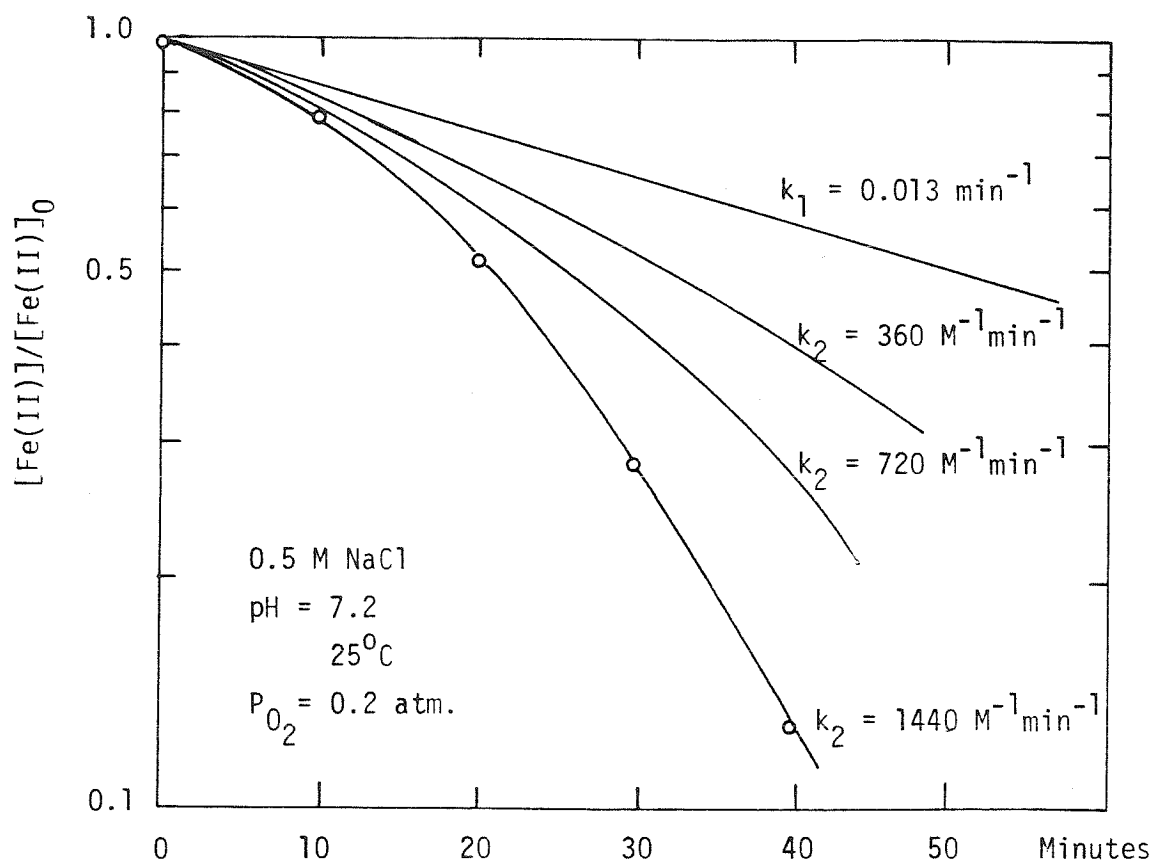
Figure 3.6 Modeling of autocatalytic oxygenation of Fe(II)
with equation (3.10) of text.
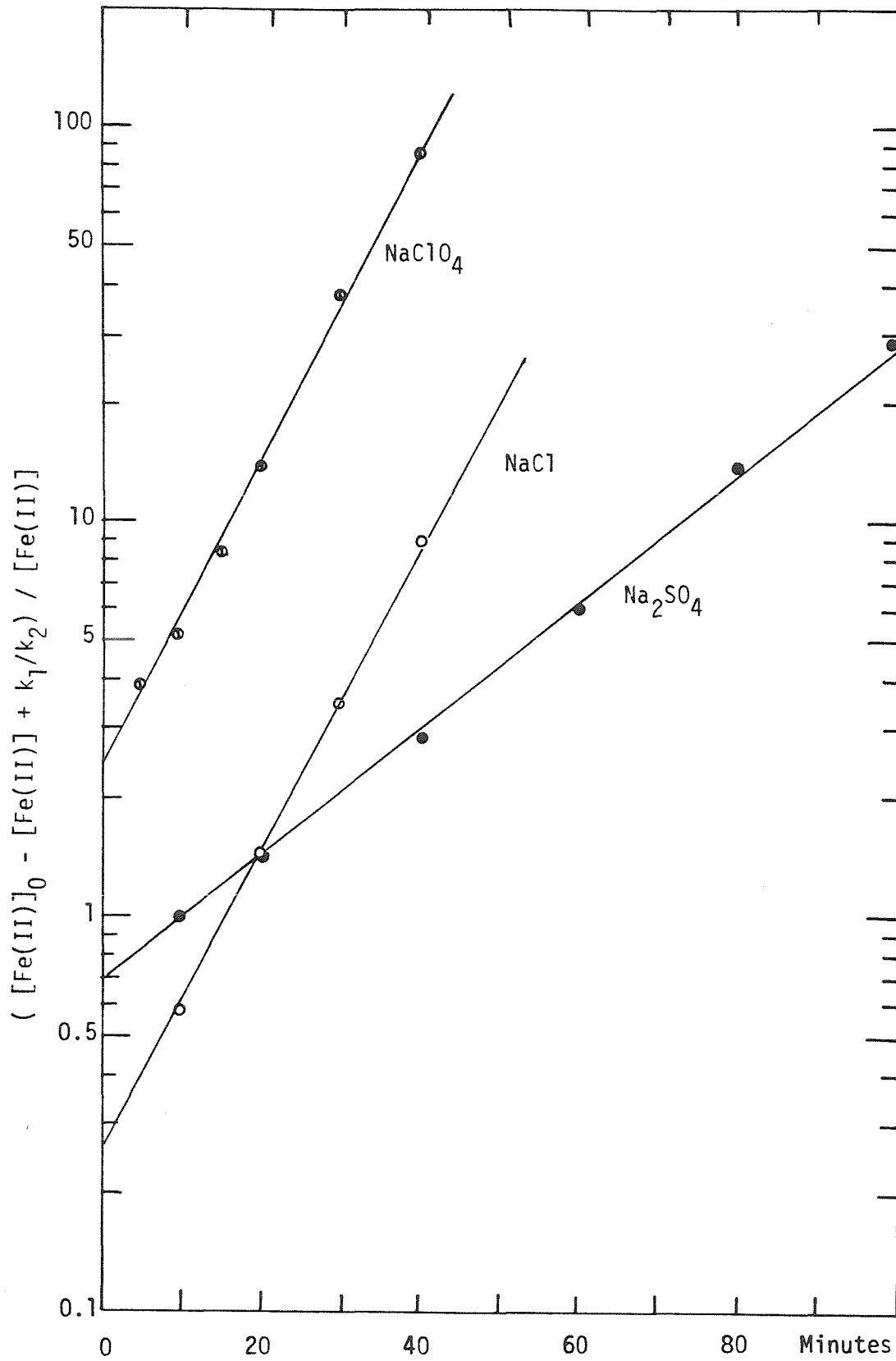
Figure 3.7 Autocatalytic plot of the data illustrated in Figure 3.5

until convergence is obtained. A consistent set of k_1 and k_2 can be obtained after about 3 trials. The procedure is illustrated in Figure 3.7, and the pertinent data summarized in Table 3.4. The agreement between the results of Tamura et al. (1966) and this study is surprisingly good, and perhaps fortuitous, since their adsorption constant was obtained for amorphous ferric hydroxide formed by hydrolysis, not by oxygenation. Following Tamura et al. (1976b) we can compare the homogeneous rate and heterogeneous rate as follows:

$$\frac{k_1}{k_2[Fe(II)]_0} = \frac{k[OH^-]^2[O_2]}{k_s[O_2]K[Fe(II)]_0/[H^+]}$$

$$= \frac{k\,K_W^2}{k_s K[H^+][Fe(II)]_0} \tag{3.13}$$

The ratio $k_1/k_2[Fe(II)]_0$ was calculated to be $9.4 \times 10^{-7}/[H^+]$ when the constants taken from Tamura et al. (1976b) were employed for $[Fe(II)]_0 = 50\ \mu M$. ($k = 2.9 \times 10^{16}\ M^{-3}min^{-1}$, $K_W = 10^{-14}\ M^2$, $k_s = 4380\ M^{-1}\ min^{-1}$, $K = 10^{-4.85}$). Therefore, $k_1/k_2[Fe(II)]_0 \approx 9.4$ at pH 7 and actually decreases with decreasing pH. But at lower pH values, the surface forms slowly and adsorption of Fe(II) is less favorable. As a result, autocatalysis is noticeable only for pH around 7. For high pH, $k_1 > k_2[Fe(II)]_0$ and we would expect pseudo-first-order kinetics again.

In our kinetic experiments we measure total ferrous iron in the system:

$$[Fe(II)] = [Fe^{2+}] + [FeOH^+] + ... + [FeCl^+] + [FeCl_2^0] + ... + [Fe^{2+}]_{ads} \tag{3.14}$$

We assume that steady state conditions apply for the complexed species,

Table 3.4 Values of k_1 and k_2

SOLUTION COMPOSITION[a]	pH	$\tau_{\frac{1}{2}}$	K_{cW} X 10^{14} [b]	k_1 (min^{-1})	k(M^{-2}atm^{-1}min^{-1})	k_2 (M^{-1}min^{-1})
0.1 M NaCl	6.50	3.108 hr	1.57	0.00372	7.5 X 10^{12}	
0.25 M NaCl	6.50	13.577 hr	1.63	0.000851	1.6 X 10^{12}	
0.50 M NaCl	6.50	22.844 hr	1.45	0.000506	1.2 X 10^{12}	
0.50 M NaCl	7.20	21 min	1.45	0.013	1.2 X 10^{12} c	1440
0.50 M NaClO$_4$	7.20	12 min	1.45	0.052	4.9 X 10^{12}	360
0.165 M Na$_2$SO$_4$	7.25	36 min	1.45[d]	0.016	1.1 X 10^{12}	360
0.70 M NaCl 2.5mM alk.	7.05	56 min	1.38	0.0079	1.6 X 10^{12}	365

a. T=25°C, alk.=5mM unless stated otherwise.

b. K_{cW}= [H$^+$][OH$^-$] calculated from (4-34) of Baes and Mesmer(1976) The concentration quotient differs significantly from that given by Harned and Owen (1958).

c. This is obtained by using the plotting form illustrated by Fig.3.7. The difference between this k and the k above,obtained at lower pH by regression,is less than 5%.

d. The actual ionization constant should be smaller because SO$_4^{2-}$would bind protons. So the actual k should be smaller.

Using(3.7) of the text and Tamura et al (1976b)'s numbers(obtained for 0.11 M NaClO$_4$) for k_s and K;[O$_2$]
= 2.2X10^{-4}M and pH=7.2 we estimate $k_2 \approx$4380M^{-1}min^{-1}X2.2X10^{-4}min^{-1}X10$^{-4.85}$/10$^{-7.2}$M = 216 M^{-1}min^{-1}.

and write:

$$[Fe(II)]=[Fe^{2+}]+K_{FeOH}[OH^-][Fe^{2+}]+\ldots+K_{FeCl}[Cl^-][Fe^{2+}]+\ldots+\frac{K[Fe(III)]}{[H^+]}[Fe^{2+}]$$

$$= [Fe^{2+}]\left\{1+K_{FeOH}[OH^-]+\ldots+K_{FeCl}[Cl^-]+\ldots+\frac{K[Fe(III)]}{[H^+]}\right\} \qquad (3.15)$$

We have neglected other complexed species because of the unavailability of equilibrium constants or because we assumed that their concentrations are small. Equilibrium constants were chosen from the compiled REDEQL data set at Caltech or from Baes and Mesmer (1976). $K_{FeCl} = 10^{-0.9}$ $K_{FeOH^+} = 10^{4.5}$. Therefore at pH 7, $[Cl^-] = 0.5$ M $>> [Fe(II)]_0 = 50$ μM,

$$[Fe(II)] = [Fe^{2+}] \{1 + 0.0032 + 0.063 + 0.00706\}$$

$$= 1.073[Fe^{2+}] \qquad (3.16)$$

This is a conservative estimate since we have not corrected the constants with respect to ionic strength. Even so, $[Fe^{2+}]_0$ is 93% of [Fe(II)], $[FeOH^+]$ is less than 0.30% of Fe(II), only 6% of the [Fe(II)] is complexed as $FeCl^+$ and $Fe(II)_{ads}$ is less than 1% of the total Fe(II), so the mass balance assumed in (3.8) is justified.

3.3 Product Identification

Initial attempts to obtain X-ray diffraction patterns for the oxygenation products were unsuccessful. They proved amorphous to X-rays.

Misawa et al. (1974) claimed that γ-FeOOH was formed in the case of rapid aerial oxidation of ferrous iron, and that Fe(II)-Fe(III) green intermediates formed in neutral and slightly acidic solutions. Upon comparing the infrared spectra of the oxygenation products shown in Figure 3.8 with the infrared spectra of the standard ferric oxyhydroxides in Figure 3.9, it was readily apparent that the oxygenation products had an infrared spectra closest to that of γ-FeOOH. Some of the oxygenation products gave recognizable X-ray patterns (tabulated in Table 3.5) confirming that γ-FeOOH is indeed the product.

Figure 3.10 shows the spectra of some products formed by hydrolyzing ferric salts. Amorphous ferric hydroxide is formed at slightly alkaline pH values, even when Cl^- is present at 0.7 M concentration. Apparently, the formation of β-FeOOH is an aging process that requires a time scale much longer than hours at such pH values. The hydrolyzed ferric oxide at pH values close to 12 exhibits goethite peaks, although X-ray diffraction shows it to be amorphous. Figure 3.11 shows the spectra of an amorphous ferric hydroxide sample aged at 0.7 M NaCl and pH 9 for one year; α-FeOOH peaks were observed. It is of interest to note that, although it is known that anions are important in determining the nature of the product in ferric salt hydrolysis, in oxygenation experiments it is γ-FeOOH that invariably forms first, whether in ClO_4^-, Cl^-, or SO_4^{2-} media. Figure 3.12 shows the spectra of a γ-FeOOH sample prepared by procedure A (outlined in Chapter 2) aged in 0.7 M NaCl and pH 9 for one year. It remained essentially the same. Although free energy calculations would indicate that γ-FeOOH is unstable with respect to α-FeOOH,
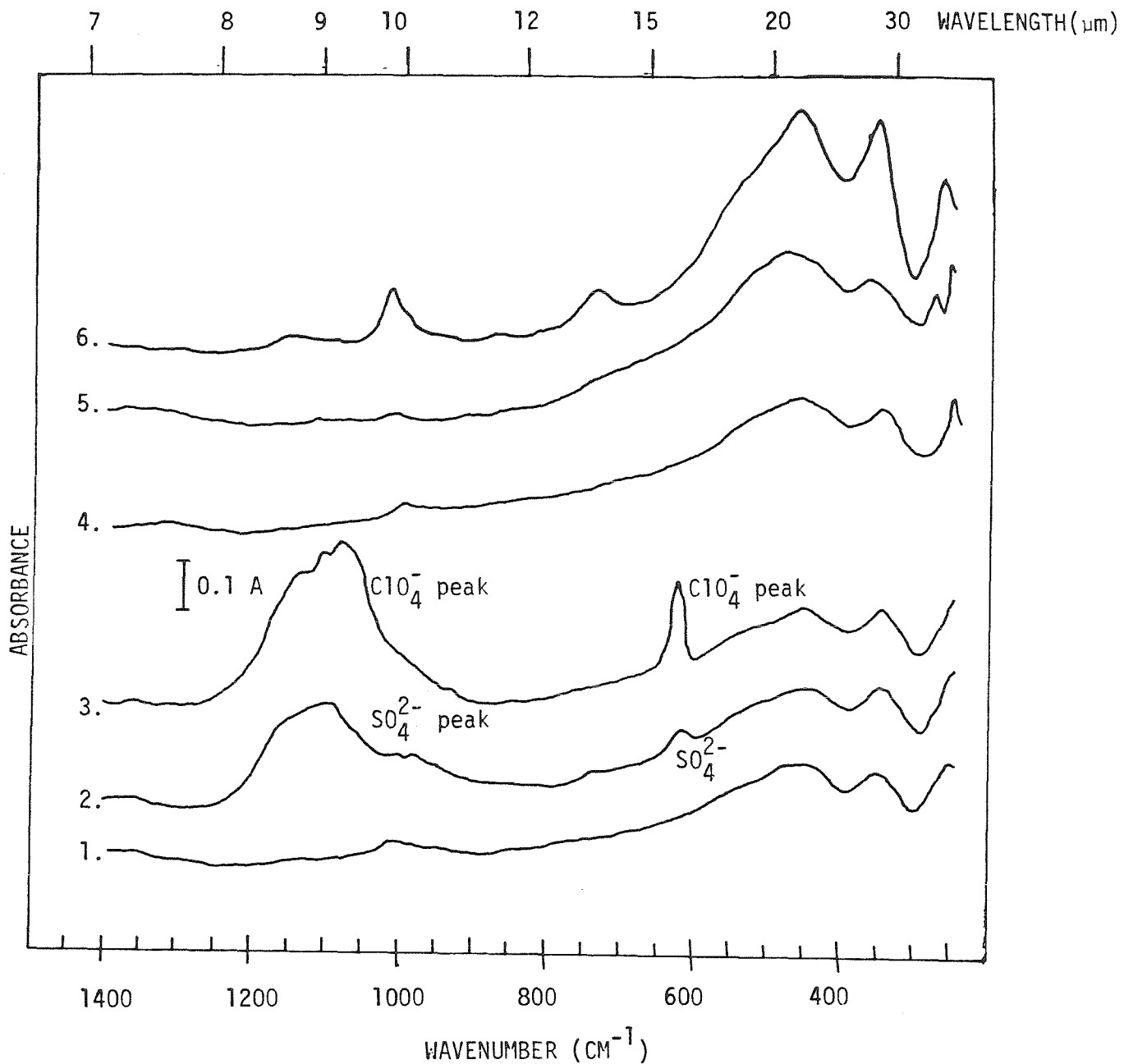
Figure 3.8 Infrared spectra of Fe(II) oxygenation product.

All spectra except 6. are run with one-mg sample in 200 mg KBr

(1)0.5 M NaCl,pH 7.2,$[Fe(II)]_0$ = 50μM. HCO_3^- buffer

(2)0.165 M Na_2SO_4,other conditions as above.

(3)0.5 M $NaClO_4$,other conditions as above.

(4)0.7 M NaCl,pH 8.3,$[Fe(II)]_0$= 10^{-3}M,HCO_3^- buffer.

(5)0.1 M $NaClO_4$,pH 9.0,$[Fe(II)]_0$= 10^{-3}M,NH_3/NH_4^+ buffer.

(6)0.6 mg of standard γ- FeOOH in 200 mg KBr.

WAVELENGTH (MICRONS)
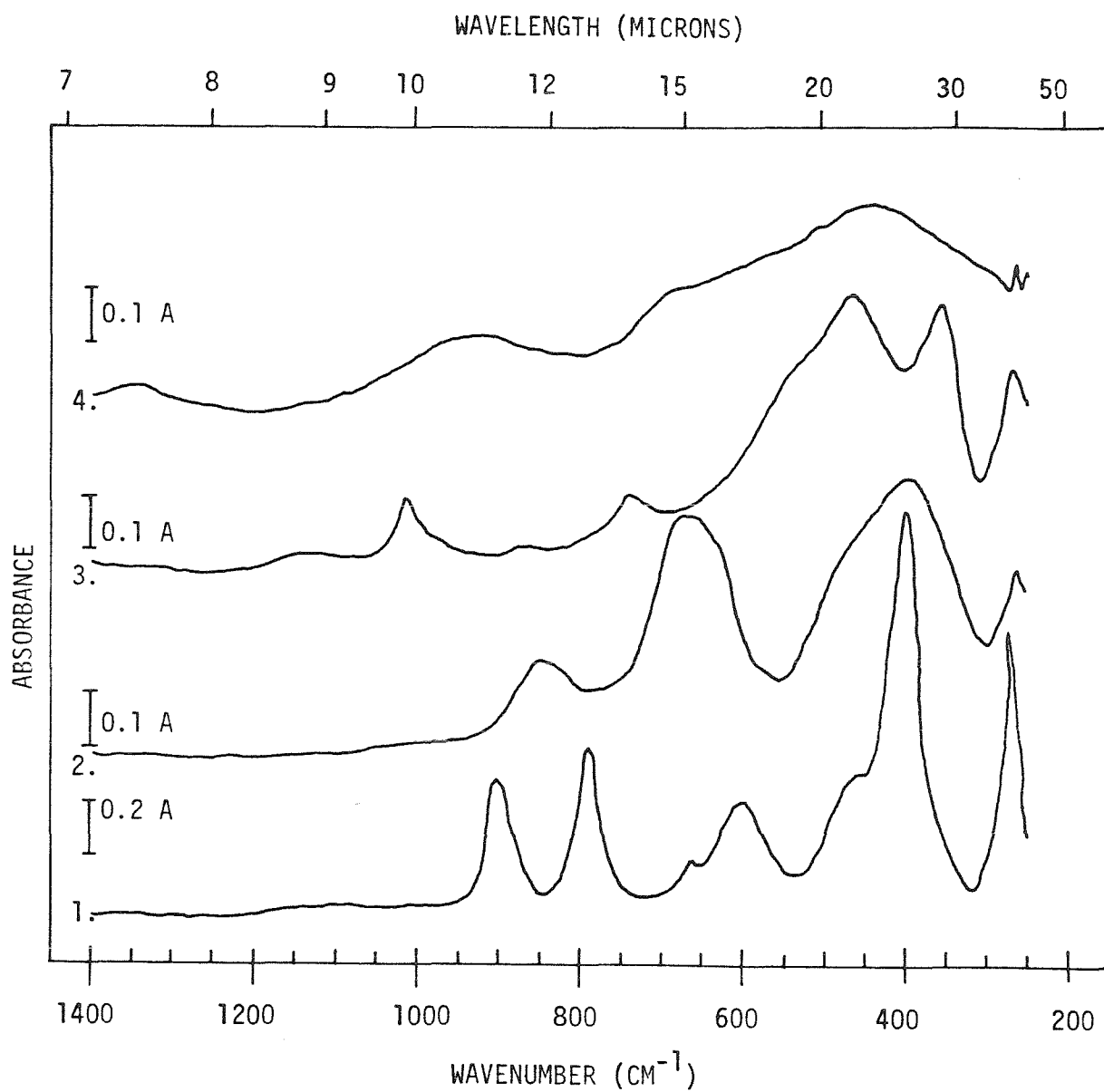
Figure 3.9 Infrared spectra of standard ferric oxyhydroxides. See Appendix C
for synthetic prosedure and characteristic peaks.

(1) α- FeOOH from Dr.G.R.Rossman. 0.8 mg in 200 mg KBr.

(2) β- FeOOH,synthetic. One-mg in 200 mg KBr.

(3) γ- FeOOH,synthetic. 0.6 mg in 200 mg KBr.

(4)   amorphous FeOOH,synthetic. One-mg in 200 mg KBr.
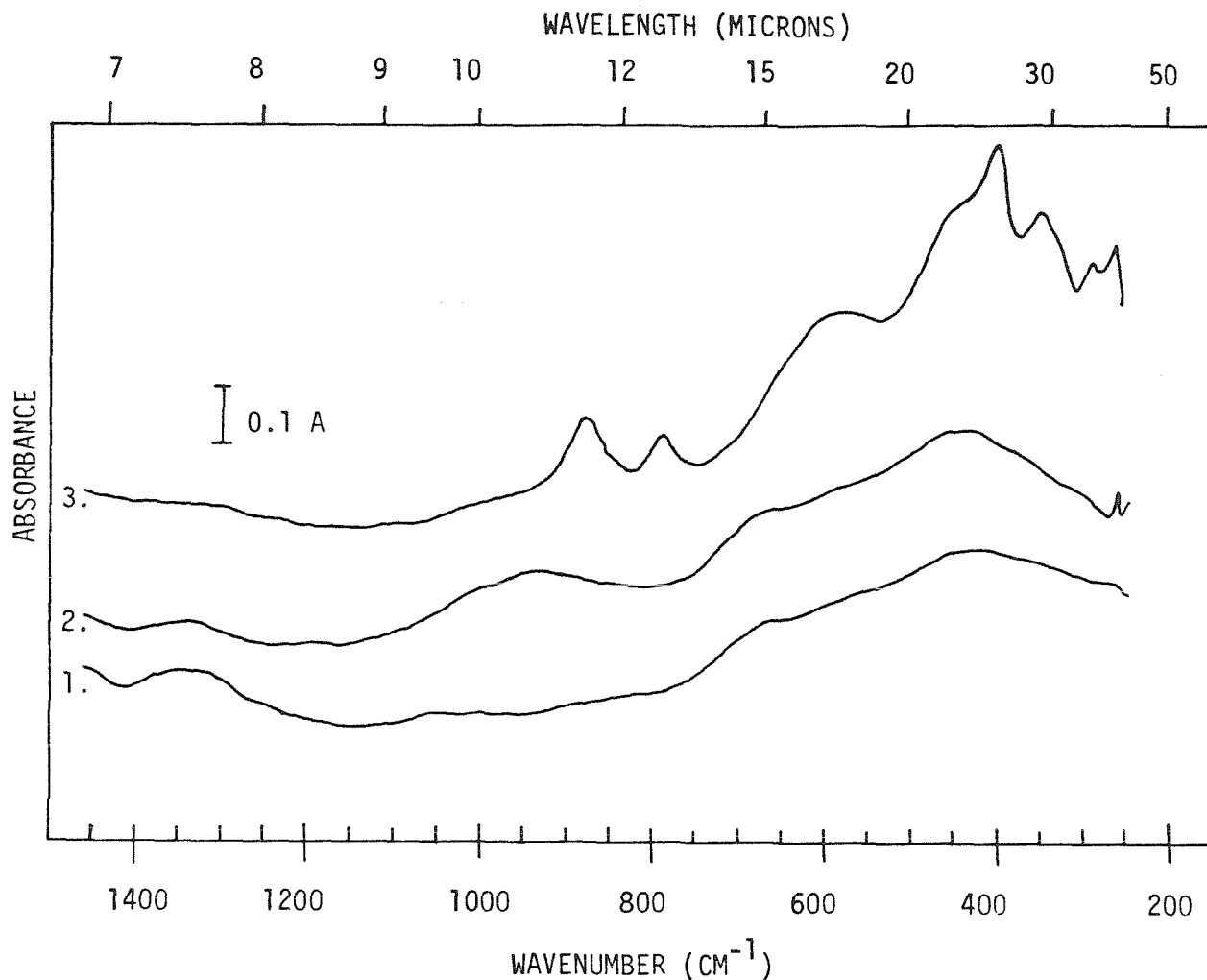
Figure 3.10 Infrared spectra of some ferric iron hydrolysis products.
All spectra run with one-mg sample in 200 mg.KBr.

(1) 10^{-3}M $Fe(ClO_4)_3$ in 0.7 M NaCl,pH = 8.3 with HCO_3^- buffer.

(2) $Fe(NO_3)_3$ in 0.1 M $NaNO_3$,pH = 8 by addition of CO_3^{2-} free NaOH. Obtained from K.Hayes,Stanford University,Dept.Civil engineering. 1978

(3) $FeCl_3$ in 0.01 M NaOH. From D.Wilson,formerly with Army corp. of engineers,Waterways Experimental Station,Vicksburg,Miss.
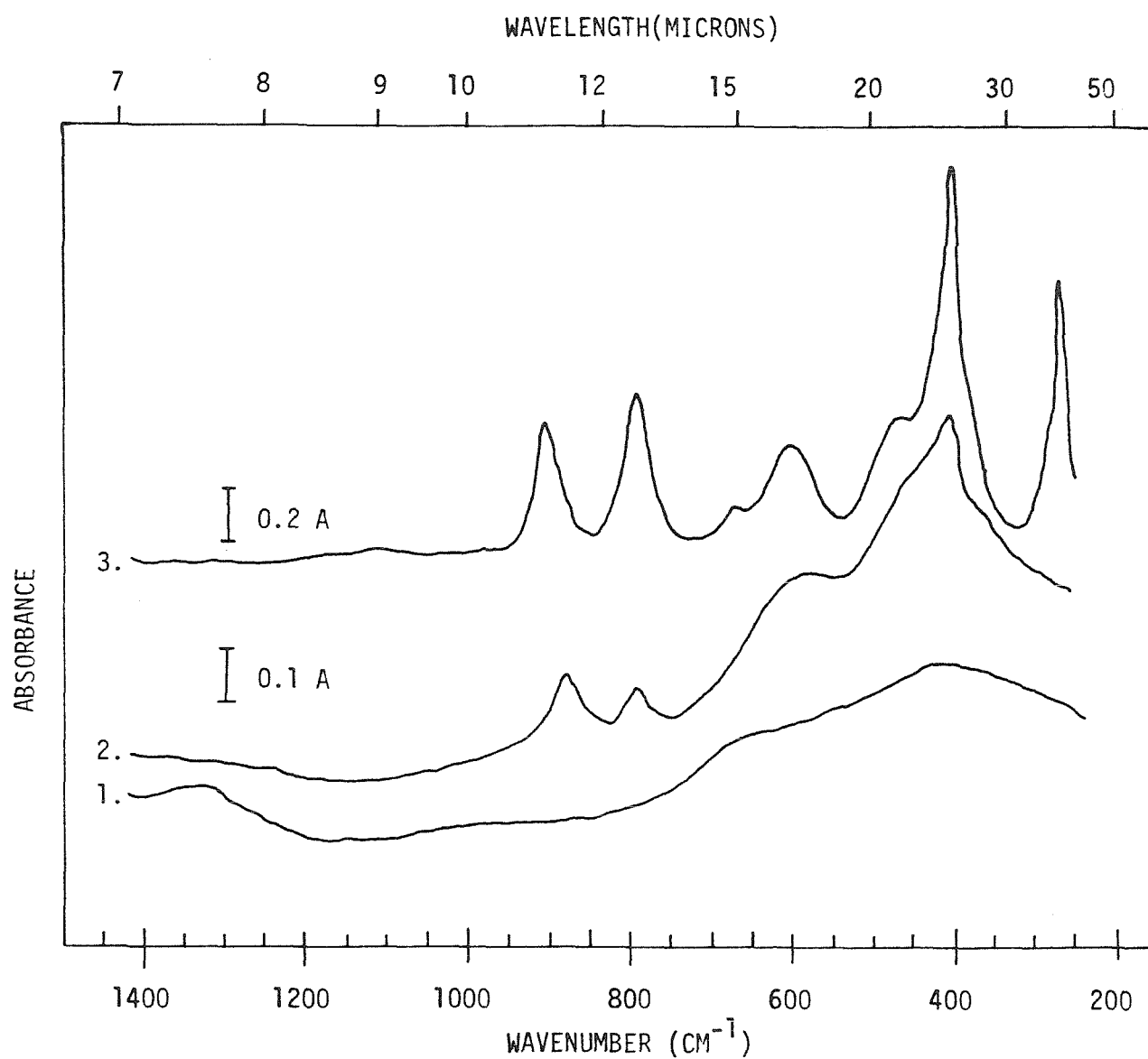
Figure 3.11 Aging of amorphous FeOOH studied by infrared spectroscopy.

(1) amorphous FeOOH synthesized by procedure in Appendix C.
0.97 mg in 200 mg KBr.

(2) same sample from (1) aged for one-year in 0.7M NaCl-
5 mM $NaHCO_3$. 1.07 mg in 200 mg KBr.

(3) spectra of standard α- FeOOH. 0.8 mg in 200 mg KBr.
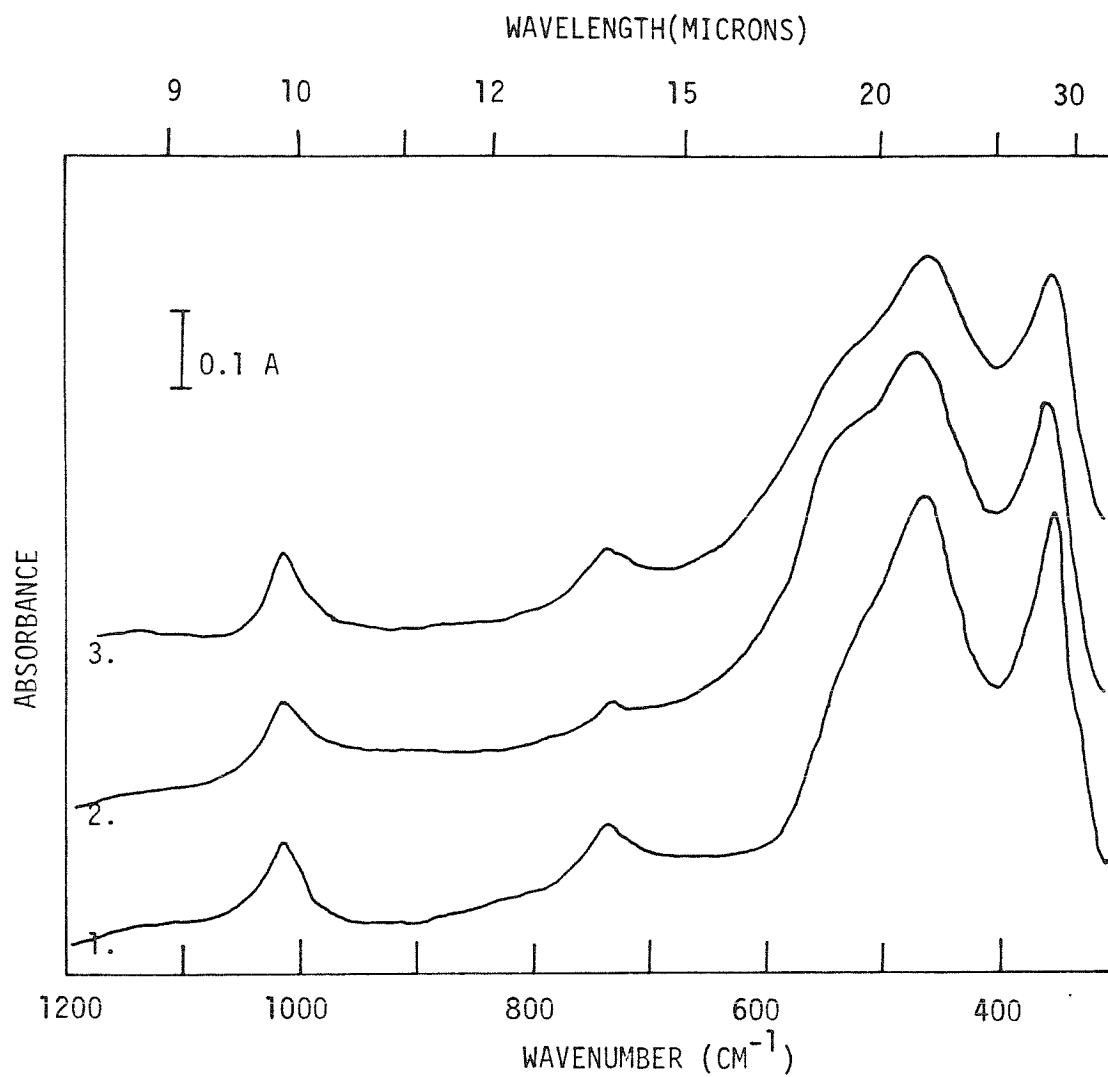
Figure 3.12 Infrared spectra of aged γ- FeOOH

(1) γ-FeOOH synthesized by procedure A in Chapter 2
0.6 mg in 200 mg KBr.

(2) same sample from (1) aged for one-year in 0.7 M NaCl-
5 mM NaHCO$_3$. 0.63 mg in 200 mg KBr.

(3) spectra of standard γ-FeOOH. 0.6 mg in 200 mg KBr.

Table 3.5 X-ray diffraction pattern of
Fe(II) oxygenation product

d ($\overset{o}{A}$)	Intensity	d ($\overset{o}{A}$)[a]	Intensity (I/I_o)
6.36	s,broad	6.26	100
3.27	s	3.29	90
2.821	ms,sharp		
2.479	broad	2.47	80
2.380	ww		
1.996	m,sharp		
1.9385	s	1.937	70
		1.732	40
1.5297	w,broad	1.524	40
		1.367	30
		1.075	40

a.Taken from ASTM card file 8-98 for lepidocrocite

we are apparently seeing slow kinetics of transformation or particle
size effects on the apparent solubility. See Table C.1 in the
appendix.

3.4 Implications for Natural Systems

The results of this study   have implications for understanding
the short-term dynamics of iron transformations in freshwater and marine
systems. It is suggested that the influences of ionic strength and
complexation in retarding oxygenation-removal helps to explain reported
differences in behavior for freshwater, estuarine and marine waters.
The relative ease of Fe(II) oxygenation indicates that amounts of true
dissolved ferrous iron would be extremely small in natural waters.
Boyle et al. (1977) reported strong evidence that the river-borne
"dissolved" iron consists almost entirely of mixed iron oxide-organic
matter colloids, of diameter less than 0.45 μm and stabilized by the
dissolved organic matter. Large-scale, rapid removal of iron from river
water occurring during estuarine mixing is interpreted as a flocculation
process whereby seawater cations neutralize the negatively charge iron-
bearing colloids. On the other hand, Fe(II) oxygenation half-time on
the order of minutes, rather than seconds, for marine waters may help
to provide an explanation for biological availabilities of Fe(II) and
Fe(III) in surface waters containing both reducing agents and dissolved
oxygen.

CHAPTER 4

SURFACE CHEMICAL PROPERTIES OF γ-FeOOH

In the preceding chapter we described the identification of the oxygenation product of Fe(II) to be γ-FeOOH, lepidocrocite. The surface thus formed was shown to have a catalytic effect on Fe(II) oxygenation kinetics. It will be shown in Chapter 5 that the same surface also catalyses Mn(II) oxygenation kinetics. This chapter summarizes the chemical properties of the γ-FeOOH surface relevant to this study.

4.1 Particle Size Distribution and Surface Area

A suspension of γ-FeOOH prepared by procedure A (outlined in Chapter 2) was analysed by Hunt (1980) with a modified Coulter counter. The Coulter counter measures voltage pulses caused by changes in resistance with the passage of particles carried by a suspending electrolyte through a small orifice. The resistance change is proportional to the particle volume, theoretically. The instrument is calibrated with known size distributions (e.g. latex spheres). Figure 4.1 shows the differential area distribution of the γ-FeOOH suspension. The area distribution was derived from the particle size distribution, and has a very sharp peak near 2 μm and the cumulative specific area was determined to be 3.3 m^2/g. This result is subject to shape factor corrections, since the distribution is based on the assumption that the particles are spheres. Kaneko et al. (1975) reported that γ-FeOOH prepared by oxidizing Fe(II) gave very thin rectangular plates and their surface area as measured by the adsorption of nitrogen was 100 m^2/g. Samples prepared by procedure A gave an
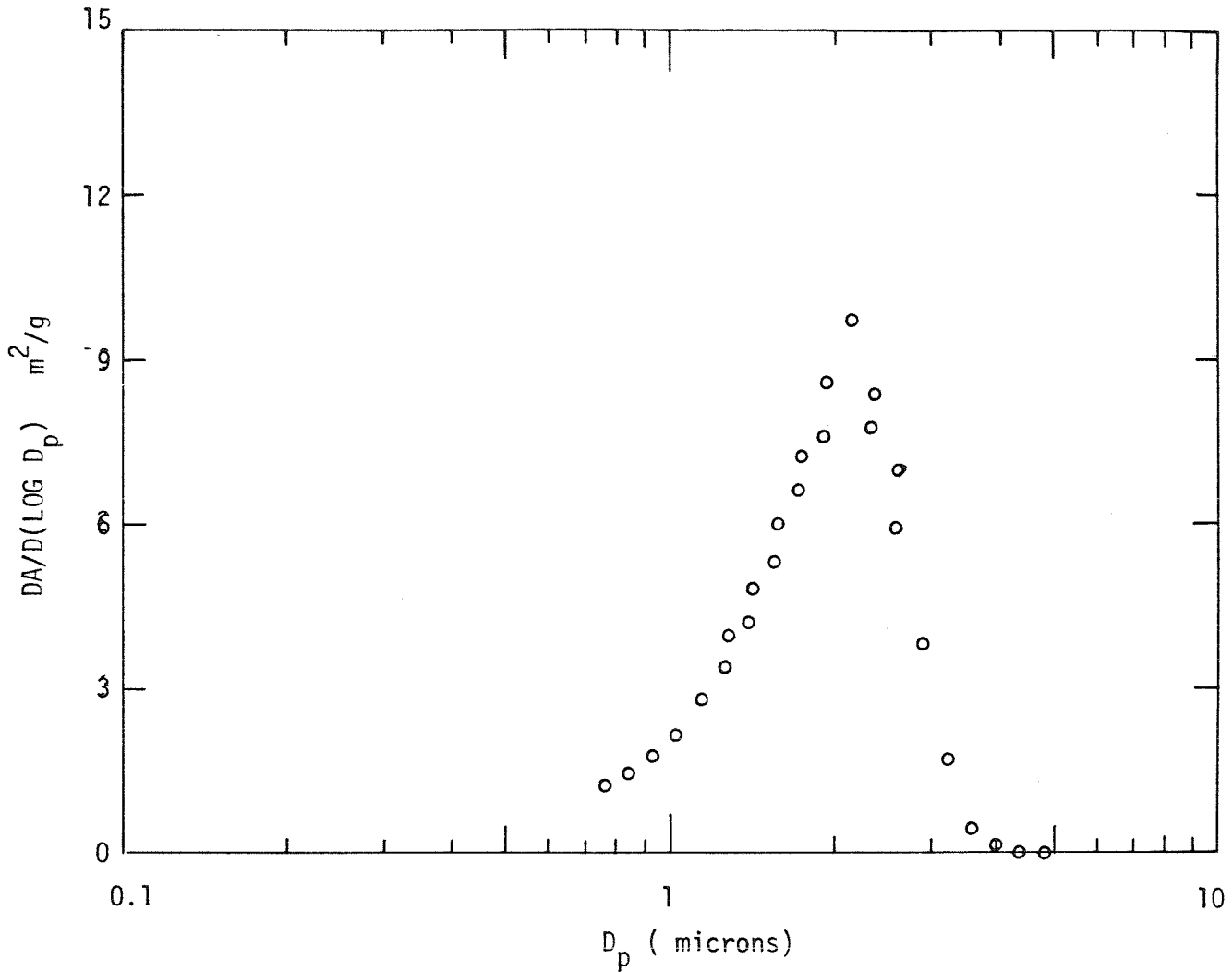
Figure 4.1 Differential Area Distribution of γ- FeOOH determined
by Hunt(1980)

average surface area of 171 m^2/g, determined by J. B. Earnest with the BET (Braunauer, Emmett, Teller) at JPL. This implies that we were either seeing strongly held aggregates of particles in the Coulter counter or that the particles were very porous, or both.

4.2 Surface Charge Distribution by Acid Titration

Solid oxides in aqueous solutions develop surface charge by the adsorption and desorption of potential-determining ions. Parks and de Bruyn (1962) first demonstrated that H^+ and OH^- are potential-determining ions for ferric oxides in aqueous suspensions.

Potentiometric titrations have been applied to study the surface charge of ferric oxides in aqueous suspensions. Operationally, the procedure measures the amount of acid or base consumed by the solid surface through the difference between the titration curves of the solid suspension and a blank solution. Balistrieri and Murray (1979) reported a titration study of the α-FeOOH, goethite surface; Murray (1978) has reported on the surface titration of β-FeOOH, akaganeite.

4.2.1 Titration Procedure

1. Suspensions prepared by procedures A and B were acidified to pH 4 to convert the remaining HCO_3^- to aqueous CO_2. The aqueous CO_2 was removed by N_2 bubbling. The pH was measured.

2. Known amounts of 0.1 N NaOH were added to raise the pH above 10 and deprotonate the surface. Onoda and de Bruyn (1966) have shown that, within these pH ranges, the solubility of ferric oxyhydroxide

was not significant to affect the proton balance.

3. The suspension was titrated with acid (0.1 N HCl, 0.6 M NaCl) from a volumetric buret. The titrant is of the same ionic strength as the suspension, 0.7 M Cl⁻ and so the ionic strength remains constant throughout the titration.

4. The pH was monitored by the glass-reference electrode cell potential as discussed in Appendix B.

Since we are ignoring the solubility of the ferric oxyhydroxide we can define the surface coverage as:

$$\Gamma = \Gamma_{H^+} - \Gamma_{OH^-} = C_B - C_A + [H^+] - [OH^-] \qquad (4.1)$$

where Γ is the surface excess of protons written in terms of M units. C_B is the concentration of strong base added, C_A is the concentration of strong acid added. $[H^+]$ is known from the pH measurement and $[OH^-]$ is calculated from a knowledge of ^cK_w.

Onoda and de Bruyn (1966) reported a kinetic study of proton adsorption at the α-Fe_2O_3, hematite/solution interface. They distinguished between a rapid step of adsorption (on the order of 2 min) and a slow diffusion step (on the order of 5 to 10 days). The interpretation that α-Fe_2O_3 in solution formed a goethite-like layer was proposed, the slow step being the diffusion of protons into or out of this interface. In the present study the glass-reference electrode cell potential reached stable values in about 30 sec, in the pH range 10.5 to 9.0; longer times, on the order of hours, were needed for pH stabilization as the titration

curve approaches the pH range 8-4. This was attributed to the unbuffered nature of these solutions, where potential drift could be expected.

4.2.2 Results on Surface Titration

Figure 4.2 shows results of a typical titration for a surface prepared by procedure A. Figure 4.3 shows a surface charge versus pH plot obtained using equation (4.1). The plot is fairly linear over a wide pH range (9.5 to 6). Such behavior has been observed in studies of oxides in high ionic strength solutions by other investigators, e.g., Breeuwsma (1973) for α-Fe_2O_3 in 1.0 M KCl, Yates (1975) for TiO_2, rutile in 0.1 M $NaClO_4$, and Balistrieri and Murray (1979) for goethite in 0.7 M NaCl. The surface charge vs. pH for γ-FeOOH in 0.7 M NaCl in this study can be represented by the equation:

$$\Gamma = -58.6(pH - 6.77) \text{ in units of } \mu M$$

$$= -659 \ (pH - 6.77) \text{ in units of } \mu moles/g \qquad (4.2)$$

Equation (4.2) is valid for the pH range 9.5 to 6 only.

Total surface sites of the γ-FeOOH prepared by procedures A and B were determined to be 2.6 moles/Kg and 2.3 moles/Kg, respectively. Using a specific surface area of 171 m^2/g, the corresponding number of surface sites per unit area were computed to be 9.2 and 8.1 OH groups/nm^2. These values compare well with the theoretical values of surface density calculated by Jones and Hockey (1971) for TiO_2, 6.1 to 12.2 OH groups/nm^2. The site density for γ-FeOOH observed here also compares well with the result of 8.4 OH groups/nm^2 for γ-FeOOH reported by Kaneko et
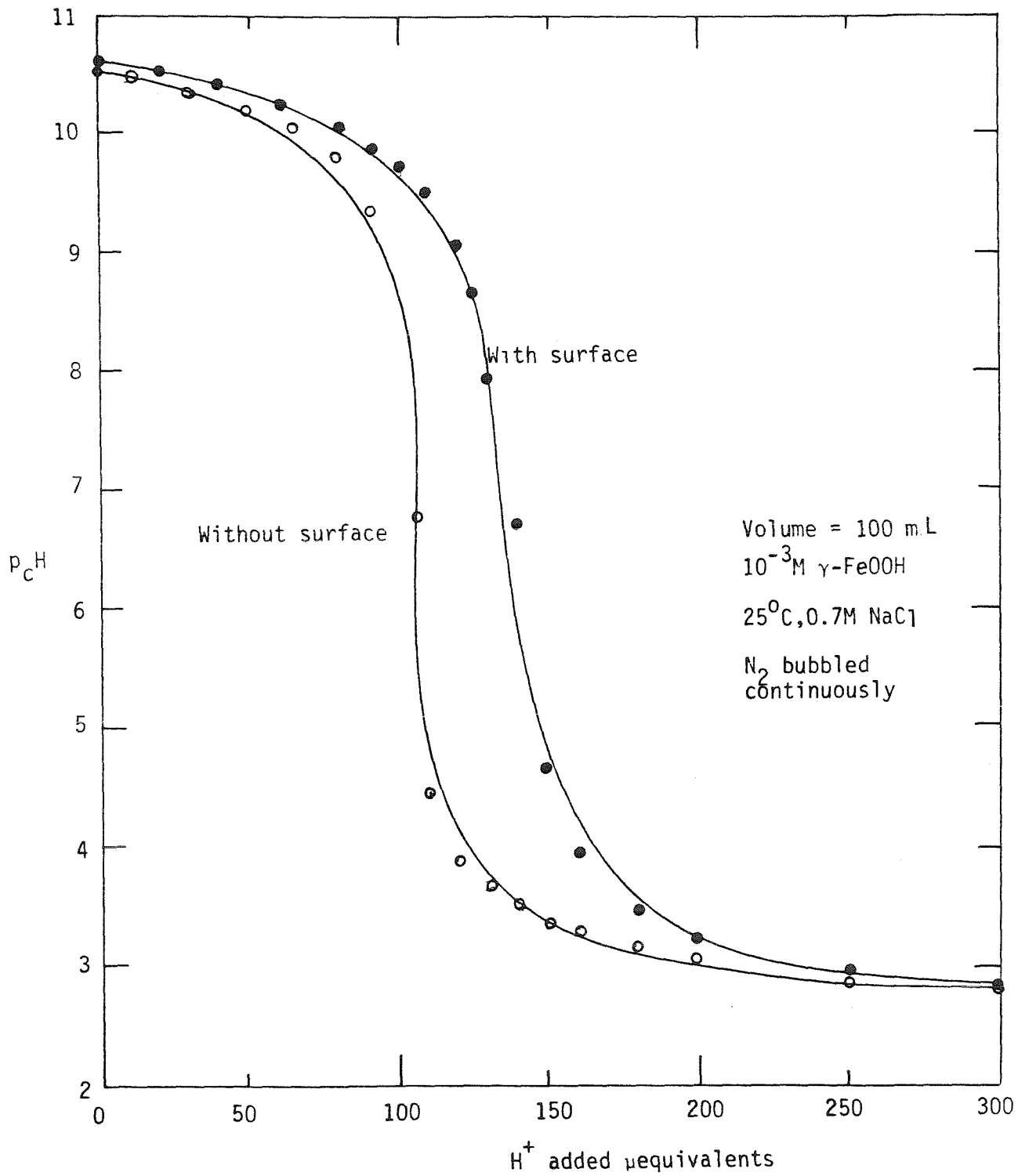
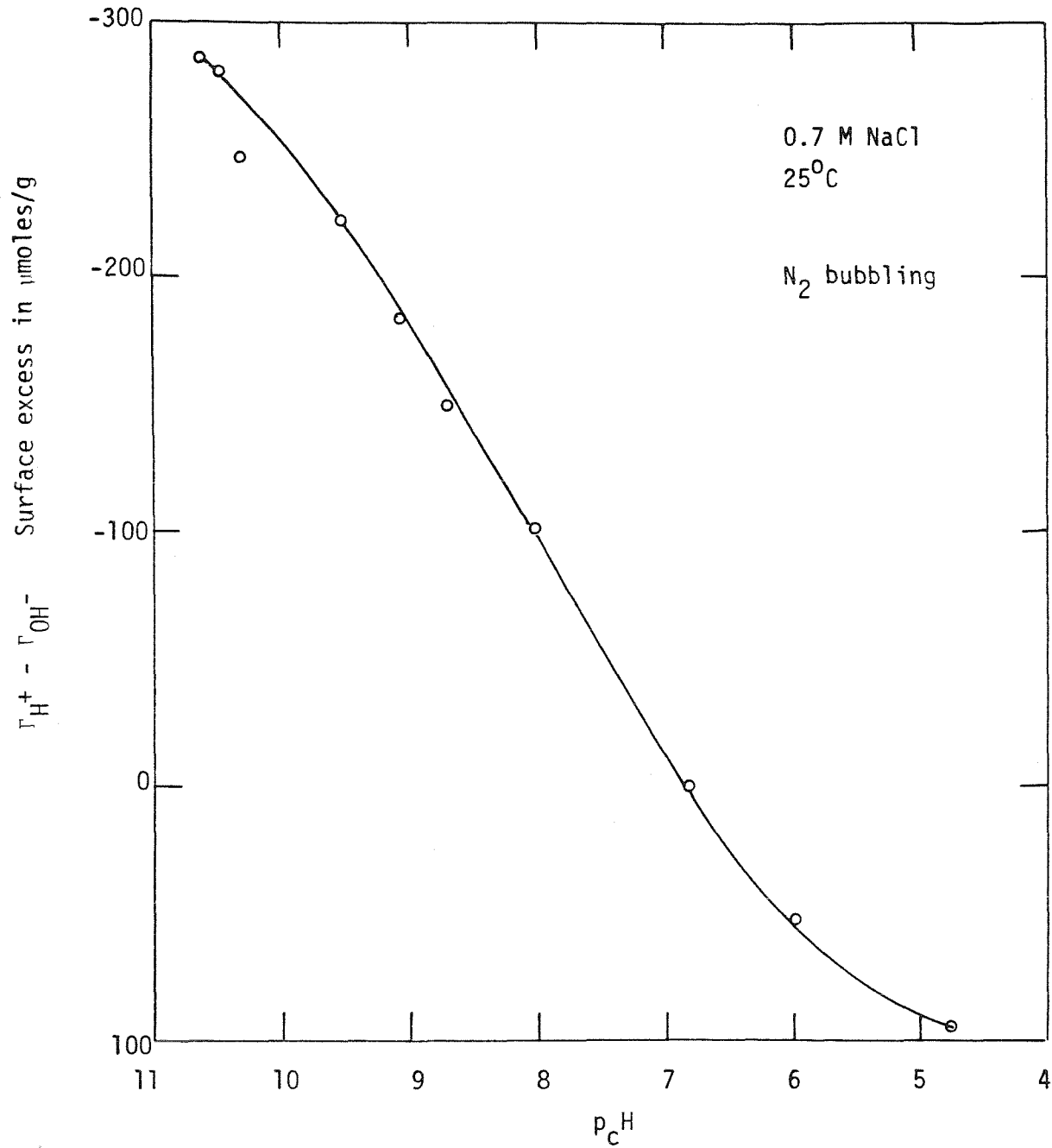Figure 4.2 Titration curve in the presence and absence of γ-FeOOH

Figure 4.3 Surface charge characteristics of γ-FeOOH as
determined by acid/base titration

al. (1975). That result was obtained from calculations based on an experimental study of the dielectric behavior of adsorbed water molecules on ferric oxyhydroxide.

The surface charge density σ, can be calculated from equation (4.2) by means of the specific surface area, A, and the Faraday constant, $F = 96500$ coulombs mole^{-1}:

$$\sigma = \frac{\Gamma}{FA} = -0.37 \frac{coulombs}{m^2} (pH - 6.77) \tag{4.3}$$

These results compare favorably with those obtained by Onoda and de Bruyn (1966) for equilibrium isotherms (5 to 10 days equilibrium time) of the α-Fe$_2$O$_3$/NaNO$_3$ solution interface.

Westall and Hohl (1980) have described five models involving different descriptions of the electrical double layer and showed that they could all represent the available data on proton excess or deficiency equally well. The simple Gouy-Chapman theory of a single flat double layer (a physical description), has been described in detail by Stumm and Morgan (1970). If pH is not greatly different from pH$_{zpc}$, the pH value where the surface has zero charge, they showed that the surface charge is approximately linearly dependent upon pH. For a temperature of 25°C, the simple double-layer theory gives:

$$\sigma = -\left(\frac{\varepsilon\kappa}{4\pi}\right) 0.05915 (pH - pH_{zpc}) \tag{4.4}$$

where ε is the dielectric constant = 89×10^{-12} coulomb volt^{-1} cm^{-1};

κ is the reciprocal double layer thickness in cm^{-1}. For water at $25^{o}C$:

$$\kappa^{-1} = 3.0 X 10^{-8} I^{-0.5} \tag{4.5}$$

where I is the total ionic strength. For a 0.7 M NaCl solution, κ^{-1} is about $3.6 X 10^{-8} cm$. Equation (4.4) predicts the numerical slope of a surface charge versus pH plot to be $-(\epsilon\kappa/4\pi)0.05915$ or $-11.6\mu coulombs/cm^2$. Our experimental slope was $-37\mu coulombs/cm^2$, a factor of 3.2 higher. We can fit our data to the Guoy-Chapman double layer theory by adjusting the product $\epsilon\kappa$ (e.g. adjusting κ^{-1} to be $1.1 X 10^{-8} cm$). Thus, the double layer may be modeled as a parallel plate condenser with a capacitance of:

$$C = \frac{\epsilon\kappa}{4\pi} = 6.3 \frac{coulombs}{volt\ m^2} = 6.3\ Farads/m^2 (630\mu Farads/cm^2) \tag{4.6}$$

The capacitance of $6.3\ Farads/m^2$ is high compared to that of the mercury surface, which has a typical value of $0.2\ Farads/m^2$ (see Bockris and Reddy,1970). Physically, a double layer thickness of $1.1 X 10^{-8}$ cm is close to molecular dimensions and the Stern treatment of the electrical double layer is preferred over the Gouy-Chapman treatment (see Adamson,1967). Modeling efforts along this line by Westall and Hohl(1980) and Davis and Leckie(1978) for surface titration data gave inner layer capacitances ranging from $1.06\ Farads/m^2$ for $\gamma-Al_2O_3$ in 0.1 M $NaClO_4$ and $1.4\ Farads/m^2$ for amorphous FeOOH in 0.1 M $NaNO_3$ respectively.

4.3 Adsorption of Manganese(II) on γ-FeOOH

All adsorption studies were performed with nitrogen bubbling to exclude oxygen and prevent oxidation of Mn(II) species. Samples were analysed for Mn(II) by the technique described in Chapter 2. The surfaces used for sections 4.3.1 to 4.3.3 were prepared by procedure A. When surface loading effects were studied in 4.3.4, procedure B was used to ensure that we are getting a consistent surface. The crystallinity of a sample was found to be dependent on $[Fe(II)]_0$. See Figure 4.4.

The mass balance that we have is:

$$[Mn(II)]_{total} = [Mn(II)]_0 = [Mn(II)]_{solution} + [Mn(II)]_{adsorbed} \quad (4.7)$$

Since our solution is 0.7 M NaCl and 5 mM $NaHCO_3$ we have:

$$[Mn(II)]_{solution} = [Mn^{2+}] + [MnOH^+] + [Mn(OH)_2^0] + [MnCl^+]$$

$$+ [MnCl_2^0] + [MnCl_3^-] + [MnHCO_3^+] + \ldots \quad (4.8)$$

Initial calculations show that the hydrolysed Mn(II) species ($[MnOH^+]$, $[Mn(OH)_2^0]$, $[MnOH_3^-]$, ...) are small at pH < 9.5 and that the important species are the chloro complexes. Since $[Mn(II)_0 = 50-100 \ \mu M << [Cl^-]$ and $[HCO_3^-]$, we assume that $[Cl^-]$ and $[HCO_3^-]$ are approximately their initial concentrations. Then,
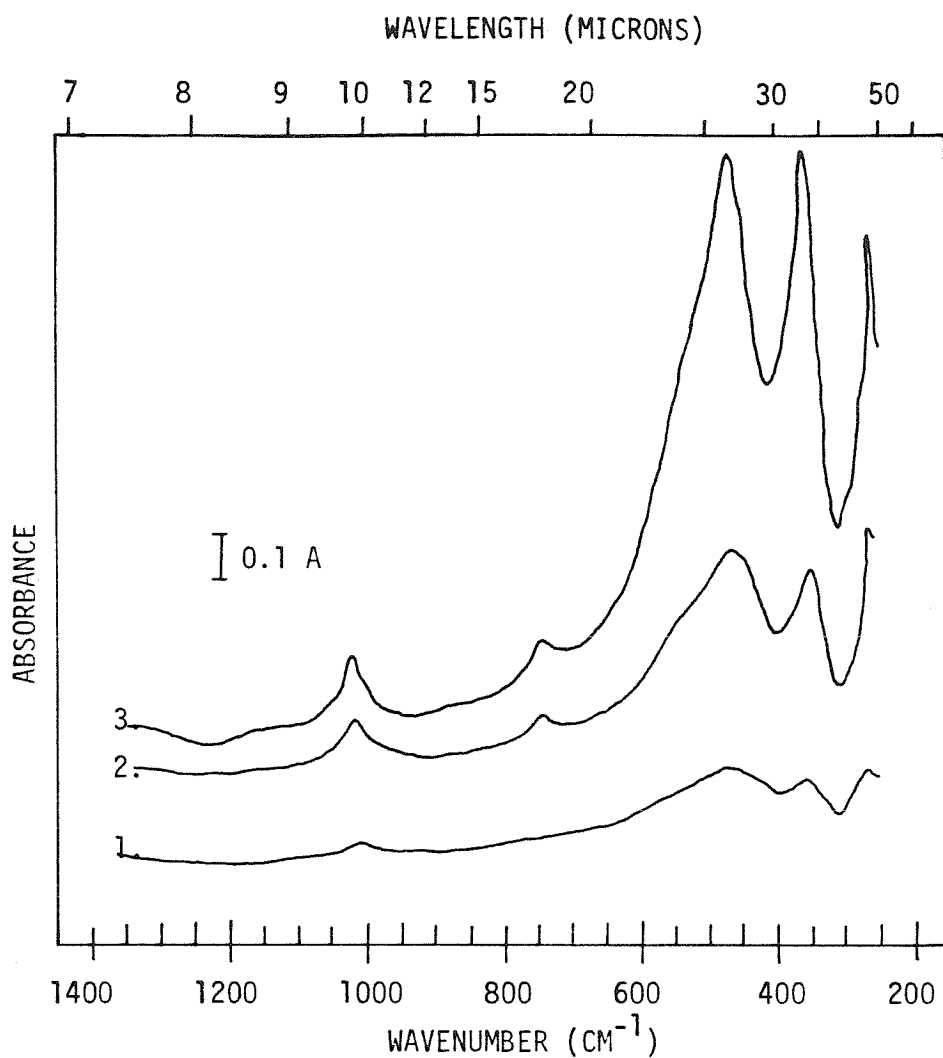
Figure 4.4 Variation of crystallinity of γ- FeOOH
due to experimental conditions.

(1) $[Fe(II)]_0$= 50 μM,0.5 M NaCl,pH 7.2

(2) $[Fe(II)]_0$= 50 μM,0.5 M NaCl,pH 6.5

(3) $[Fe(II)]_0$= 10^{-3}M,0.7 M NaCl,pH 7.3

All spectra ran with one-mg sample in 200 mg KBr.

$$[Mn(II)]_{solution} = [Mn^{2+}]\{1 + K_{MnCl}[Cl^-] + K_{MnCl_2}[Cl^-]^2 + K_{MnCl_3}[Cl^-]^3$$

$$+ K_{MnHCO_3}[HCO_3^-]\} \tag{4.9}$$

Using the REDEQL data set at Caltech and the Davies equation to estimate the activity coefficient of individual charged ions, we obtain the following speciation. As a percentage of $[Mn(II)]_{solution}$, $[Mn^{2+}]$ is 18.6%, $[MnCl^+]$ is 53%, $[MnCl_2^0]$ is 21%, $[MnCl_3^-]$ is 4.7% and $[MnHCO_3^+]$ is 2.8%. In the following discussions $[Mn(II)]$ will stand for $[Mn(II)]_{solution}$ and $[Mn(II)]_{ads}$ will stand for $[Mn(II)]_{adsorption}$.

The adsorption of Mn(II) species on the γ-FeOOH surface can include the following possibilities:

$$Mn^{2+} + \equiv FeOOH \rightleftharpoons \equiv FeOOMn^+ + H^+ \tag{4.10}$$
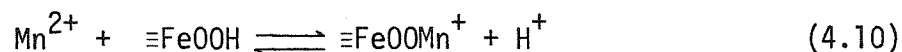
where $\equiv FeOOH$ is a schematic representation of a surface site.

$$Mn^{2+} + 2\equiv FeOOH \rightleftharpoons (\equiv FeOO)_2Mn + 2H^+ \tag{4.11}$$

$$MnCl^+ + \equiv FeOOH \rightleftharpoons \equiv FeOOMnCl + H^+ \tag{4.12}$$

$$MnCl_2^0 + \equiv FeOOH \rightleftharpoons \equiv FeOOMnCl_2^- + H^+ \tag{4.13}$$
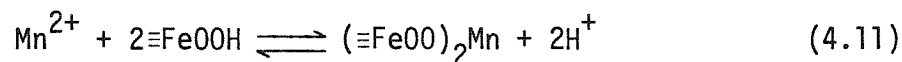
Forbes, Posner and Quirk (1974) studied the specific adsorption of Hg^{2+} on goethite as a function of pH and $[Cl^-]$ and reported that complexing

the mercuric ion with chloride to give $HgCl_2^0$ reduces adsorption to

negligible amounts, so maybe (4.13) is not important.

Each of the reactions in (4.10) to (4.12) entails the formation

of a surface complex and we could in principle write equilibrium

constants for each of them. It is important to note that each of the

reactions also entails a different charge balance on the surface.

Schindler (in press) and Westall and Hohl (1980) discussed the theoreti-

cal developments and the necessary mathematical techniques for a general

approach to surface equilibria. In the end, a set of parameters (hope-

fully minimal) are obtained for an optimal fit of the model to experi-

mental results.

In light of the complexity discussed above we will first try an

empirical approach; we write the following mass expression:

$$aMn(II) + b\equiv FeOOH \rightleftharpoons (\equiv FeOO)_{b/a} aMn + bH^+ \qquad (4.14)$$
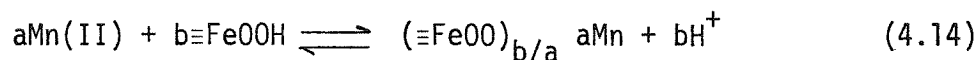
where a and b are stoichiometric coefficients.

4.3.1 Kinetics of Adsorption

Figure 4.5 shows typical data on the kinetics of manganese(II)

adsorption on γ-FeOOH. The reaction approaches steady values in about

20 min. There are various ways to model adsorption kinetics, depending

on how one formulates the mechanism of adsorption. At constant pH one

could write:

$$Mn(II) + S \underset{k_4 \text{ desorption}}{\overset{k_3 \text{ adsorption}}{\rightleftharpoons}} Mn(II) \cdot S \qquad (4.15)$$
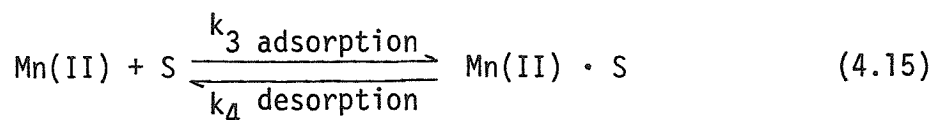
where S is a surface site in this case and Mn(II) · S denotes adsorbed
Mn(II). The mathematical treatment is simplified if we assume that the
surface sites are not limiting, then:

$$-\frac{d[Mn(II)]}{dt} = k_3[Mn(II)] \, [S] - k_4[Mn(II) \cdot S]$$

$$= k_3'[Mn(II)] - k_4[Mn(II) \cdot S] \qquad (4.16)$$

k_3' and k_4 have units of inverse time. Since $[Mn(II) \cdot S] =$
$[Mn(II)]_0 - [Mn(II)]$, we can write:

$$-\frac{d[Mn(II)]}{dt} = (k_3' + k_4) \, [Mn(II)] - k_4 \, [Mn(II)]_0 \qquad (4.17)$$

At equilibrium, the rate is zero and we define an equilibrium [Mn(II)]

$$[Mn(II)]_e = \frac{k_4[Mn(II)]_0}{k_3' + k_4} \qquad (4.18)$$

Integrating (4.17) with $[Mn(II)] = [Mn(II)]_0$ at $t = 0$;

$$[Mn(II)] = ([Mn(II)]_0 - [Mn(II)]_e)\exp[-(k_3' + k_4)t] + [Mn(II)]_e \qquad (4.19)$$

(4.19) is the form of the equations plotted in Figure 4.5. We note that
at $t = 0$, the exponential becomes one and $[Mn(II)] = [Mn(II)]_0$ while for
large t, the exponential becomes zero and $[Mn(II)]$ approaches $[Mn(II)]_e$.
k_3' was not dependent on pH and its numerical value was determined to be

10^{-3}M γ-FeOOH

0.7 M NaCl

25^0C

pH = 8.33

$[Mn(II)] = 21.6\exp(-0.30t) + 28.4$

pH = 8.70

$[Mn(II)] = 29.7\exp(-0.40t) + 20.3$

concentration in μM; t in minutes
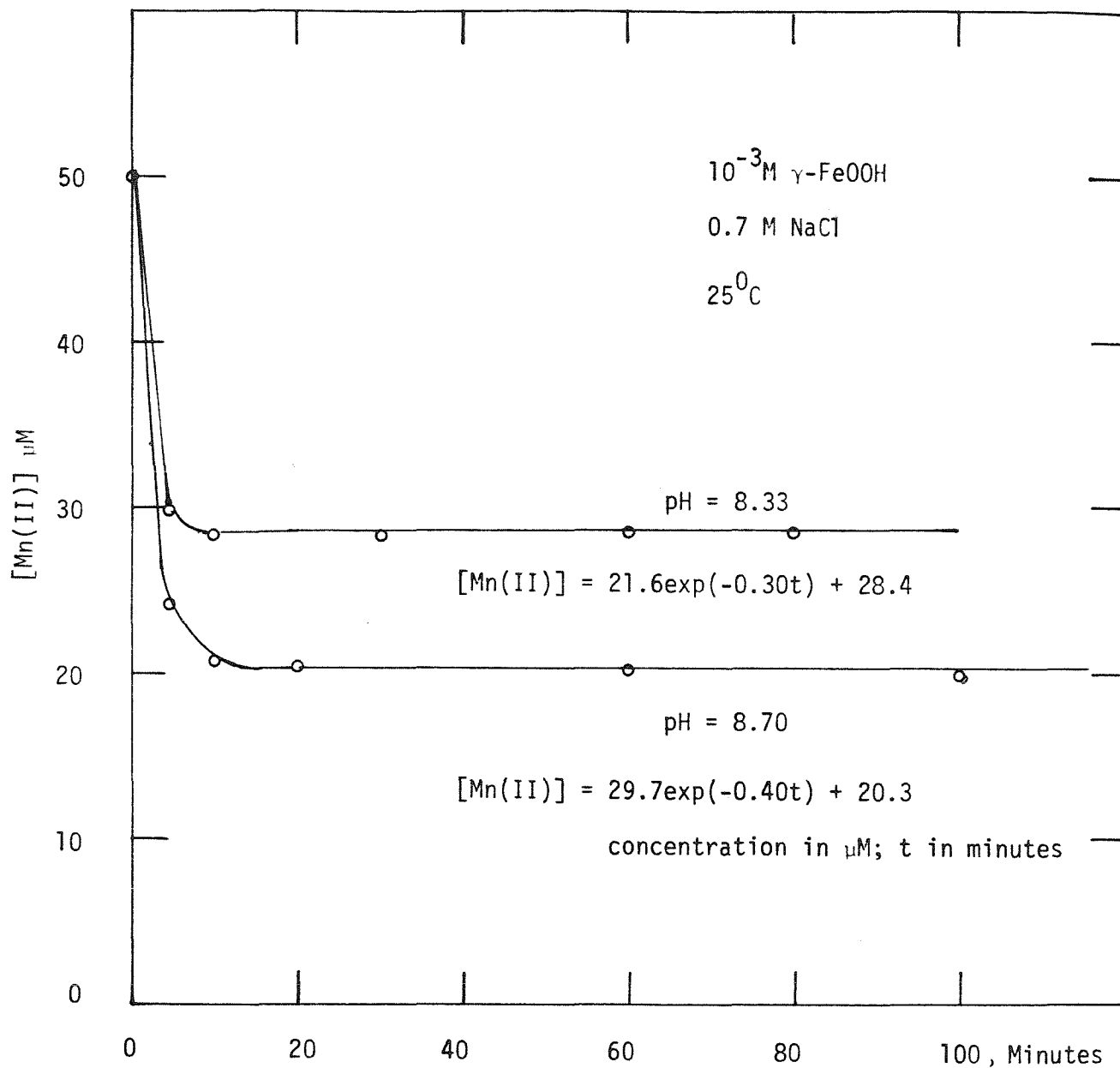
Figure 4.5   The kinetics of Mn(II) adsorption on γ-FeOOH.
Equations are in the form (4.19) in the text.

about 0.24 min^{-1}.

All subsequent descriptions of adsorption are in terms of equilibrium results, with 30-60 minutes taken as the equilibrium time.

4.3.2 Dependence of Adsorption on pH

The experimental data are summarized in Table 4.1 and presented in Figures 4.6 and 4.7. The percentage of Mn(II) adsorbed versus pH plot is a linear one for the range 8 to 9.7. The following discussions are applicable to this range only. The complete percentage adsorption vs. pH curve is generally an S-shaped curve.

The linear regression of $log[Mn(II)]_{ads}/[Mn(II)]$ vs. pH (Figure 4.7) was done to examine the mass-law expression (4.14) written as:

$$Mn(II) + \equiv FeOOH \; \rightleftharpoons \; \equiv FeOOMn + H^+ \qquad (4.20)$$
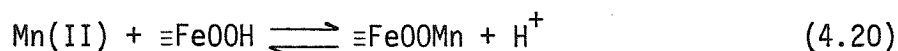
The slope obtained was 0.76, close to unity as expected from the work of Grimme (1968), who studied the adsorption of Mn(II) on α-FeOOH. A possible reason for a non-integral stoichiometry for the proton-Mn(II) is discussed further in the following sections.

4.3.3 Adsorption Isotherm

Another way to test (4.14) is to hold pH constant and vary $[Mn(II)]_0$. Superficially, this may be viewed as an adsorption isotherm experiment. Weber (1972) discussed various forms of adsorption isotherms, which are functional expressions for the variation of adsorption with concentration of adsorbate in bulk solution at constant temperature.
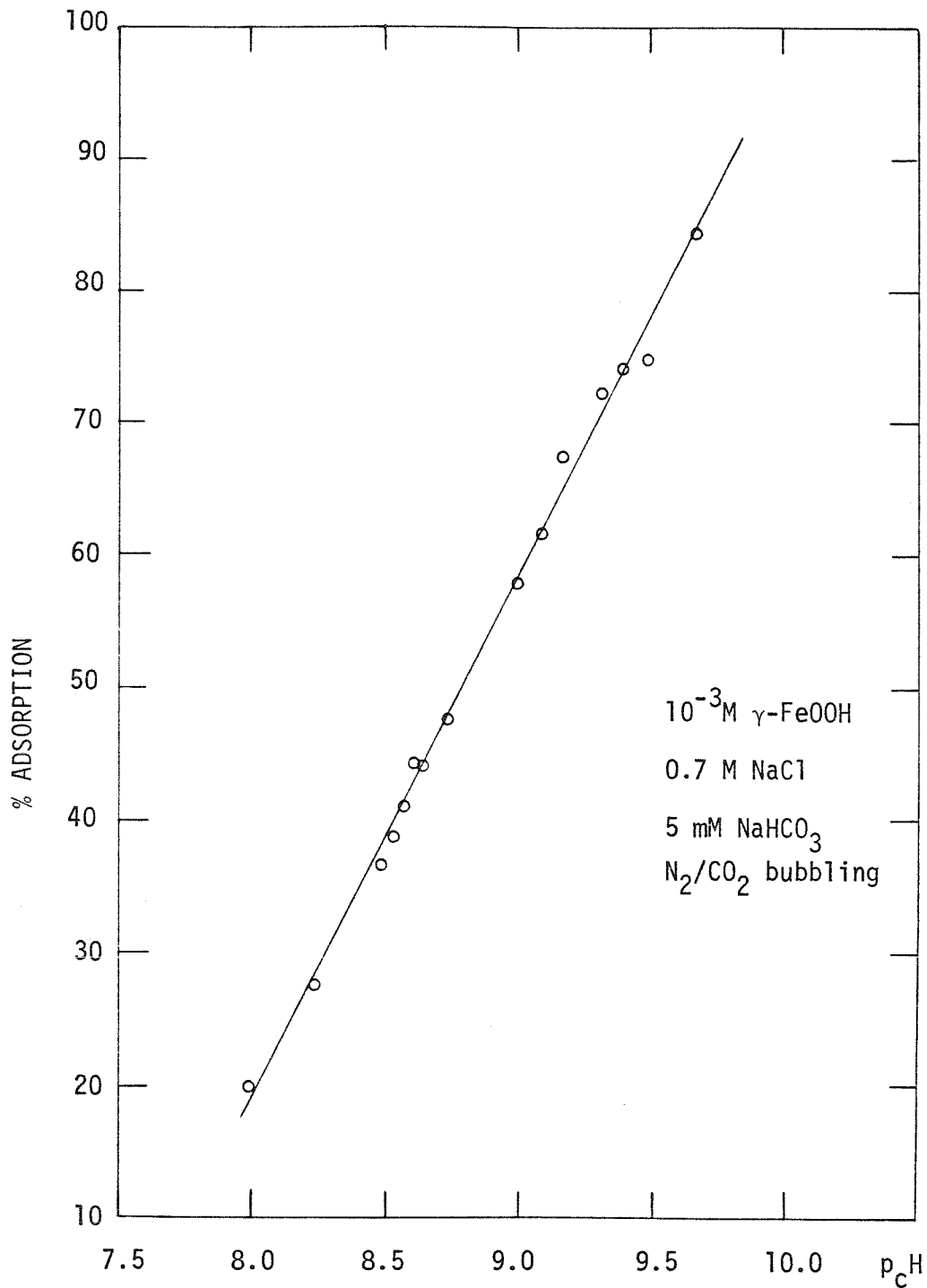
Figure 4.6   % Mn(II) adsorption as a function of p_cH

Linear regression: % Adsorption

$$= 39.45 p_cH - 296.86 \quad r^2 = 0.99$$
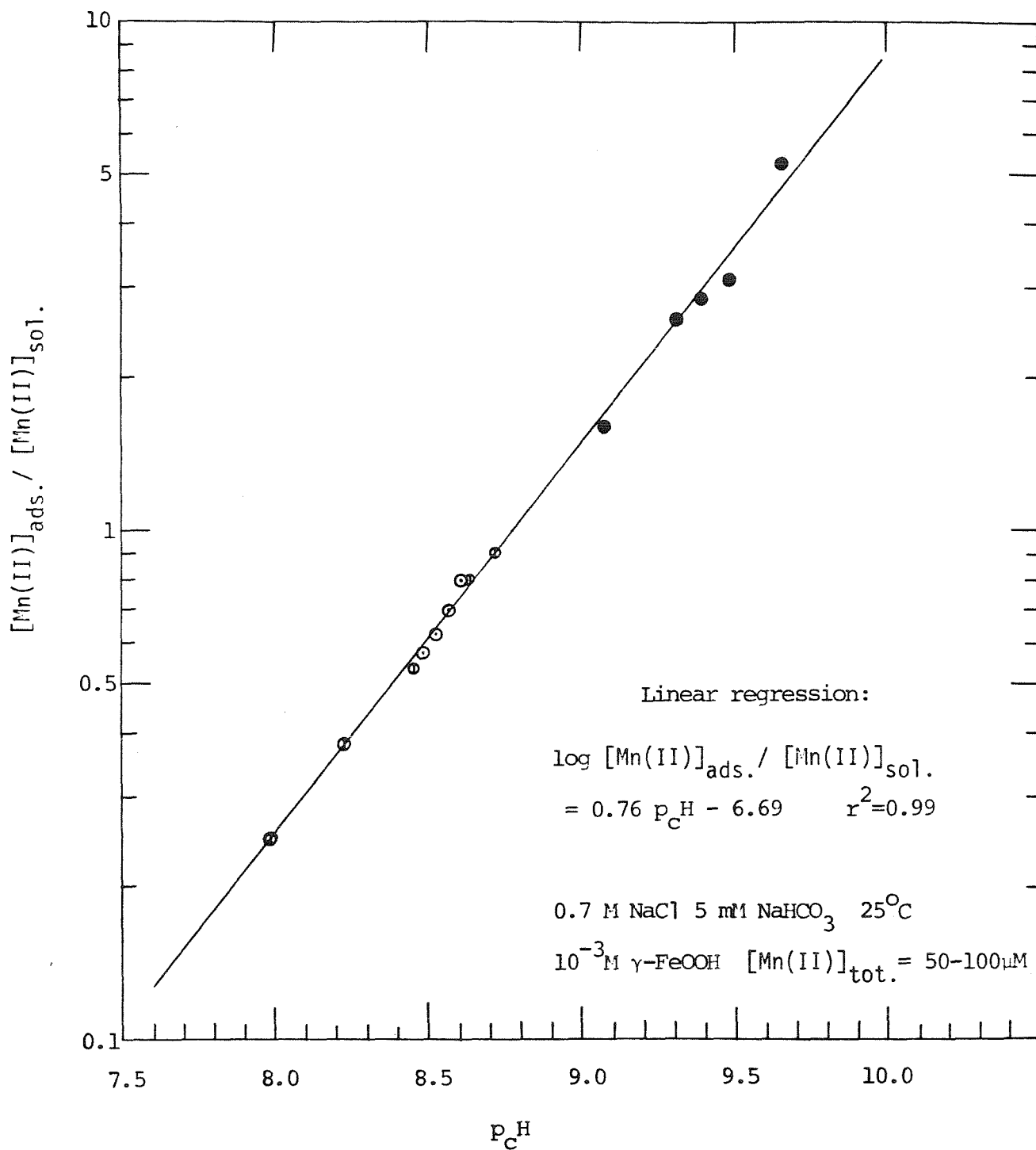
Figure 4.7 Data from Table 4.1 plotted to test
mass law expression of text

Table 4.1 Adsorption of Mn(II) on γ-FeOOH as
a function of pH, 0.7 M NaCl, 25°C

pH	$[Mn(II)]\mu M$	$[Mn(II)]_{ads}\mu M$	% Adsorbed	(multiply by 5.63 to get)
8.00	40.9	10.1	20.1	$\underline{\mu moles}$
8.24	36.1	13.9	27.8	g
8.47	32.4	17.6	34.7	
8.50	31.7	18.3	36.6	
8.53	30.7	19.3	38.6	
8.57	29.5	20.5	41.0	
8.60	27.8	22.2	44.4	
8.64	27.7	22.3	44.6	
8.74	26.2	23.8	47.6	
9.09	18.9	30.5	61.7	
9.33	13.3	34.7	72.3	
9.41	12.7	36.3	74	
9.49	12.1	37.9	75.7	
9.68	7.6	42.4	84.8	

An adsorption isotherm such as the classical Langmuir isotherm can be derived rigorously thermodynamically and/or kinetically, see Adamson (1967). As such, the derivation assumes reversibility. The adsorption data for Mn(II) and the γ-FeOOH surface, summarized in Table 4.2 and plotted in Figure 4.8, were obtained from one direction only. However, the shape of the isotherm is similar to that of the standard BET (Brunauer, Emmett, Teller) model, which is usually interpreted as reflecting multilayer adsorption or the existence of different kinds of surface sites.

An empirical isotherm equation, the Freundlich or van Bemmelan equation is also widely used. It can be viewed as a special case for heterogeneous surface energies. The mathematical form for the Freundlich isotherm for our system is:

$$[Mn(II)]_{ads} = K_F [Mn(II)]^{1/n} \qquad (4.21)$$

K_F is the Freundlich constant and n is a constant related to the energy of adsorption. The adsorption data are shown as a log-log plot in Figure 4.9, the r^2 is 0.95. The slope of 0.6 implies that at constant pH, $[Mn(II)]_{ads} = K_F[Mn(II)]^{0.6}$. This suggests that the coefficient a in (4.14) is 0.6, so we try the plot $\log[Mn(II)]_{ads}/[Mn)II)]^{0.6}$ versus pH, as in Figure 4.10. The slope obtained this time was 0.6. This gives us a conditional constant that is dimensionless:

$$\frac{[Mn(II)]_{ads}}{[Fe(III)]_T} \left(\frac{[H^+]}{[Mn(II)]} \right)^{0.6} = K_{conditional} \qquad (4.22)$$
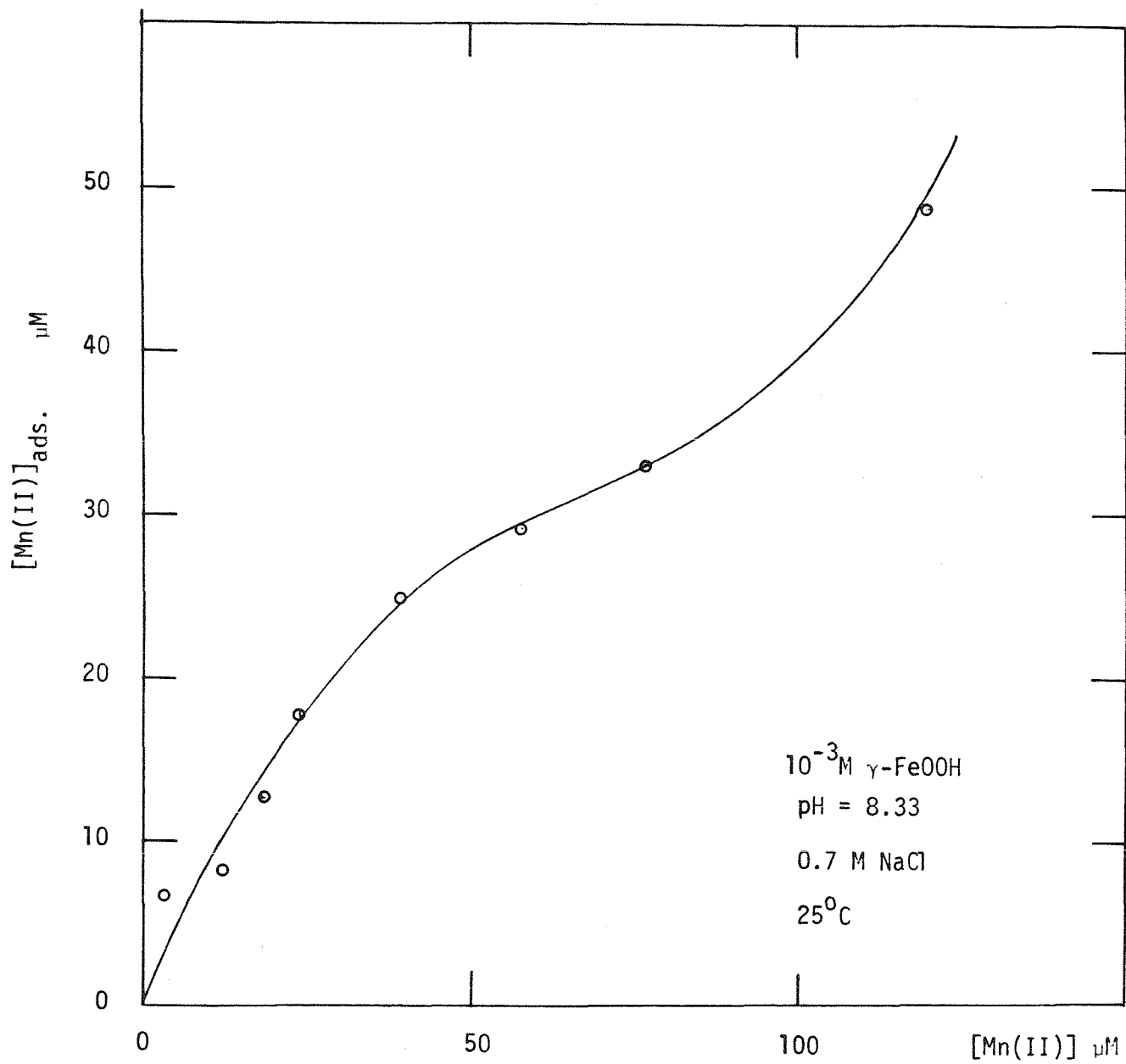
Figure 4.8 Adsorption isotherm for Mn(II) adsorption on γ-FeOOH
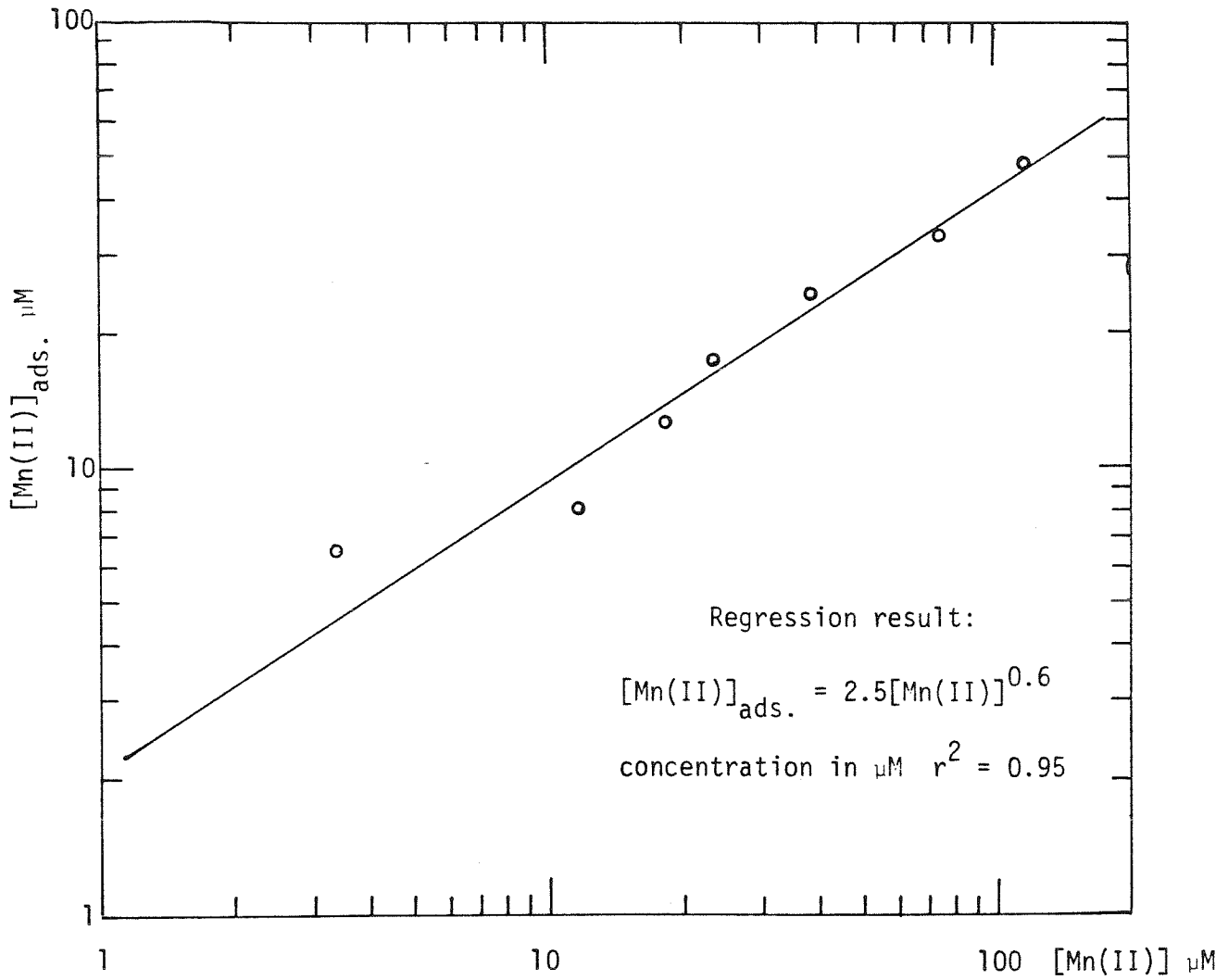
Figure 4.9   Log-log plot of the adsorption data.

Table 4.2 Relation between equilibrium [Mn(II)] and
[Mn(II)]$_{ads}$ for 10^{-3}M γ-FeOOH, 0.7 M NaCl

T = 25°C, pH = 8.33

[Mn(II)]$_e$μM	[Mn(II)]$_{ads}$μM	(multiply by 11.25 to get) μmole/g
3.4	6.6	
12.0	8.2	
18.0	12.7	
23.8	17.9	
39.1	24.9	
57.5	29.1	
76.7	33.0	
119.5	48.7	
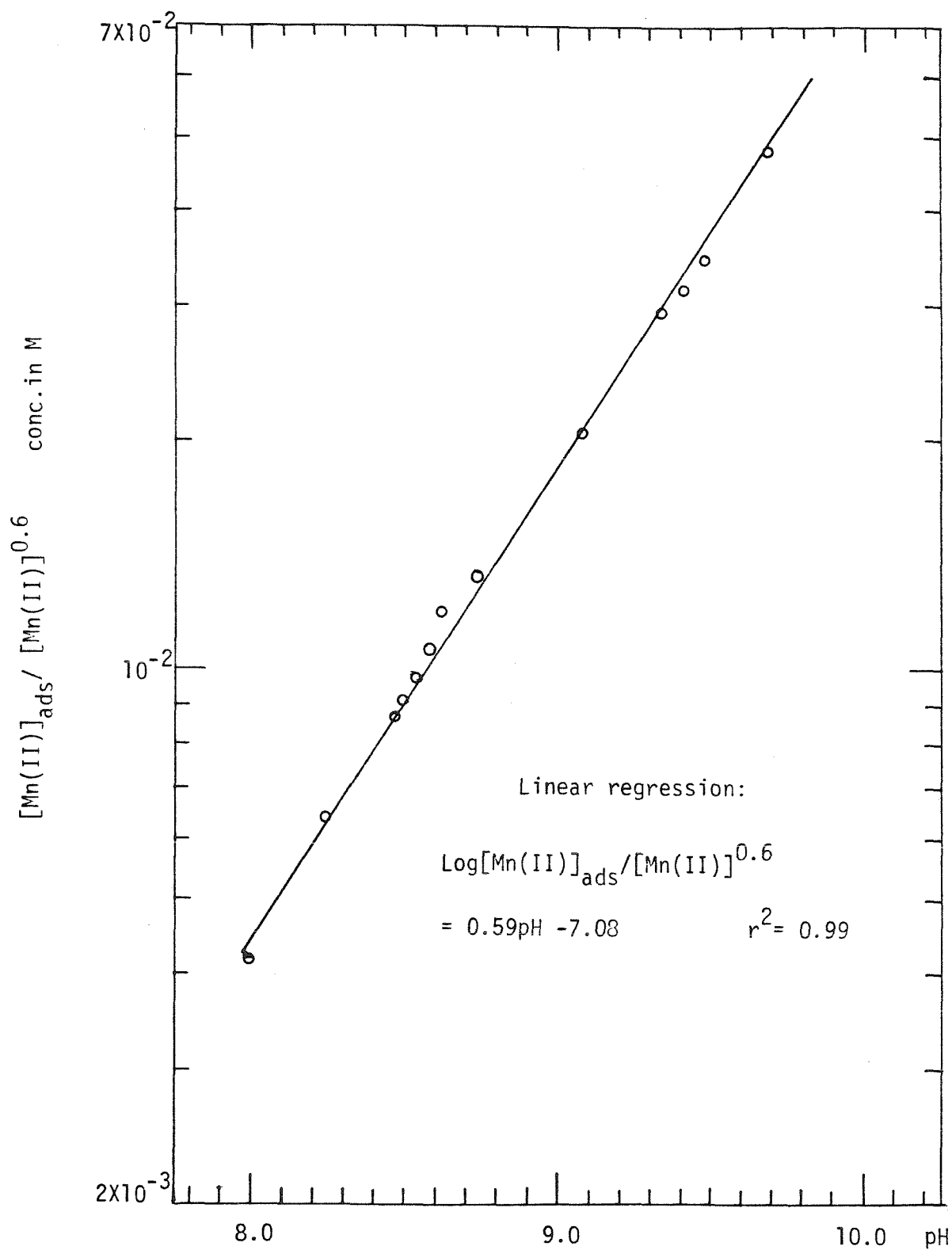
Figure 4.10   Replotting the data of Table 4.1 to
evaluate the conditional constant

and the numerical value turns out to be $7.4\pm0.8\times10^{-5}$.

4.3.4 Dependence of Adsorption on Amount of Surface

The dependence of the amount of Mn(II) adsorption as a function of the amount of surface is summarized in Table 4.3 and presented in Figure 4.11. The conditional constant as calculated by (4.22) was determined to be $1.6\pm0.4\times10^{-4}$. This is reassuring since the surface used for this study was synthesized by procedure B (to ensure consistent surface characteristics) and the variation of the constant is less than a factor of 2 compared with the constant determined for surfaces prepared by procedure A.

4.3.5 Summary

In this section we have computed other formulations of the conditional constant and show their variability.

$$K' = \frac{[Mn(II)]_{ads}[H^+]}{[Fe(III)]_T[Mn(II)]} \quad \text{dimensionless} \tag{4.23}$$

K' was calculated to be $1.7\pm0.9\times10^{-6}$. The variability was calculated for 2σ and amounted to 53%. This formulation is similar to the one formulated by Tamura et al. (1976b) for [Fe(II)] adsorption on amorphous ferric oxyhydroxide (see Chapter 3.2).

$$K'' = \frac{[Mn(II)]_{ads}[H^+]}{[\equiv FeOOH][Mn(II)]} \quad \text{dimensionless} \tag{4.24}$$
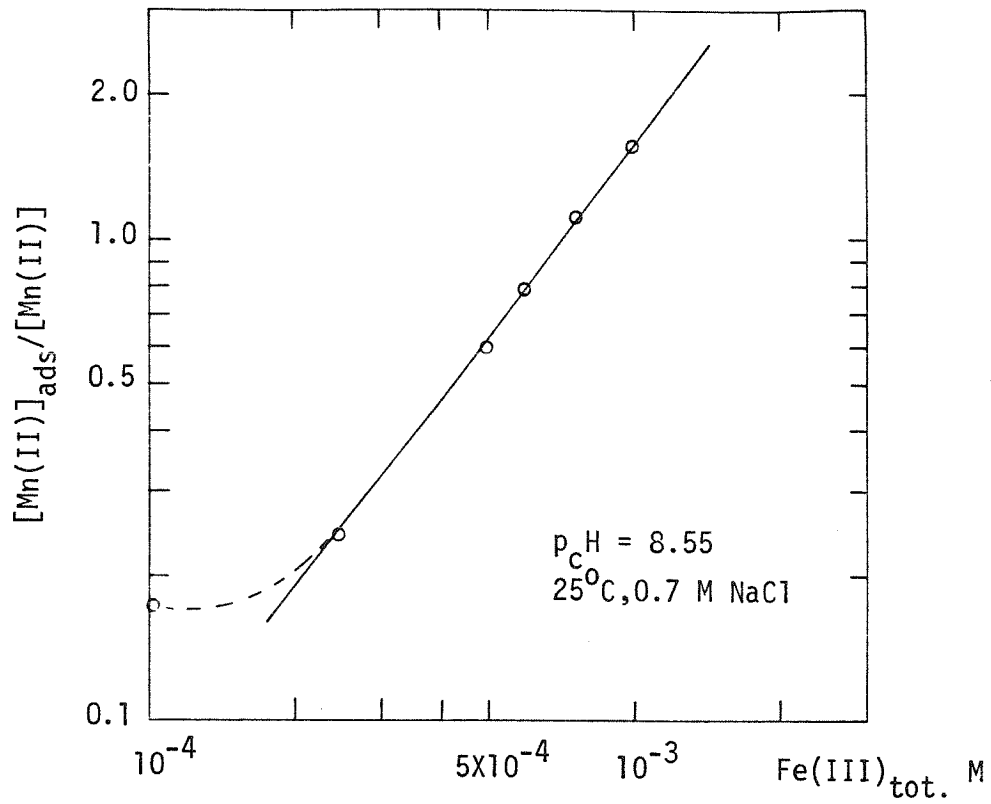
Figure 4.11 Mn(II) adsorption as a function
of total ferric iron

Table 4.3 Adsorption of Mn(II) on γ-FeOOH as a
function of the amount of surface

pH = 8.55, 0.7 M NaCl, T = 25°C

Surface x 10^4 M	[Mn(II)]μM	[Mn(II)]$_{ads}$μM	%Adsorption
10	19.9	30.1	60.2
7.5	23.8	26.2	52.3
6.0	27.7	22.3	44.6
5.0	31.2	18.8	37.5
2.5	40.4	9.6	19.1
1.0	42.5	7.5	14.9

The difference between K' and K_2'' is that we have imposed the mass balance on the surface sites in the latter. Total surface sites were assumed to be the number determined from acid titration, thus:

$$S_T = [\equiv FeOOH] + [\equiv FeOO^-] + [\equiv FeOOMn^+] \qquad (4.25)$$

S_T = 231 μM, $[\equiv FeOOMn^+]$ is just the adsorbed [Mn(II)], and $[\equiv FeOO^-]$ was calculated as surface excess hydroxide from equation (4.2) and $[\equiv FeOOH]$ was obtained by mass balance. This is subject to large errors at high pH values (above 9) since we are subtracting two large numbers. Consequently the variation in the numerical value of K_2 was 100%. However, if we calculate K'' for the data from pH 8 to 9 only, the numberical value was $1.8\pm0.3\times10^{-5}$. This formulation is similar to that of Davis and Leckie (1978). Grimme (1968) reported the affinities of metal ions for α-FeOOH in 0.1 M KNO_3 to increase in the order: Mn < Co < Zn < Cu. The sequence was confirmed and extended by Forbes et al. (1976) for α-FeOOH in 0.075 M $NaNO_3$, in the order: Cd < Co < Zn < Pb < Cu. Assuming the sequence to hold for the γ-FeOOH surface in 0.7 M NaCl, we predict that the affinity of Cd and Mn should be similar. For amorphous FeOOH in 0.1 M $NaNO_3$, Davis and Leckie (1978) reported the constants 7.9×10^{-5} for Cu and 1.3×10^{-5} for Cd. The agreement is reasonable.

It is difficult to apply electrostatic corrections to K'' without further modeling. If we approximate the surface charge by (4.3), assume that the surface potential = σ/C by a constant capacitance model, use some sort of exponential function (e.g. $\exp(-F\psi/RT)$) as a correction to

$K^{\prime\prime}$; we obtain the correct trend but variability is around a factor of 5.

If the ultimate goal is to obtain a reasonable fit between experiment and calculations, perhaps the simplest way is to use the conditional constant as formulated by (4.22), which is an empirical relation that combined all the effects discussed above.

CHAPTER 5

MANGANESE(II) OXYGENATION KINETICS

5.1 Autocatalysis of Mn(II) Oxygenation

Nichols and Walton (1942), in their study of the kinetics of oxygen

consumption of manganous chloride in ammonia-ammonium buffers, first

suggested that the reaction is autocatalytic and that the rate is a strong

function of pH. Since then, the oxidation-removal kinetics of Mn(II) have

been studied by Nordell (1953), Asada (1959), Hem (1963), Morgan (1967)

and Coughlin and Matsui(1976). Because the oxygenation rate is strongly

dependent on pH, quantitative treatment of the rate data can be performed

only for buffered solutions, without undue mathematical treatment. Of the

studies above, only those of Morgan (1967) and Coughlin and Matsui (1976)

fall into this category.

5.1.1 Kinetic Expression

The experimental data of Mn(II) oxygenation kinetics can be

modeled by an integrated rate expression identical to the one formulated

for Fe(II) oxygenation in Chapter 3, Equation (3.10). The differential

form at constant pH and P_{O_2} is:

$$-\frac{d[Mn(II)]}{dt} = k_1[Mn(II)] + k_2[MnO_x]\,[Mn(II)] \qquad (5.1)$$

$[MnO_x]$ denotes oxidized manganese. It is known that these oxide products

are usually non-stoichiometric, i.e., x is not an integer. Morgan (1967)

showed that x ranged from 1.24 to 1.43 when Mn(II) was oxygenated in the pH range 9 to 10.

Figures 5.1 and 5.2 show the experimental results of Morgan (1967) and Coughlin and Matsui (1976) modeled by the integrated rate expression. Morgan (1964) reported a combined rate, $k_{obs} = \dfrac{k_1}{[Mn(II)]_0} + k_2$ and showed a second-order relationship between the reaction rate and the OH^- activity. Following Morgan (1964), we write:

$$k_{obs} = k'\{OH^-\}^2 \qquad (5.2)$$

k' was determined to be $8.5\pm2\times10^{11}$ $M^{-3}min^{-1}$ in ammonia-ammonium buffers, about $2\times10^{12}M^{-3}min^{-1}$ in carbonate/bicarbonate buffers. The rate constants of Coughlin and Matsui (1976), where pH was maintained by base titration, gave a k' of $7.5\times10^{12}M^3min^{-1}$. The difference could be attributed to complexation of the Mn^{2+} by ammonia and bicarbonate, or to the formation of localized regions of high $[OH^-]$ in the titration procedure, or a combination of both.

For $[Mn(II)]_0 = 50$ μM, we can calculate $\tau_{1/2}$ using (3.11). It ranged from 15 hr to 335 hr at pH 8 using the data of Coughlin and Matsui (1976) or Morgan (1964), respectively. The presence of high concentrations of NaCl(0.7 M) is expected to increase $\tau_{1/2}$ as in the case of Fe(II). Preliminary experiments with solutions of the composition 0.7 M Cl^-, 5 mM $NaHCO_3$, $P_{O_2} = 0.21$ atm., 25°C and $[Mn(II)]_0$ of 50 μM showed no significant (1%) removal of Mn(II) at pH 8.5 for a period of 24 hr. No greater than 7% of the initial $[Mn(II)]_0$ was removed at pH 8.7 over a 20-hr period.
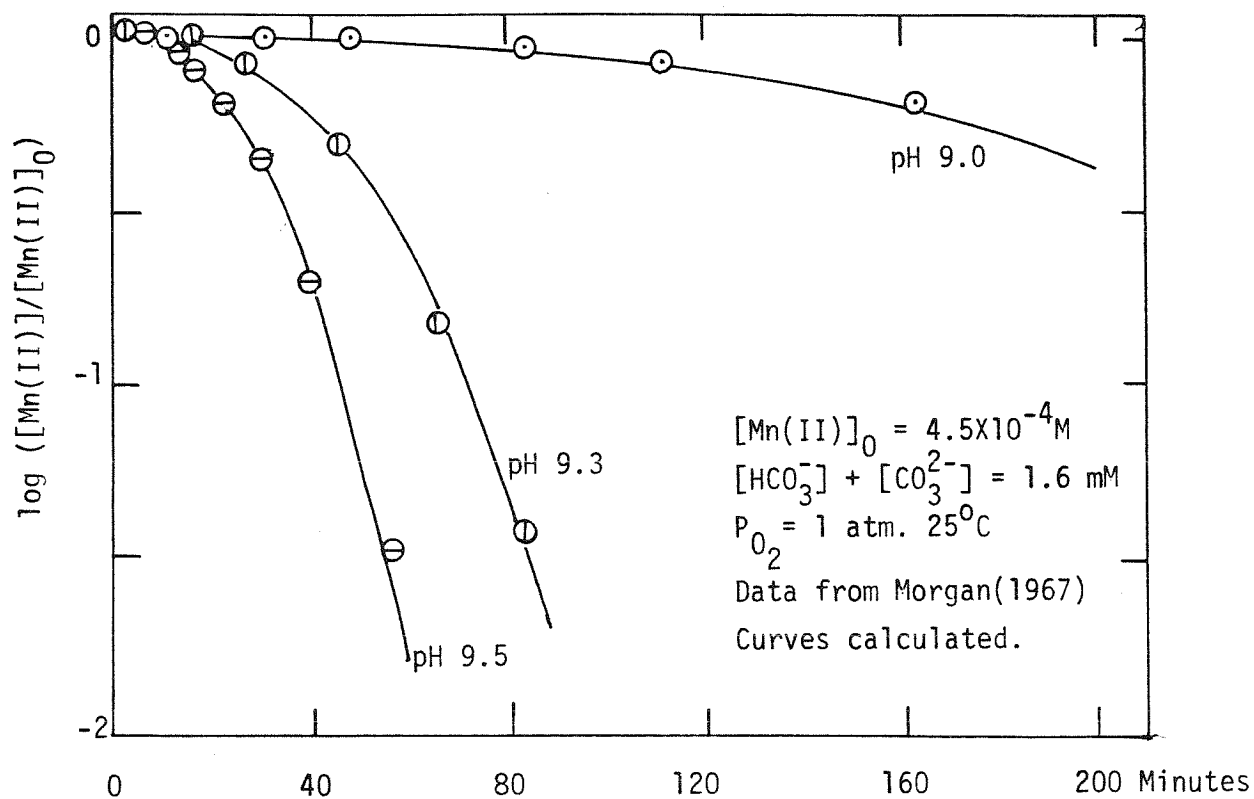
Figure 5.1 Mn(II) oxygenation removal kinetics data from Morgan(1967)
modeled with the integrated rate expression equation(3.10)

pH	$k_1(min^{-1})$	$k_2(M^{-1}min^{-1})$
9.0	3.6×10^{-4}	50.4
9.3	1.7×10^{-3}	185.7
9.5	4.2×10^{-3}	265.7

$$\frac{[Mn(II)]}{[Mn(II)]_0} = \frac{k_1 + k_2[Mn(II)]_0}{k_2[Mn(II)]_0 + k_1 exp[(k_1 + k_2[Mn(II)]_0)t]}$$
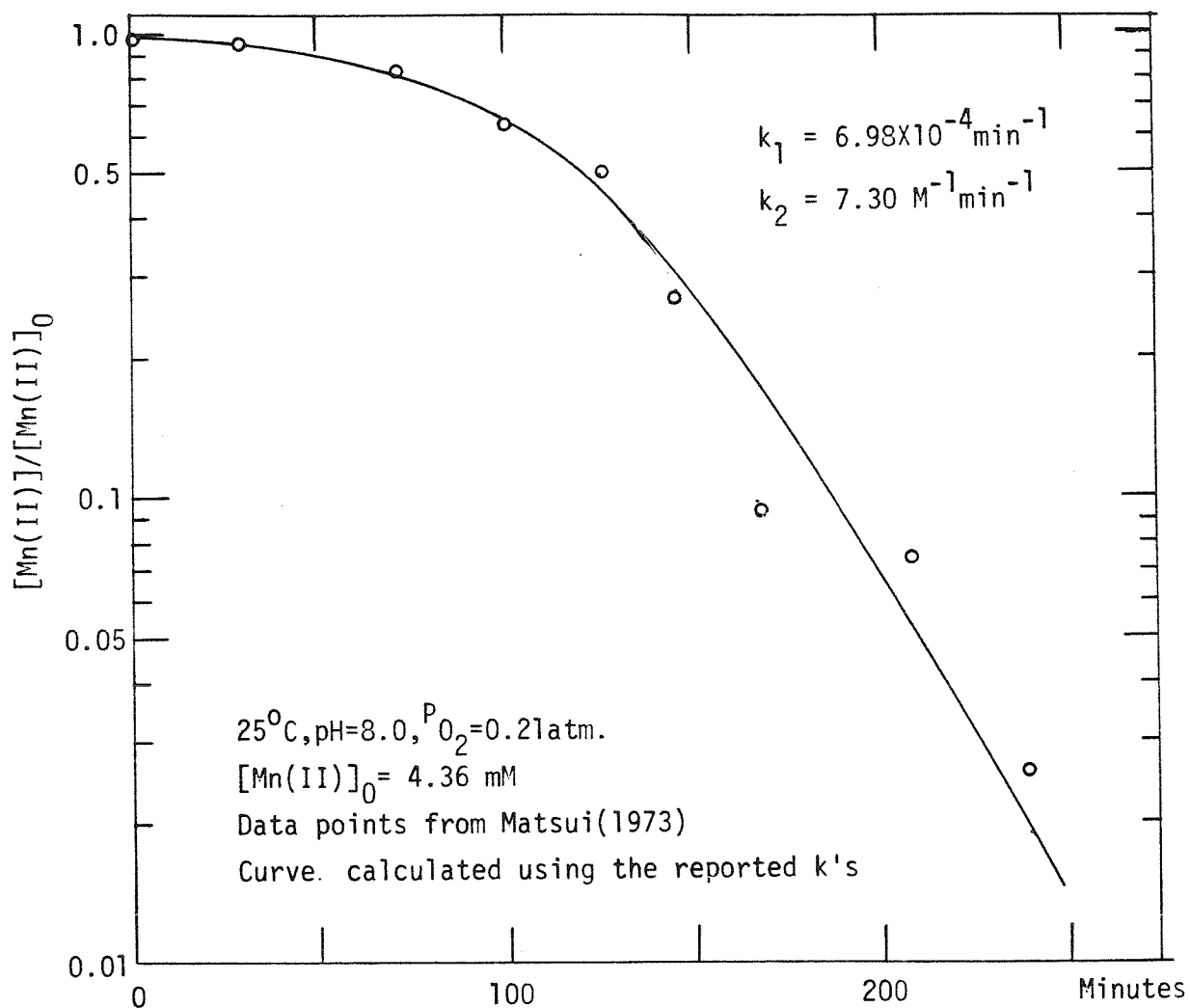
Figure 5.2 The oxygenation removal kinetics data of Matsui(1973) modeled with the integrated rate expression and reported rate constants.

The presence of a pre-existing γ-FeOOH surface will be shown to significantly decrease $\tau_{1/2}$.

5.1.2 Oxygenation Product

The manganese oxides are difficult to identify by conventional means such as X-ray diffraction. The non-stoichiometric nature of the manganese(IV) oxides may be due to the large amounts of adsorbed Mn(II). It is difficult chemically to distinguish between Mn(III) and mixtures of Mn(II) and Mn(IV). Even physical-chemical methods do not give unambigous conclusions. For example, Robin and Day (1967) reported that while X-ray analysis showed the structure of γMnOOH, manganite, to be based on sheets of O^{2-} and OH^- ions enclosing Mn(III); measurements of magnetic anisotropy appear to suggest a 50-50 mixture of Mn(II) and Mn(IV).

Stumm and Giovanoli (1976) reported the formation of γ-MnOOH when 5-10 μM Mn(II) was oxygenated in simulated lake waters. The present study showed the presence of β-MnOOH (X-ray diffraction lines of 4.62 $\overset{\circ}{A}$, 2.67 $\overset{\circ}{A}$ and 2.37 $\overset{\circ}{A}$) when millimolar levels of $[Mn(II)]_0$ were oxygenated both in the presence and absence of HCO_3^-. Bricker (1965) also reported the formation of β-MnOOH and Mn_3O_4 under similar conditions.

5.2 Mn(II) Oxygenation Kinetics in the Presence of a Ferric Iron Oxide Surface

Van der Weijden (1975) reported experiments on adsorption and oxidation of Mn(II) and Co(II) under marine conditions. A contribution of oxidative removal to the total adsorption was found in experiments for Mn

with the surfaces of sand, clay, carbonate, iron hydroxide and manganese oxides. Similarly, Coughlin and Matsui (1976) reported the catalytic effect of the surfaces of α-MnO$_2$, β-MnO$_2$, γ-MnO$_2$, δ-MnO$_2$, Mn(II) · manganite, manganese nodules, plagioclase, microcline, olivine, rutile, hematite and silica gel on the oxygenation kinetics of 4.36 mM initial Mn(II) concentrations at pH 8. Their results for iron oxide surface are illustrated in Figure 5.3. It is difficult to ascertain the surface oxidative step in the study of van der Weijden (1975) since the difference between the removal curves is small. The results of Coughlin and Matsui (1976) are not straightforward to analyse as the Mn(II) in solution appeared to undergo significant oxidation without any external surface under their conditions. They modeled their observations with a set of 5 coupled differential equations.

5.2.1 Surface Kinetics Formation

Figure 5.4 shows typical kinetics of Mn(II) removal from solution with γ-FeOOH in the presence and absence of oxygen. The [Mn(II] was plotted logarithmically in anticipation of a first order kinetic behavior. The kinetics were dominated by the process of adsorption in the first few minutes with [Mn(II)] approaching a steady value in the absence of oxygen, as discussed in Chapter 4.3.1. Mn(II) was further removed from the solution phase in the presence of oxygen, implying some sort of surface oxidation step. A surface oxidized species was postulated to form from the adsorbed Mn(II) and dissolved oxygen. Adsorption equilibrium was assumed to be reestablished at the expense of solution Mn(II) as adsorbed Mn(II) was removed irreversibly by a surface oxidation step.
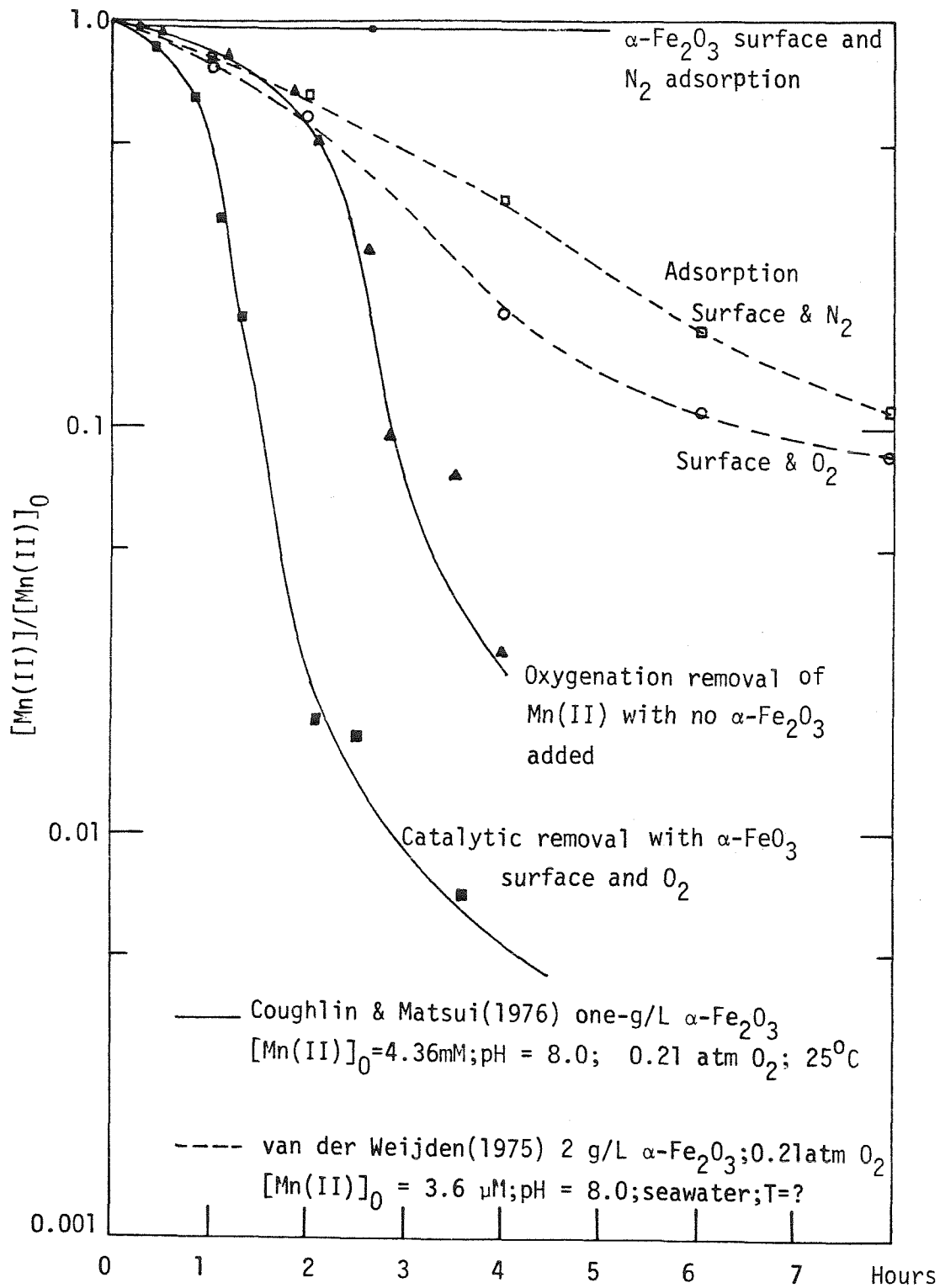
Figure 5.3 Summary of previous work on Mn(II) oxygenation
kinetics in the presence of ferric oxide.

The mass balance is

$$[Mn]_{total} = [Mn(II)]_0 = [Mn(II)] + [Mn(II)]_{ads} + [MnO_x]_{surface} \qquad (5.3)$$

$$\frac{-d[Mn]_{total}}{dt} = 0 = \frac{d[Mn(II)]}{dt} + \frac{d[Mn(II)]_{ads}}{dt} + \frac{d[MnO_x]_{surface}}{dt} \qquad (5.4)$$

If Mn(II) were assumed to come into equilibrium with respect to adsorption prior to oxygen bubbling, subsequent removal of Mn(II) from solution when oxygen is introduced would be dominated by the surface oxidation step. In addition, the following assumptions were made:

1. That adsorption/desorption kinetics is fast compared to the surface oxidation kinetics, allowing us to relate $[Mn(II)]_{ads}$ to [Mn(II)] by an equilibrium constant of adsorption.

2. That the surface is not altered significantly with the formation of the surface oxidized species.

3. That oxygen gas transfer from bubbling is fast compared to the surface oxidation rate.

Schematically, at constant pH and $[O_2]$, we have:

$$Mn(II) + S \underset{\longleftarrow}{\overset{fast}{\longrightarrow}} Mn(II)_{ads}$$
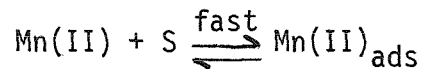
where S denotes a surface site.

$$Mn(II)_{ads} + O_2 \overset{k_S}{\longrightarrow} MnO_{x,surface}$$
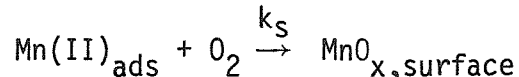
If we write $[Mn(II)]_{ads} \approx K[Mn(II)]$, where K is the equilibrium constant of adsorption related to $\acute{K}$ of equation (4.2.3), the Equation (5.4) becomes:

$$\frac{-d[Mn(II)]}{dt} = \frac{1}{1 + K} \frac{d[MnO_x]_{surface}}{dt} \qquad (5.5)$$

Figure 5.5 shows data for the removal of Mn(II) plotted logarithmically versus time to test for first order kinetics. This and all subsequent kinetic data were obtained by the establishment of adsorption equilibria prior to oxygen bubbling. The fit is quite good by the r^2 criteria. Figure 5.6 shows the effect of pH on the removal kinetics. The rate was observed to decrease at high pH (pH > 8.5) with the passage of time. This was not totally unexpected, since [Mn(II)] was decreasing with time, the rate of adsorption would be decreasing as well, so that assumption 1 would not be a good one for longer times. As surface oxidation goes to completion we would expect to get a surface coverage of 3.3 μmoles Mn/m^2. A monolayer coverage of hydrated Mn would be on the order of 4 μmoles/m^2, so assumption 2 is also not valid as time progresses.

If we deal only with initial rates, say for the first five minutes or so, we can write:

$$[Mn(II)] = [Mn(II)_0 \exp(-\acute{k}t) \qquad (5.6)$$

$$[Mn(II)]_{ads} = K[Mn(II)]$$
$$= K[Mn(II)_0 \exp(-\acute{k}t) \qquad (5.7)$$
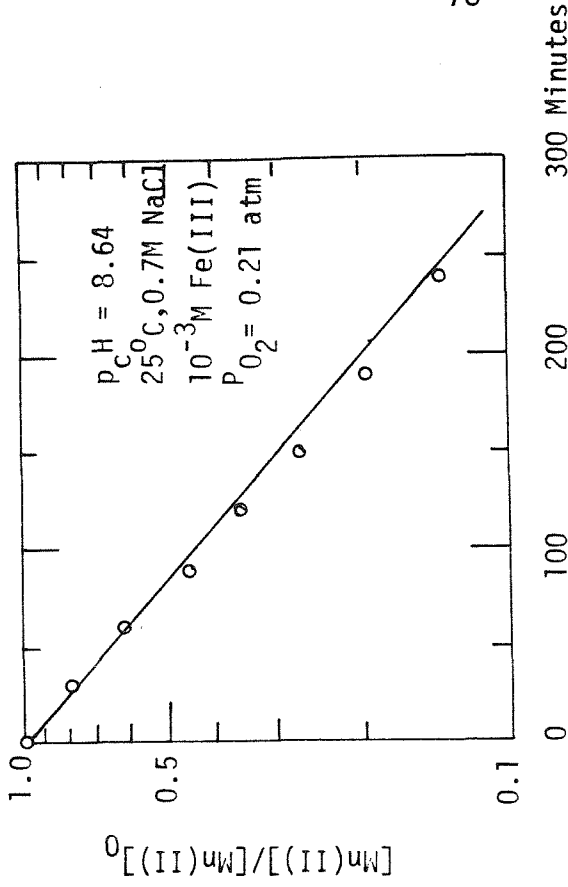
Figure 5.5 Test of first-order kinetics for Mn(II) removal when surface was in prior equilibrium with respect to adsorption before O_2 bubbling. Regression gave: $\log([Mn(II)]/[Mn(II)]_0) = -0.0037t + 0.0038; r^2 = 0.99$. The surface was generated by procedure A.
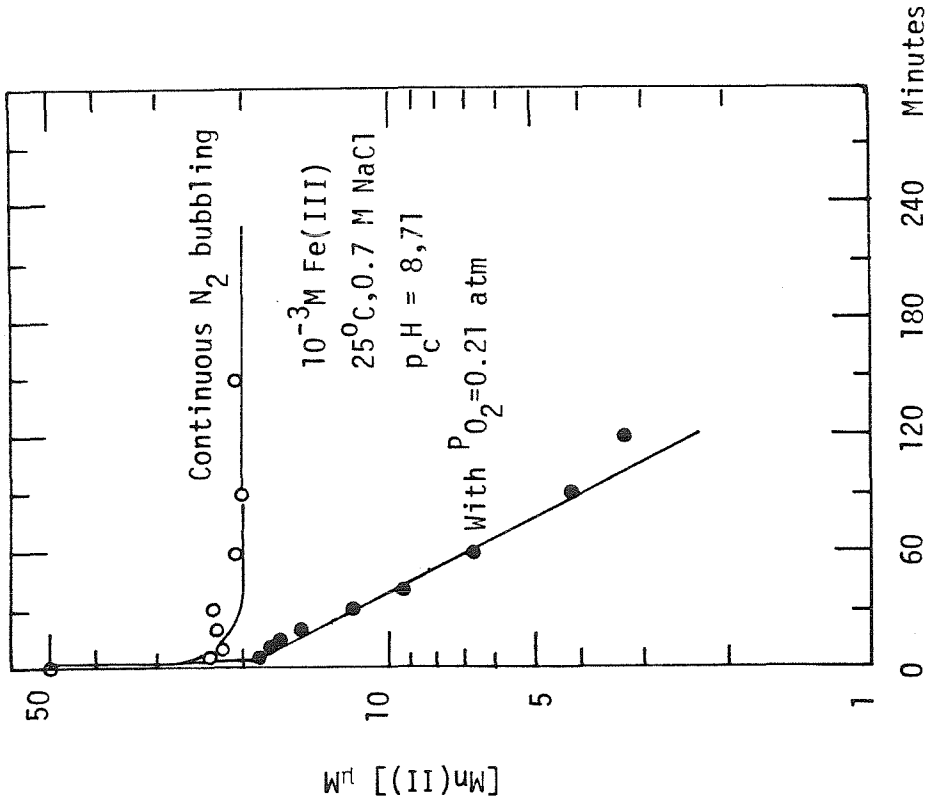
Figure 5.4 Removal kinetics of Mn(II) with γ-FeOOH in the presence and absence of oxygen. The surface was generated by procedure B.
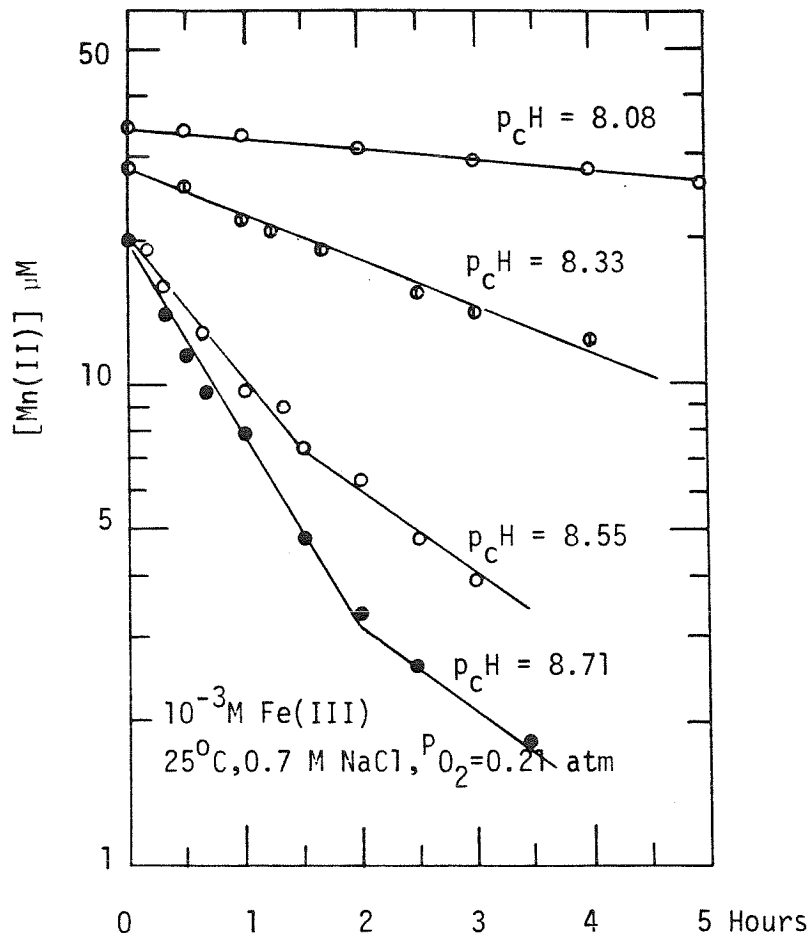
Figure 5.6 The effect of pH on the oxygenation removal kinetics of Mn(II) with γ-FeOOH.The surface was in prior equilibrium with respect to adsorption before the introduction of oxygen. The surface was generated by procedure B.

$$[MnO_x]_{surface} = [Mn]_{total} \{1 - \exp(-k't)\} \tag{5.8}$$

Equation (5.8) would tend to overestimate the rate of formation of MnO_x on the surface at longer times for the reasons discussed above. We note that at $t = 0$, $[MnO_x]$ surface $= 0$; for small t (on the order of 10 minutes) we can approximate the exponential by $1 - k't$ and $[MnO_x]_{surface}$ becomes a linear function of time; as $t \to \infty$, $[MnO_x]_{surface} \to [MnO_x]_{total}$. We calculate the initial rate of MnO_x formation at pH 8.7 to be about $8 \times 10^{-7} M\ min^{-1}$. Matsui (1973) studied the rate of oxygen transfer by bubbling air under similar laboratory conditions. The rate of oxygen solution was given as:

$$[O_2] = [O_2]_{saturation} \{1 - \exp(-bt)\} \tag{5.9}$$

Saturation concentration of oxygen in 0.7 M NaCl and 25°C is about 2.13×10^{-4} M. b was a transfer coefficient determined by Matsui (1973) to be 3.8 min^{-1}. Conservatively allowing a factor of 100 lower than 3.8 min^{-1} for our system the rate of oxygen supply for the first 10 minutes was calculated to be 5.5×10^{-6} M min^{-1}. Since one mole of O_2 can oxidize two moles of Mn(II), our rate of oxygen supply is at least a factor of 14 greater than needed, and assumption 3 is justified.

5.2.2 Rate Law Formulations

In this section we examine the effect of pH and the amount of iron oxide surface on the oxygenation removal kinetics of Mn(II). The key result is the value of $\tau_{1/2}$ obtained by linear regression of the

initial logarithmic variation of Mn(II) with time. We define k'
= $\ell n2/\tau_{1/2}$. Initial rates of surface oxidized species formation were
calculated by differentiating (5.8):

$$\frac{d[MnO_x]_{surface}}{dt} = [Mn]_{total} \, k' \exp(-k't) \qquad (5.10)$$

The time scale of 5 minutes was arbitrarily chosen to study the
initial rates. Tables 5.1 and 5.2 summarize the dependence of $\tau_{1/2}$ on
pH and the amount of iron oxide surface. Figures 5.7 and 5.8 show the
dependence graphically. The observed rate can be described by:

$$\frac{d[MnO_x]_{surface}}{dt} = constant \frac{Fe(III)_{total}}{[H^+]^2} \qquad (5.11)$$

Part of the proton concentration dependence comes from the
adsorption equilibrium of Mn(II) on the surface. Another part of the
proton dependence must involve the oxidative step. A detailed mechanistic
interpretation cannot be tested with the data at hand. Kaneko and Inouye
(1979) studied the adsorption of water on ferric oxyhydroxide. They also
reported (1976) on chemisorption of oxygen on the γ-FeOOH surface.
Electrical conductivity measurement results were interpreted as a defect
property of the surface. Possibly a reasonable model would include the
adsorption of aqueous oxygen on the surface prior to surface oxidation,
e.g.,
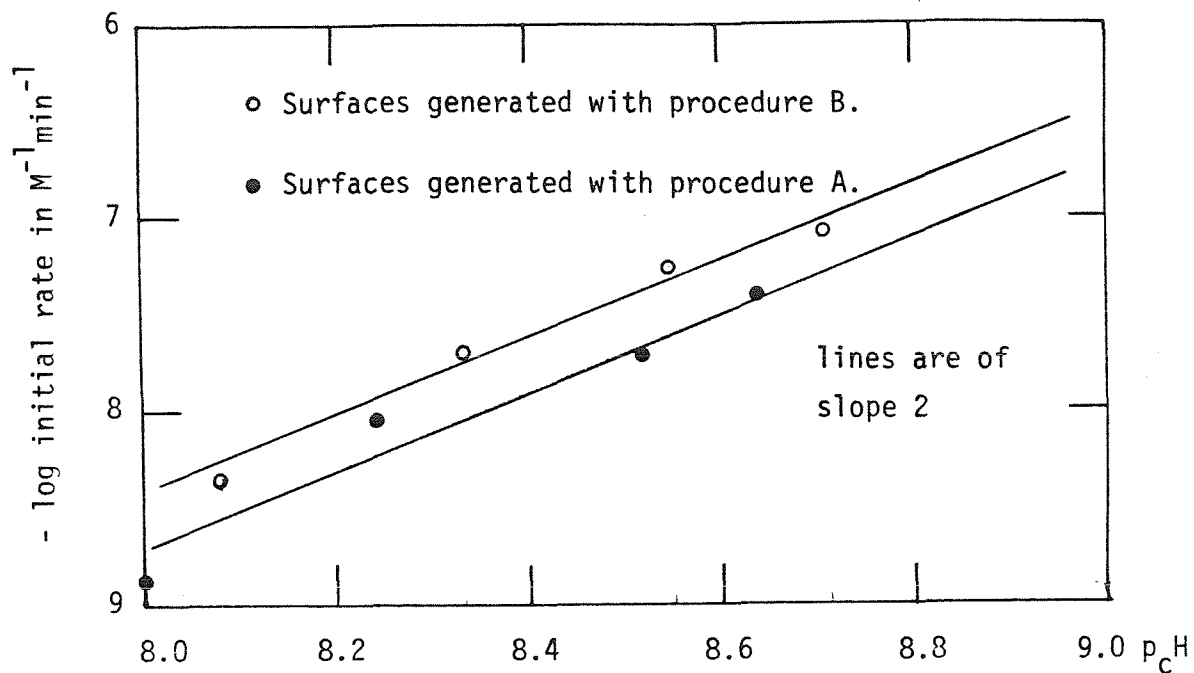
Figure 5.7 The effect of pH on the initial rate of surface oxidized Mn formation. See Table 5.1
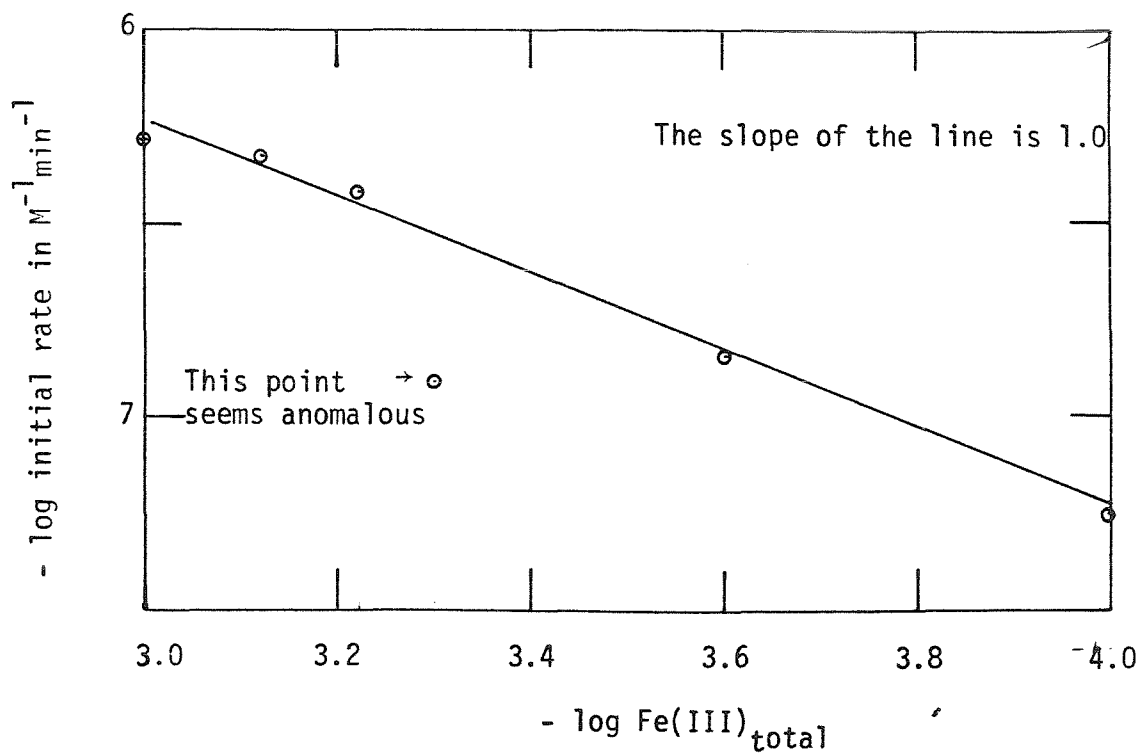
Figure 5.8 The effect of total ferric loading on the initial rate of formation of surface oxidized manganese. The surfaces were generated by procedure B.

TABLE 5.1 $\tau_{1/2}$ as a function of pH

$10^{-3}M$ γ-FeOOH, 0.7 M NaCl, 25°C

Surface prepared by procedure A

pH	$[Mn(II)]_0(\mu M)^a$	$\tau_{1/2}(min)$	Initial rate of formation of $[MnO_x](M\ min^{-1})^b$
8.00	40.0	2559	1.35×10^{-8}
8.24	35.5	370.7	9.26×10^{-8}
8.52	32.5	174	1.95×10^{-7}
8.64	27.5	83.7	3.98×10^{-7}

log $\tau_{1/2}$= -2.17pH + 20.66 r^2=0.95   log initial rate=2.14pH - 24.92 r^2=0.95

Surface prepared by procedure B

8.08	34.7	785	4.40×10^{-8}
8.33	28.5	164.9	2.06×10^{-7}
8.55	20.0	57.8	5.50×10^{-7}
8.71	20.3	36.8	8.57×10^{-7}

log $\tau_{1/2}$= -2.13pH + 20.08 r^2=0.98   log initial rate= 2.06pH - 23.97 r^2=0.98

a. $[Mn(II)]_0$ is the equilibrium $[Mn(II)]$ in solution prior
   to oxygen bubbling. $[Mn]_{total}$ = 50 μM.

b. Calculated initial rate at 5 minutes with Equation (5.10)

TABLE 5.2 $\tau_{1/2}$ as a function of Fe(III)$_{total}$

surface prepared by procedure B, pH = 8.55, T = 25°C

Fe(III)$_{total}$ (x10^{4}M)	[Mn(II)]$_0^a$ μM	$\tau_{1/2}$ (min)	Initial rate of MnO$_x$ formation (M min^{-1})^b
10	19.9	57.8	5.28x10^{-7}
7.5	23.8	65.2	4.75x10^{-7}
6.0	27.7	82.0	3.87x10^{-7}
5.0	31.2	218.6	1.54x10^{-7}
2.5	40.4	233.0	1.44x10^{-7}
1.0	42.5	610.0	0.56x10^{-7}

a. [Mn(II)]$_0$ is the equilibrium [Mn(II)] in solution prior to oxygen bubbling. [Mn]$_{total}$ = 50 μM

b. Calculated using equation (5.11) at 10 minutes.

Linear regression : $\tau_{1/2}$ = 6.24X10^{-2}(Fe(III))$^{-1}$ - 14.9 r^2= 0.96

log initial rate = 1.02 log[Fe(III)]$_{total}$ - 3.17

r^2 = 0.99

$$O_2(aq) + S \overset{K^*}{\rightleftharpoons} O_2 \text{ adsorbed} \qquad (5.12)$$
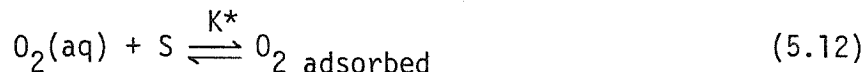
If the adsorption of oxygen also displaces a proton, we would have the $[H^+]^2$ dependence. Preliminary studies show that adsorption of oxygen, if it occurs in solution, would involve very small amounts and below our measurement capabilities (about 15 μM using an Orion oxygen electrode). Alternatively, we would assign the proton dependence to the oxidation step. The experimental data could be described by the following rate law:

$$\frac{d[MnO_x]_{surface}}{dt} = k_s [Mn(II)]_{ads} [O_2]_{ads}$$

$$= \frac{k_s K^*}{[H^+]} \frac{K'Fe(III)_{total}}{[H^+]} [O_2][Mn(II)] \qquad (5.13)$$

where we could obtain the combined rate constant $k_s K^*$ in units min^{-1}. The observed initial rates were tested with this formulation and $k_s K^*$ was calculated to be $1.8 \pm 0.7 \times 10^{-7}$ min^{-1}. (Average of eight values for surfaces prepared by both procedures A and B.)

Brewer (1975) reported the surface catalytic rate of Mn(II) oxygenation on colloidal MnO_2. The rate law was given as:

$$\frac{-d[Mn(II)]}{dt} = k_{Mn} [OH^-]^2 [MnO_2] [O_2] [Mn(II)] \qquad (5.14)$$

k_{Mn} was reinterpreted by Emerson et al. (1980) to be 5×10^{18} $M^{-4} d^{-1}$.

Equation (5.13) can be rewritten for the rate of change of Mn(II):

$$-\frac{d[Mn(II)]}{dt} = \frac{k_s K^* K'}{K_w^2} [OH^-]^2 \, Fe(III)_{total} \, [O_2] \, [Mn(II)] \qquad (5.15)$$

We define k_{Fe} to be $k_s K^* K'/K_w^2$. Using results from this study, k_{Fe} was calculated to be $2.0 \times 10^{18} \, M^{-4} \, d^{-1}$. So the γ-FeOOH surface can be just as effective as colloidal MnO_2 in catalysing Mn(II) oxygenation. Formation of ferric oxyhydroxide under most natural water conditions would be easier to accomplish, however.

5.3 Implications for Natural Systems

We can estimate the reaction time scales for Mn(II) in natural waters using Equation (5.15). For seawater-like systems, $[OH^-]$ is reported by Dyrssen and Wedborg (1974) to be $10^{-5.65}M$; saturation $[O_2]$ is about $2 \times 10^{-4}M$; $Fe(III)_{total}$ was chosed to be about 10 μM from Boyle et al. (1977). The rate then becomes:

$$-\frac{d[Mn(II)]}{dt} = 2.0 \times 10^{-2} d^{-1} [Mn(II)]$$

and the half-life calculated to be about 35 days. Emerson et al. (in press) studied redox species in Saanich inlet and modeled the Mn(II) profile in the water column with a vertical eddy diffusion coefficient and a first order removal rate. The calculated residence time of Mn(II) was on the order of 2 days, and was interpreted as bacterial catalysis. Other calculated residence times for Mn(II) in seawater range from 6

to 50 years (see Spencer and Brewer, 1971 and Emerson et al. in press).

Mn(II) behavior in estuaries has been reported by Moore et al. (1979), Morris and Bale (1979) and Wollast et al. (1979). The latter two investigations reported removal times of Mn(II) in reaerated river waters on the order of days. Morris and Bale (1979) in particular reported zero-order kinetics with respect to dissolved manganese for the loss of dissolved manganese in natural river waters, the rate being proportional to the amount of particulate load. They also reported that removal of dissolved manganese from estuarine waters approximated to first-order kinetics with respect to dissolved manganese. The present study is in accord with these observations.

CHAPTER 6

SUMMARY AND CONCLUSIONS

The cycling of iron and manganese in natural systems depends strongly upon their redox chemistries, and is of interest in environmental science. This work presents new experimental data on the oxygenation kinetics of Fe(II) in aqueous systems and on the identity of the solid phase formed in the reaction. New experimental data on the surface oxidation kinetics of Mn(II) in the presence of γ-FeOOH are also presented.

The experimental data on oxygenation kinetics of Fe(II) or Mn(II) in aqueous systems at constant pH and P_{O_2} can be adequately described by the following integrated rate expression:

$$X = \frac{X_0(k_1+k_2X_0)}{k_2X_0 + k_1\exp[(k_1+k_2X_0)t]} \qquad (6.1)$$

where X stands for [Fe(II)] or [Mn(II)],the subscript 0 stands for the concentration at t=0; k_1 is the homogeneous rate constant in units of min^{-1},and k_2 is the heterogeneous rate constant in units of $M^{-1}min^{-1}$. The half-life in this context is:

$$\tau_{\frac{1}{2}} = \frac{\ln[(2k_1+k_2X_0)/k_1]}{k_1+k_2X_0} \qquad (6.2)$$

If $k_1 \gg k_2X_0$, equations(6.1) and (6.2) reduce to their first-order counterparts:

$$X = X_0\exp(-k_1t) \qquad (6.3)$$

$$\tau_{\frac{1}{2}}=\frac{\ln2}{k_1} \qquad (6.4)$$

Although the rate expressions for both Fe(II) and Mn(II) are similar, the relative importance of the homogeneous rate and the heterogeneous rate is quite different in each case. In the following discussion, we will use k_1 to denote the homogeneous rate constant and $k_2 X_0$ to denote the effective heterogeneous rate constant. The concentration of either Fe(II) or Mn(II) for purposes of illustration is taken to be at the ppm level(e.g. 50 μM).

In the case of Fe(II) oxygenation, k_1 was shown to be dependent on ionic strength(I), temperature(T) and solution anion(X^-) concentration, in addition to the generally reported $[OH^-]^2$ and P_{O_2} dependence. i.e.

$$k_1 = k(I,T,X^-)[OH^-]^2 P_{O_2} \qquad (6.5a)$$

$$= k'(I,T,X^-)[OH^-]^2[O_2] \qquad (6.5b)$$

k is in units of $M^{-2} atm^{-1} min^{-1}$, k' is related to k by the Henry's law constant for oxygen solubility and has units of $M^{-3} min^{-1}$. The effective heterogeneous rate constant for Fe(II) is a combination of a surface oxidation rate constant and an adsorption equilibrium constant. The surface formed by Fe(II) oxygenation is apparently an excellent catalyst for Fe(II) oxygenation (judging from the high numerical value of the surface rate constant = 4380 $M^{-1} min^{-1}$) and the $k_2 X_0$ term is limited only by the ability of the surface to adsorb Fe(II). Using an electrostatic model, we would predict that adsorption of positively charged ions such as Fe^{2+} would only be promoted by a negatively charged surface. The pH_{zpc}

values for ferric oxyhydroxides are generally reported to be around pH 7. Consequently,Fe(II) oxygenation is dominated by the k_1 term for pH < ca.7. k_1 and $k_2 X_0$ are comparable in magnitude for pH 7-8.

On the other hand, the homogeneous rate of Mn(II) oxygenation is difficult to study because of its slowness when pH < 9. Experimental conditions that promote faster rates introduce ambiguity due to Mn(II) phase supersaturations. The observed rates for pH > 9 are dominated by the heterogeneous rate, due in no small part to the efficiency of adsorption of the oxidized product surface for Mn(II). The pH_{zpc} for colloidal manganese dioxide is generally reported to be around pH 2. The $[OH^-]^2$ dependence of $k_{obs.}$ is also dominated by the $k_2 X_0$ term. While in some cases k_1 for Mn(II) oxygenation can be shown to have a $[OH^-]^2$ dependence (HCO_3^-/CO_3^{2-} medium), in other cases the pH dependence of k_1 is more complex (e.g. in NH_3/NH_4^+ buffers) and may reflect complexation effects also. However,the oxygenation rate of ppm levels of Mn(II) between pH 8 - 9 was shown to be slow and required on the order of days before we could observe measurable oxygenation.

Comparison of the infrared spectra of products of our oxygenation experiments under various solution conditions with the infrared spectra of standard ferric oxyhydroxides showed that the product spectrum was invariably closest to that of γ-FeOOH, lepidocrocite. This observation was confirmed by comparison of the X-ray diffraction patterns of the Fe(II) oxygenation product with that of standard lepidocrocite.

The γ-FeOOH surface was investigated with respect to its catalytic effect on Mn(II) oxygenation kinetics. In a seawater-like medium (0.7 M NaCl and mM levels of $NaHCO_3$), adsorption of Mn(II) is noticeable for pH > 7 and can be modeled as a surface-complex formation. The surface showed an added capacity for Mn(II) removal in the presence of dissolved oxygen and reduced the half-life of Mn(II) from days to hours. The initial rate of formation of surface oxidized Mn was shown to have a $[OH^-]^2$ dependence, and was proportional to the total amount of ferric oxyhydroxide in solution. A model of surface oxidation accounts well for these observations.

Suggestions for future work:

1. The ferric oxyhydroxide surface should be studied with respect to dissolved oxygen adsorption.

2. The influence of some representative organic ligands on the adsorption and catalytic properties of the ferric oxyhydroxide surface should be studied.

3. The influence of temperature on the adsorption and catalytic properties of the ferric oxyhydroxide surface should be examined.

APPENDIX A

THE BICARBONATE/CARBON DIOXIDE BUFFER SYSTEM

Oxygenation of Fe(II) and Mn(II) produces protons. In order to keep pH essentially constant we require some sort of buffer. The HCO_3^-/ CO_2 buffer was chosen because it is the predominant buffer in nature.

Following Stumm and Morgan(1970), we define the acid-neutralizing capacity, or alkalinity as:

$$Alk. = [HCO_3^-] + 2[CO_3^{2-}] + [OH^-] - [H^+] \qquad (A.1)$$

For solutions with pH less than 9 and alk. on the order of milli-equivalents/L we can neglect the terms following the bicarbonate.

$$Alk. \simeq [HCO_3^-]$$

The following equilibrium constants are defined:

$$\frac{\{H^+\}[HCO_3^-]}{[H_2CO_3^*]} = K_1' \qquad (A.2)$$

$$\frac{[H_2CO_3^*]}{P_{CO_2}} = K_{CO_2} \qquad (A.3)$$

where $[H_2CO_3^*] = [CO_2] + [H_2CO_3]$.

Then we have the following relation:

$$Alk. = [NaHCO_3]_0 = K_1' K_{CO_2} P_{CO_2} / \{H^+\} \qquad (A.4)$$

For 0.7 M NaCl, it is preferable to use $[H^+]$:

$$Alk. = {}^cK_1 K_{CO_2} P_{CO_2} / [H^+] \qquad (A.5)$$

i.e. $p_cH = \log(alk.) - \log(P_{CO_2}) - \log({}^cK_1 K_{CO_2}) \qquad (A.6)$

The product ${}^cK_1 K_{CO_2}$ was measured experimentally in this study to be $2.77 \pm 0.19 \times 10^{-8} M^2 atm^{-1}$. For seawater, Stumm and Morgan(1970) reported

K_{CO_2} = 0.0295 Matm^{-1} and $^cK_1 \simeq 10^{-6.02}$ M at 25°C; therefore, the product $^cK_1K_{CO_2}$ = 2.82X10^{-8}M^{2}atm^{-1}, in a seawater medium. The agreement is quite satisfactory.

APPENDIX B

MEASUREMENTS OF pH

This appendix summarizes the procedure used to calibrate the glass electrode. For conventions and detailed discussions see Bates(1975). The pH of the solutions in this study was monitored with a Beckman glass electrode and an Orion double-junction reference electrode (inner chamber matches characteristics of standard KCl calomel electrode) via an Orion 801A pH meter.

For Fe(II) experiments with I $\leq$ 0.11 M, the outer chamber of the reference electrode was filled with the 10% KNO_3 solution provided, and the electrode calibrated with pH 4.00 and 7.00 NBS buffers. [OH^-] was calculated from the measured pH = - log {H^+} and the compiled K_w={H^+}{OH^-} from Harned and Owen(1958), using the Davies equation (see Stumm and Morgan, 1970) to estimate the activity coefficient of OH^-.

For I > 0.11 M, the outer chamber of the reference electrode was filled with a solution of the major ions of the experimental solution (e.g.0.7M NaCl). HCl solutions of different concentrations, at the same ionic strength, were obtained by diluting 0.1 N HCl(from Dilutit$^{®}$) with warious amounts of NaCl. This was to minimize the variation of the junction potentials. A calibration curve was obtained by the use of the Nernst equation:

$$E = E_0' + \frac{RT}{F}\log[H^+] \qquad (B.1)$$

where E is the potential registered by the glass-reference electrode pair. E_0' a standard potential that incoporates the activity coefficient of the proton and liquid-junction potentials. Figure B.1 shows a calibration. Solution pH was calculated from knowing E and E_0'.
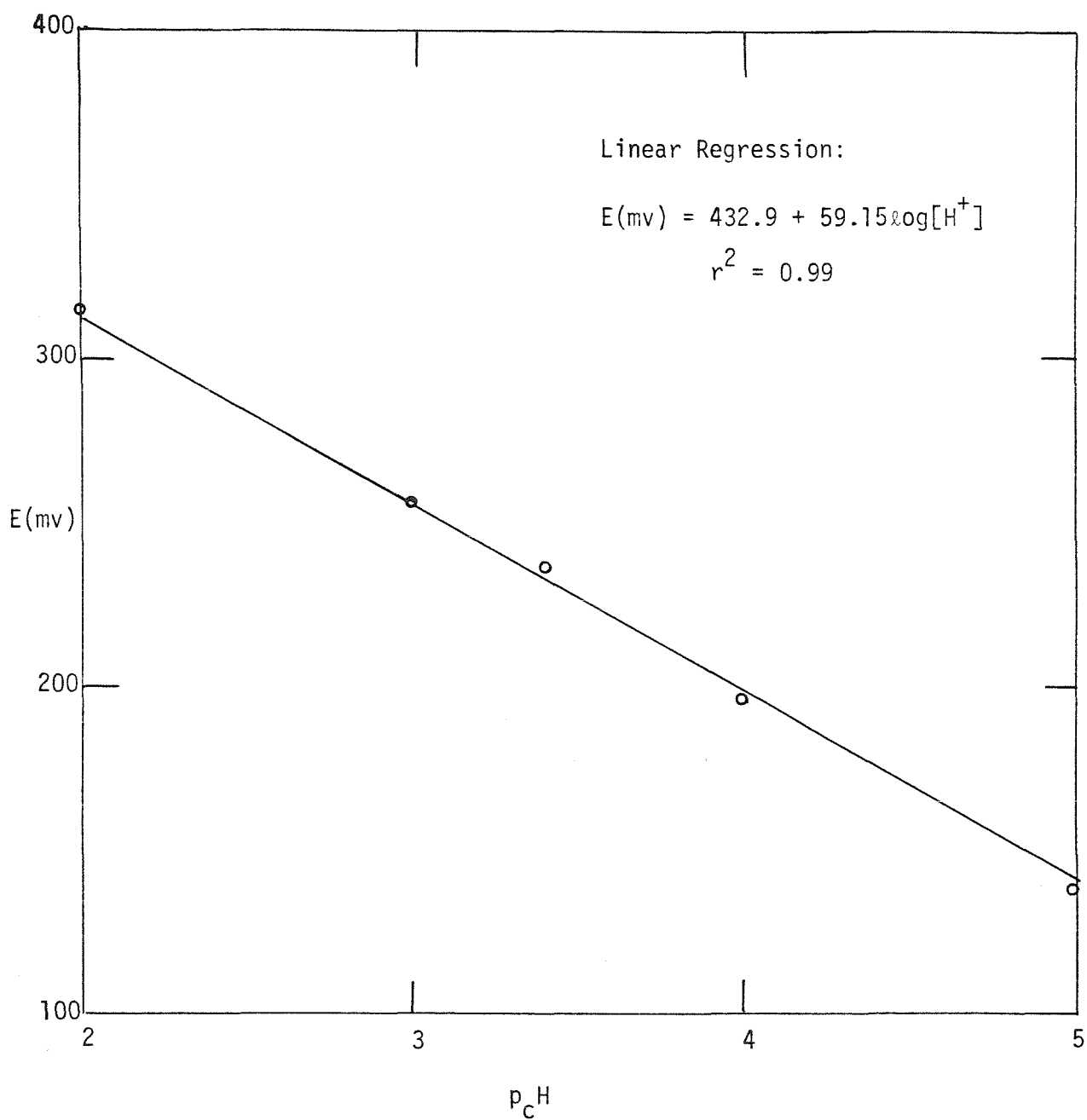
Figure B.1 Typical calibration curve of glass-reference

electrode. 25°C; total ionic strength = 0.7 M Cl⁻.

APPENDIX C

SYNTHETIC PROCEDURE FOR STANDARD Fe(III) OXYHYDROXIDES

This appendix summarizes the procedures for synthesizing standard ferric oxyhydroxides. These standard ferric oxyhydroxides were used to obtain standard X-ray diffraction patterns and infrared spectra for identification purposes. Table C.1 summarizes some of the more important characteristics of these solids.

I. Synthesis of α-FeOOH, goethite.

Goethite was prepared according to the method of Atkinson et al.(1967).

1. Fifty-g of reagent grade $Fe(NO_3)_3 \cdot 9H_2O$ (M.W.403.85) was weighed out and dissolved in 825 mL of distilled deionized water.

2. Two hundred mL of 2.5 N KOH was added to the solution with mixing; rapid precipitation should occur. The Fe/OH ratio = 0.25 and the final pH should be near 12. The precipitate is golden-yellow in color.

3. The precipitate was aged in the original solution for 24 hours in a $60^{\circ}C$ oven.

4. The precipitate was centrifuged and washed with distilled deionized water. It could be freeze-dried or dried in a $60^{\circ}C$ oven.

   Balistrieri(1977) used the same procedure. BET N_2 specific surface area ranged from 48.5 to 70.9 m^2/g. A sample of goethite was obtained from Dr.G.R.Rossman of Caltech(Pfeizer Minerals and Pigments).

II. Synthesis of β-FeOOH, akaganeite.

Matijevic and Scheiner (1978) discussed the morphology of synthetic akaganeite by hydrolysing $FeCl_3$ in HCl. Nightingale and Benck(1960)

discussed the use of complexing agents (N,N-dihydroxyethylglycine) in obtaining crystalline β-FeOOH. This study used the following procedure:

1. An amount of 15.75 g of $FeCl_3.6H_2O$ was weighed out and dissolved in one-liter 10^{-3}M HCl.

2. The solution was filtered through 0.22 μm Millipore® filter.

3. The solution was placed in 20 mL aliquots in test-tubes.

4. The test-tubes were sealed and placed in a 100^oC oven overnight.

5. The precipitate is reddish-brown in color and can be washed and dried as in the case for goethite. BET N_2 specific surface area is about 8 m^2/g.

III. Synthesis of γ-FeOOH, lepidocrocite.

Baudisch and Albrecht(1932) first synthesized gamma ferric hydroxide with the use of pyridine.

1. An amount of 19.88 g of $FeCl_2.4H_2O$ was weighed out and dissolved under N_2 bubbling in 500 mL distilled deionized water.

2. The greenish solution was filtered through 0.22 μm Millipore® filter.

3. Fifty-mL of pyridine was added. A greenish-black precipitate should form.

4. Air was bubbled into the solution for 30 min. An orange-red precipitate should form.

5. The precipitate was allowed to settle, decant and washed free of Cl^-. It was then dried as before.

A sample of γ-FeOOH was obtained from Dr.D.L.Janes of the 3M company.

IV.Synthesis of amorphous ferric hydroxide.

There exist in the literature several recipes for amorphous ferric

hydroxide. See Kauffman and Hazel,1975; and Gadde & Latinen (1974). The pro-

cedure adopted here is a similar procedure to that employed by Dr.J.O.Leckie's

group at Stanford University.

1.One hundred mL of 3.5 M NaCl, 5 mL of 1.0 M $NaHCO_3$ was mixed with 345

   mL of distilled deionized water.

2.Pre-mixed gas with P_{CO_2} = 0.0018 atm was bubbled until pH stabilizes

   about 8.3.

3.Fifty mL of stock 10^{-2}M $Fe(ClO_4)_3$ was added.

4.The precipitate was aged for 4 hours, filtered and dried in a

   dessicator.

Samples of amorphous ferric hydroxide were obtained from K.Hayes

of Stanford University(Dept.Civil Engineering,1978) and D.Wilson,formerly

with the army corp. of engineers,Waterways Experimental Station,Vicksburg,

Mississippi.(1978)

Table C.1   SOME CHARACTERISTICS OF THE FERRIC OXYHYDROXIDES

Mineral	X-Ray Diffraction Spacings (1)	Infra-Red Absorption Peaks (cm^{-1}) (2)	Solubility Products	pH zpc By Acidimetric titration
Goethite α-FeOOH	4.18,2.69,2.45	900,780,600,400	pFe + 3pOH = 43.3-44.0 (3)	7.5 ± 0.1 (7)
Akaganeite β-FeOOH	7.40,3.31,1.635	840,660,380	pFe + 3pOH = 38.43±0.06 (4)	8.1 (8)
Lepidocrocite γ-FeOOH	6.26,3.29,2.47	1020,750,460,350	pFe + 3pOH = 39.5 (5) = 40.6-42.5 (6)	6.8 this study
Amorphous ferric oxyhydroxide	Nil	3 small peaks at 1610,1470,1330 and a broad peak at 430	pFe + 3pOH = 37.0-39.4 (6)	7.9 (9)

(1) Only the 3 strongest lines are recorded from ASTM files. Burns and Burns (1977) lists eight diffraction lines.

(2) There are some differences in the positions of the peaks between this study and other reports due to different machines and operating conditions.

(3) After Schwertmann and Taylor (1977).

(4) After Makovskaya and Spivakovskii (1974), their compound had a chemical formula of $Fe(OH)_{2.86}Cl_{0.14}$.

(5) After Misawa (1973)

(6) After Schwertmann and Taylor (1977), table 5-1 of this report lists much other useful information.

(7) Ballistieri (1977).

(8) Murray (1978).

(9) Davis and Leckie (1978).

REFERENCES

Adamson, A. D. (1967) Physical Chemistry of Surfaces, 2nd ed. Wiley-Interscience, New York.

Anderson, B. J., E. A. Jenne and T. T. Chao (1973) The sorption of silver by poorly crystallized manganese oxides. Geochim. Cosmochim. Acta 37, 611-622.

Asada, H. (1959) Study on manganese treatment in polluted supply-water. Suido Kyokai Zasshi (Japan) No. 293, 26-29.

Atkinson, R. J., A. M. Posner and J. P. Quirk (1967) Adsorption of potential-determining ions at the ferric oxide-aqueous electrolyte interface. J. Phys. Chem. 71 (3), 550-558.

Baes, C. F. and R. E. Mesmer (1976) The Hydrolysis of Cations. Wiley, New York.

Balistrieri, L. S. (1977) The Basic Surface Characteristics of Geothite. M.S. thesis, University of Washington. Seattle, Washington.

Balistrieri, L. S. and J. W. Murray (1979) Surface of goethite (α-FeOOH) in seawater. E. Q. Jenne, editor, Chemical Modeling in Aqueous Systems: Speciation, Solubility and Kinetics. A.C.S. Symposium, series 93.

Bates, R. G. (1975) pH scales for seawater. E. D. Goldberg, editor, The Nature of Seawater, Dahlem Workshop Report, Berlin, Germany.

Baudisch, O. and W. H. Albrecht (1932) Gamma-ferric oxide hydrate. J. Am. Chem. Soc. 54, 943-947.

Bockris, J. O'M. and A. K. N. Reddy (1970) Modern Electrochemistry. 2 volumes, Plenum Publish. Corp. New York.

Bowen, H. J. M. (1966) Trace Lements in Biochemistry. Academic Press, New York.

Boyle, E. Q., J. M. Edmond and E. R. Sholkovitz (1977) The mechanism of iron removal in estuaries. Geochim. Cosmochim. Acta 41, 1313-1324.

Breeuwsma, A. (1973) Adsorption of Ions on Hematite (α-Fe_2O_3). H. Veenman and Zonen B. V.-Wageningen, The Netherlands.

Brewer, P. G. (1975) Minor elements in seawater. J. P. Riley and G. Skirrow, editors, Chemical Oceanography, 1,445-496. Academic Press, New York.

Bricker, O. (1965) Some stability relations in the system Mn-O_2-H_2O at 25° and one atmosphere total pressure. Amer. Mineral, 50, 1296-1354.

Burns, R. G. and V. M. Burns (1977) Mineralogy of ferromanganese nodules. G. P. Glasby, editor, Marine Manganese Deposits, Elsevier, New York.

Coughlin, R. W. and I. Matsui (1976) Catalytic oxidation of aqueous Mn(II). J. of Catalysis 41, 108-123.

Davis, J. A. and J. O. Leckie (1978) Surface ionization and complexation at the oxide/water interface. J. Colloid Interface Sci. 67, 90-107.

Dyrssen, D. and M. Wedborg (1974) Equilibrium calculations of the speciation of elements in seawater. E. D. Goldberg, editor, The Sea. v. 5, Marine Chemistry. Wiley-Interscience, New York.

Emerson, S., R. E. Cranston and P. S. Liss (in press). Redox species in a reducing fjord: equilibrium and kinetic considerations.

Ewing, F. J. (1935) The crystal structure of lepidocrocite. J. Chem. Phys. 3, 420-424.

Forbes, E. A., A. M. Posner and J. P. Quirk (1974) The specific adsorption Hg(II) species and Co(III) complex ions on geothite. J. Colloid. Interface Sci. 49, 403-409.

Forbes, E. A., A. M. Posner and J. P. Quirk (1976) The specific adsorption of divalent Cd, Co, Cu, Pb and Zn on goethite. J. Soil S . 27(2), 154-166.

Gadde, R. Rao and H. A. Laitinen (1974) Studies of heavy metal adsorption by hydrous iron and manganese oxides. Anal. Che. 46 (13), 2022-2026.

Ghosh, M. M., J. T. O'Connor and R. S. Engelbrecht (1966) Precipitation of iron in aerated ground waters. ASCE J. Sanit. Engr. Div. 16(SAI), 199-213.

Goldberg, E. D. (1954) Chemical scavengers of the sea. J. Geol. 62, 249-265.

Goldberg, E. D. (1961) Chemistry in the oceans. M. N. Hill, editor, Oceanography, Amer. Assoc. Adv. Sci. Publ. no. 67.

Goto, K., H. Tamura and M. Nagayama (1970) The mechanism of oxygenation of ferrous ion in neutral solution. J. Inorg. Chem. 9(4), 962-964.

Grimme, H. (1968) Die adsorption von Mn, Co, Cu und Zn durch goethit aus verdüennten löesungen. Z. Pflanzern Dürg. Bodenk 121, 58-65.

Hammond, G. S. and C. H. S. Wu (1968) Oxidation of iron(II) chloride in nonaqueous solvents. R. F. Gould, editor, Oxidation of Organic Compounds (III), Adv. Chem. Ser. 77.

Harned, H. S. and B. B. Owen (1958) The Physical Chemistry of Electrolytic Solutions. 3rd ed. Reinhold Publ. Corp. New York.

Hem, J. D. (1963) Chemical equilibria and rates of manganese oxidation. U. S. Geol. Survey Water-Supply Paper 1667-A, 64 p.

Hem, J. D. (1972) Chemical factors that influence the availability of iron and manganese in aqueous systems. Geol. Sco. Amer. Special Paper 140, 17-24.

Hem, J. D. (1978) Redox processes at surfaces of manganese oxide and their effects on aqueous metal ions. Chem. Geol. 21, 199-218.

Hunt, J. R. (1980) Coagulation in Continuous Particle Size Distributions: Theory and Experimental Verification. Ph.D. thesis, California Institute of Technology, Pasadena, California.

Jenne, E. A. (1968) Controls on Mn, Fe, Co, Ni, Cu and Zn concentrations in soils and water: the significant role of hydrous Mn and Fe oxides. R. F. Gould, editor, Trace Inorganics in Water. Adv. Chem. Ser. 73.

Jones, P. and J. A. Hockey (1971) Infra-red studies of rutile surfaces-hydroxylation, hydration and structure of rutile surfaces. Trans. Faraday Soc. 67, 2679-2685.

Kaneko, K., M. Serizawa, T. Ishikawa and K. Inouye (1975). Dielectric behavior of water molecules adsorbed on iron (III) oxide hydroxides. Bull. Chem. Soc. Jpn. 48, 1764-1769.

Kaneko, K. and Inouye (1976) Electrical conductivity as a defect property of γ-FeOOH. J. Chem. Soc. Faraday Trans. 1, 72, 1258-1266.

Kaneko, K. and K. Inouye (1979) Adsorption of water on FeOOH as studied by electrical conductivity measurements. Bull. Chem. Soc. Jpn. 52, 315-320.

Kauffman, K. and F. Hazel (1975) Infrared and Mössbauer spectroscopy, electron microscopy and chemical reactivity of ferric chloride hydrolysis products. J. Inorg. Nucl. Chem. 37, 1139-1148.

Kessick. M. A., J. Vuceta and J. J. Morgan (1972) Spectrophotometric determination of oxidized manganese with leuco crystal violet. Env. Sci. Tech. 6, 642-644.

Kester, D. A., R. H. Byrne and Y. J. Liang (1975) Redox reactions and solution complexes of iron in marine systems, T. M. Church, editor, Marine Chemistry in the Coastal Environment. A.C.S. Symposium series 18.

Krauskopf, K. B. (1956) Factors controlling the concentrations of thirteen rare metals in seawater. Geochim. et Cosmochim. Acta. 9, 1-26.

Landa, E. R. and R. G. Gast (1973) Evaluation of crystallinity in hydrated ferric oxides. Clays and Clay Minerals. 21, 121-130.

Larson, T. E. (1967) Oxidation of metals and ions in solution. S. D. Faust and J. V. Hunter, editors, Principles and Applications of Water Chemistry. Wiley and Sons, Inc., New York.

Liang, Y. J. and D. R. Kester (1977) Kinetics of ferrous oxygenation in aqueous media. EOS, Trans. A.G.U. 58, 1168.

Loganathan, P. and R. G. Burau (1973) Sorption of heavy metal ions by a hydrous manganese oxide. Geochim. et Cosmochim. Acta 37, 1277-1293.

Makovskaya, G. V. and V. B. Spivakovskii (1971) Conditions for the precipitation of iron (III) basic chlorides and hydroxide from chloride solutions. Russ. J. Inorg. Chem. 16, 18.

Mason, B. (1958) Principles of Geochemistry, 2nd ed. Wiley & Sons, Inc., New York.

Matijevic E. and P. Scheiver (1978) Ferric hydrous oxide sols III. J. Colloid Interface Sci. 63, 509-524.

Matsui, I. (1973) Catalysis and Kinetics of Manganous Ion Oxidation in Aqueous Solution and Adsorbed on the Surfaces of Solid Oxides. Ph.D. thesis, Lehigh University. Bethlehem, Pennsylvania.

Michelson, A. M., J. M. McCord and I. Fridovich (1977), editors, Superoxide and Superoxide Dismutases. Academic Press, New York.

Misawa, T. (1973) The thermodynamic consideration for $Fe-H_2O$ system at 25°C. Corrosion Sci. 13, 659-676.

Misawa, T., K. Hashimoto and S. Shimodaira (1974), The mechanism of formation of iron oxide and oxyhydroxides in aqueous solutions at room temperature. Corrosion Sci. 14, 131-149.

Moore, M., J. D. Burton, P. J. LeB. Williams and M. L. Young (1979) The behaviour of dissolved organic material, iron and manganese in estuarine mixing. Geochim. et Cosmochim. Acta 43, 919-926.

Morgan, J. J. (1964) Chemistry of Aqueous Manganese(II) and (IV). Ph.D. thesis, Harvard University. Cambridge, Massachusetts.

Morgan, J. J. (1967) Chemical equilibria and kinetic properties of manganese in natural waters. S. D. Faust and J. V. Hunter, editors, Principles and Applications of Water Chemistry. Wiley and Sons, Inc. New York.

Morgan, J. J. and W. Stumm (1965) Analytical chemistry of aqueous manganese. J. Amer. Water Works Assoc. 57, 107-119.

Morgan, J. J. and F. B. Birkner (1966) Discussions on precipitation of iron in aerated ground water. ASCE J. Sanit. Engr. Div. 16(SA6), 137-143.

Morris, A. W. and A. J. Bale (1979) Effect of rapid precipitation of dissolved Mn in river water on estuarine Mn distributions. Nature 279, 318-319.

Murray, D. J., T. W. Healy and D. W. Fuerstenau (1968) The adsorption of aqueous metal on colloidal hydrous manganese oxide. W. J. Weber and E. Matijevie, editors, Adsorption From Aqueous Solution. Adv. in Chem. Series 79.

Murray, J. W. (1975) The interaction of metal ions at the manganese dioxide-solution interface. Geochim. et Cosmochim. Acta 39, 505-519.

Murray. J. W. (1978) β-FeOOH in marine sediments. EOS, Trans. A.G.U. 59, 411.

Murray, J. W. and G. Gill (1978) The geochemistry of iron in Puget Sound. Geochim. et Cosmochim. Acta 42, 9-19.

National Academy of Science (1973) Medical and biological effects of environmental pollutants: manganese. National Academy of Sciences, Washington, D.C.

National Research Council (1977) Geochemistry and the environment. National Academy of Sciences, Washington, D.C.

National Research Council (1979) Medical and Biological Effects of Environmental Pollutants: Iron. University Park Press, Baltimore.

Nichols, A. R. and J. H. Walton (1942) The autoxidation of manganous hydroxide. J. Amer. Chem. Sco. 64, 1866.

Nightingale, E. R. Jr. and R. F. Benck (1960) Precipitation of crystalline iron (III) oxide from homogeneous solution. Anal. Chem. 32, 566-567.

Nordell, E. (1953) Iron and manganese removal. Water and Sewage Works, 11(5), 181-185.

Onoda, G. Y. Jr. and P. L. de Bruyn (1966) Proton adsorption at the ferric oxide/aqueous solution interface. I. A kinetic study of adsorption. Surf. Sci. 4, 48-63.

Parks, G. A. and P. L. de Bruyn (1962) The zero point of charge of oxides. J. Phys. Chem. 66, 967-972.

Phipps, D. A. (1976) Metals and Metabolism. Clarendon Press, Oxford.

Posselt, H. S., F. J. Anderson and W. J. Weber, Jr. (1968) Cation sorption on colloidal hydrous manganese dioxide. Env. Sci. Tech. 2, 1087-1093.

Potter, R. M. and G. R. Rossman (1979) The tetravalent manganese oxides: identification, hydration, and structural relationships by infrared spectroscopy. Amer. Mineral.64, 1199-1218.

Powers, D. A. (1975) Magnetic Behaviour of Delta Ferric Oxide Hydroxide. Ph.D. thesis, California Institute of Technology. Pasadena, California.

Robin, M. B. and P. Day (1967) Mixed valence chemistry. Adv. Inorg. Chem. and Radiochem. 10, 288-304.

Schenk, J. E. and W. J. Weber, Jr. (1968) Chemical interactions of dissolved silica with iron(II) and (III). J. Amer. Water Works Assoc. 60, 199-212.

Schindler, P. W. (in press) Surface complexes at oxide water interfaces. M. Anderson and A. Rubin, editors, Adsorption of Inorganics at the Solid-Liquid Interface. Ann Arbor Science.

Schwertmann, U. and R. M. Taylor (1977) Iron Oxides. J. B. Dixon, editor, Minerals in soil environments. Amer. Soc. Agron. Publ., Madison.

Sholkovitz, E. R. (1976) Flocculation of dissolved organic and inorganic matter during the mixing of river water and seawater. Geochim.et Cosmochim. Acta 40, 831-845.

Spencer, E. W. and P. G. Brewer (1971) Vertical advection diffusion and redox potentials as controls on the distribution of manganese and other trace metals dissolved in waters of the black sea. J. Geophys. Res. 76(24), 5877-5892.

Stumm, W. and G. F. Lee (1961) Oxygenation of ferrous iron. Ind. Eng. Chem. 53, 143-146.

Stumm, W. and J. J. Morgan (1970) Aquatic Chemistry. Wiley-Interscience, New York.

Stumm, W. and R. Giovanoli (1976) On the nature of particulate manganese in simulated lake waters. Chimia 30(9), 423-425.

Swallow, K. C. (1978) Adsorption of Trace Metals by Hydrous Ferric Oxide in Seawater. Ph.D. thesis, Massachusetts Institute of Technology. Cambridge, Massachusetts.

Takai, T. (1973) Studies on the mechanisms of catalytic deferrization (in Japanese) J. Jpn. Water Works Assoc. 466, 22-33.

Tamura, H., K. Goto, T. Yotsuyanagi and M. Nagayama (1974) Spectrophotometric determination of iron (II) with 1, 10-phenanthroline in the presence of large amounts of iron (III). Talanta 21, 314-318.

Tamura, H., K. Goto and M. Nagayama (1976a) The effect of anions on the oxygenation of ferrous ion in neutral solutions. J. Inorg. Nucl. Chem. 38, 113-117.

Tamura, H., K. Goto and M. Nagayama (1976b) The effect of ferric hydroxide on the oxygenation of ferrous ions in neutral solutions. Corrosion Science 16, 197-207.

Theis, T. L. (1972) The Stabilization of Ferrous Iron by Natural Organic Compounds in Oxygen-Rich Environments. Ph.D. thesis, Notre Dame Univ., Notre Dame, Indiana.

van der Weijden, C. H. (1975) Sorption Experiments Relevant to the Geochemistry of Manganese Nodules. Ph.D. thesis, University Utrecht. Utrecht, Netherlands.

Weber, W. J. Jr. (1972) Physiochemical Processes for Water Quality Control. Wiley-Interscience, New York.

Westall, J. and H. Hohl (1980) A comparison of electrostatic models for the oxide/solution interface. Adv. in Colloid and Interface Sci. 12, 265-294.

Wollast, R., G. Billen and J. C. Duinker (1979) Behaviour of manganese in the Rhine and Scheldt estuaries. Part I, physico-chemical aspects. Estuarine and Coastal Marine Sci. 9, 161-169.

Yates, D. E. (1975) The Structure of the Oxide/Aqueous Electrolyte
    Interface. Ph.D. thesis, University of Melbourne, Melbourne,
    Australia.